ELSEVIER

Neurochemistry International 36 (2000) 595–645

NEUROCHEMISTRY International

www.elsevier.com/locate/neuint

Localization of agonist and competitive antagonist binding sites on nicotinic acetylcholine receptors

Hugo Rubén Arias*

Instituto de Matemática de Bahía Blanca, Consejo Nacional de Investigaciones Científicas y Técnicas (CONICET) and Universidad Nacional del Sur, Av. Alem 1253, 8000 Bahía Blanca, Argentina

Received 20 August 1999; accepted 1 November 1999

Abstract

Identification of all residues involved in the recognition and binding of cholinergic ligands (e.g. agonists, competitive antagonists, and noncompetitive agonists) is a primary objective to understand which structural components are related to the physiological function of the nicotinic acetylcholine receptor (AChR). The picture for the localization of the agonist/competitive antagonist binding sites is now clearer in the light of newer and better experimental evidence. These sites are located mainly on both α subunits in a pocket approximately 30–35 Å above the surface membrane. Since both α subunits are identical, the observed high and low affinity for different ligands on the receptor is conditioned by the interaction of the α subunit with other non-α subunits. This molecular interaction takes place at the interface formed by the different subunits. For example, the high-affinity acetylcholine (ACh) binding site of the muscle-type AChR is located on the αδ subunit interface, whereas the low-affinity ACh binding site is located on the αγ subunit interface. Regarding homomeric AChRs (e.g. α7, α8, and α9), up to five binding sites may be located on the αα subunit interfaces. From the point of view of subunit arrangement, the γ subunit is in between both α subunits and the δ subunit follows the α aligned in a clockwise manner from the γ. Although some competitive antagonists such as lophotoxin and α-bungarotoxin bind to the same high- and low-affinity sites as ACh, other cholinergic drugs may bind with opposite specificity. For instance, the location of the high- and the low-affinity binding site for curare-related drugs as well as for agonists such as the alkaloid nicotine and the potent analgesic epibatidine (only when the AChR is in the desensitized state) is determined by the αγ and the αδ subunit interface, respectively. The case of α-conotoxins (α-CoTxs) is unique since each α-CoTx from different species is recognized by a specific AChR type. In addition, the specificity of α-CoTxs for each subunit interface is species-dependent.

In general terms we may state that both α subunits carry the principal component for the agonist/competitive antagonist binding sites, whereas the non-α subunits bear the complementary component. Concerning homomeric AChRs, both the principal and the complementary component exist on the α subunit. The principal component on the muscle-type AChR involves three loops-forming binding domains (loops A–C). Loop A (from mouse sequence) is mainly formed by residue Y^{93},

Abbreviations: AChR, nicotinic acetylcholine receptor; $GABA_AR$, γ-aminobutyric acid type A receptor; $GABA_CR$, γ-aminobutyric acid type C receptor; GlyR; glycine receptor; $5\text{-}HT_3R$, 5-hydroxytryptamine type 3 receptor; GluR; glutamate receptor; P2XR; ATP receptor; 5-HT, 5-hydroxytryptamine; ACh, acetylcholine; CCh, carbamylcholine; TC, *d*-tubocurarine; DMT, dimethyl-*d*-tubocurarine; DHβE, dihydro-β-erythroidine; α-BTx, α-bungarotoxin; κ-BTx, κ-bungarotoxin; α-CTx, α-cobratoxin; κ-FTx, κ-flavitoxin; UV, ultraviolet; K_d, apparent dissociation constant; TDF, trimethylammonium diazonium fluoroborate; MBTA, 4-(*N*-maleimido)benzyltrimethylammonium iodide; BrACh, bromoacetylcholine; ACh mustard, 2-[(*N*-2′-chloroethyl)-*N*-methylamino]ethyl acetate; MPTA, 4-(*N*-maleimido)phenyltrimethylammonium iodide; DAPA, bis(3-azidopyridinium)-1; 10-decane perchlorate; DDF, *p*-*N*; *N*-(dimethylamino)phenyldiazonium fluoroborate; dansyl-C_6-choline, 6-(5-dimethylaminonaphtalene-1-sulfonamido)hexanoic acid-β-(*N*-trimethylammonium)ethyl ester; BCNI, bis(choline)-*N*-(4-nitrobenzo-2-oxa-1; 3-diazol-7-yl)-iminodiproprionate; MTSET, [2-(trimethylammonium)ethyl]methanetiosulfonate; C_{12}-eosin, 5-(*N*-dodecanoyl)aminoeosin; C_{18}-rhodamine, octadecyl rhodamine B; NBD, 4-[*N*-[(acetoxyethyl]-*N*-methylamino]-7-nitrobenz-2-oxa-1; 3-diazole; 5-SASL, 5-doxylstearate; FRET, fluorescence resonance energy transfer; NMR, nuclear magnetic resonance; EPR, electron paramagnetic resonance; NCI, noncompetitive inhibitor; AChE, acetylcholinesterase; tacrine, 1,2,3,4-tetrahydro-9-amino-acridine.

* Present address: Department of Pharmacology, School of Medicine, Texas Tech University Health Sciences Center, Lubbock, TX 79430, USA. Tel.: +1-806-743-2425, ext. 257; fax: +1-806-743-2744.

E-mail address: inarias@criba.edu.ar (H.R. Arias).

PII: S0197-0186(99)00154-0

loop B is molded by amino acids W^{149}, Y^{152}, and probably G^{153}, while loop C is shaped by residues Y^{190}, C^{192}, C^{193}, and Y^{198}. The complementary component corresponding to each non-α subunit probably contributes with at least four loops. More specifically, the loops at the γ subunit are: loop D which is formed by residue K^{34}, loop E that is designed by W^{55} and E^{57}, loop F which is built by a stretch of amino acids comprising L^{109}, S^{111}, C^{115}, I^{116}, and Y^{117}, and finally loop G that is shaped by F^{172} and by the negatively-charged amino acids D^{174} and E^{183}. The complementary component on the δ subunit, which corresponds to the high-affinity ACh binding site, is formed by homologous loops. Regarding α-neurotoxins, several snake and α-CoTxs bear specific residues that are energetically coupled with their corresponding pairs on the AChR binding site. The principal component for snake α-neurotoxins is located on the residue sequence $\alpha 1W^{184}$–D^{200}, which includes loop C. In addition, amino acid sequence 55–74 from the α1 subunit (which includes loop E), and residues γL^{119} (close to loop F) and γE^{176} (close to loop G) at the low-affinity binding site, or δL^{121} (close to the homologous region of loop G) at the high-affinity binding site, are involved in snake α-neurotoxin binding. The above expounded evidence indicates that each cholinergic molecule binds to specific residues which form overlapping binding sites on the AChR.

Monoclonal antibodies have been of fundamental importance in the elucidation of several aspects of the biology of the AChR. Interestingly, certain antibodies partially overlap with the agonist/competitive antagonist binding sites at multiple points of contact. In this regard, a monoclonal antibody directed against the high-affinity ACh binding site (αδ subunit interface) induced a structural change on the AChR where the low-affinity ACh locus (αγ subunit interface) approached to the lipid membrane.

The α subunits also carry the binding site for noncompetitive agonists. Noncompetitive agonists such as the acetylcholinesterase inhibitor (−)-physostigmine, the alkaloid galanthamine, and the opioid derivative codeine are molecules that weakly activate the receptor without interacting with the classical agonist binding sites. This binding site was found to be located at K^{125} in an amphipathic domain of the extracellular portion of the α1 subunit. Interestingly, the neurotransmitter 5-hydroxytryptamine (5-HT) also binds to this site and enhances the agonist-induced ion flux activity. This suggests that 5-HT may act as an endogenous modulator (probably as co-agonist) of neuronal-type AChRs. The enhancement of the agonist-evoked currents elicited by noncompetitive agonists seems to be physiologically more important than their weak agonist properties.

1. Introduction

The nicotinic acetylcholine receptor (AChR) is the prototype of the superfamily of ion channel-coupled receptors which are gated by specific neurotransmitters. In addition to both neuronal- and muscle-type AChRs, this superfamily includes the γ-aminobutyric acid ($GABA_AR$ and $GABA_CR$ types), the glycine (GlyR), and the 5-hydroxytryptamine (5-HT) ($5\text{-}HT_3R$ type) receptor (reviewed in Changeux and Edelstein, 1998; Ortells and Lunt, 1995; Karlin and Akabas, 1995; Hucho et al., 1996). A scheme of the primary, the tertiary, and the quaternary basic structural features of these ionotropic receptors is shown in Fig. 1. One of the reasons by which these receptors are considered a superfamily is the existence of high homology between the amino acid sequences of each receptor subunit (Fig. 1(A)) (reviewed in Ortells and Lunt, 1995). For example, between neuronal and muscle AChR α subunit sequences homologies of 48–70% are found. The homology between the $5\text{-}HT_3A_L$ subunit and either the α1 or the α7 AChR subunit is about 30%. However, a higher homology is found when key amino acid sequences are compared (e.g. ligand binding domains or the M2 transmembrane domain).

A second characteristic, shared by all members, is that each subunit can be divided in three portions: (1) an extracellular; (2) a transmembrane; and (3) a cytoplasmic portion (Fig. 1(B)).

1. The NH_2-terminal hydrophilic extracellular portion bears the neurotransmitter binding sites, several glycosylation sites, and the 15-residue Cys-loop between amino acids 128–142 corresponding to the *Torpedo* α subunit (reviewed in Ortells and Lunt, 1995). Regarding the AChR subunit, a long extracellular region comprising about 210 amino acids is oriented 55–65 Å towards the synaptic cleft. The amino-terminal domain is essential for a correct AChR assembly (Chavez and Hall, 1992; Verrall and Hall, 1992). In addition to the loci for classical cholinergic agonists and competitive antagonists, this large domain contains: (a) the site for noncompetitive agonists (this subject will be addressed later); (b) the main immunogenic region (comprising at least residues 67–76 of the α1 subunit) which is involved in the autoimmune disease myasthenia gravis (Wahlsten et al., 1993; reviewed in Conti-Tronconi et al., 1994); (c) the high-affinity binding site for the noncompetitive inhibitor (NCI) ethidium (Johnson and Nuss, 1994; reviewed in Arias, 1996, 1997, 1998a); and (d) the Cys residue in the δ subunit that links, by means of a disulfide bridge, two different 9 S AChR monomers to form the 13 S AChR dimer (DiPaola et al., 1989).
2. The transmembrane domain of each subunit is formed by four highly hydrophobic segments named M1, M2, M3, and M4 (Fig. 1(B)). These putative membrane-spanning α helices have a dimension of

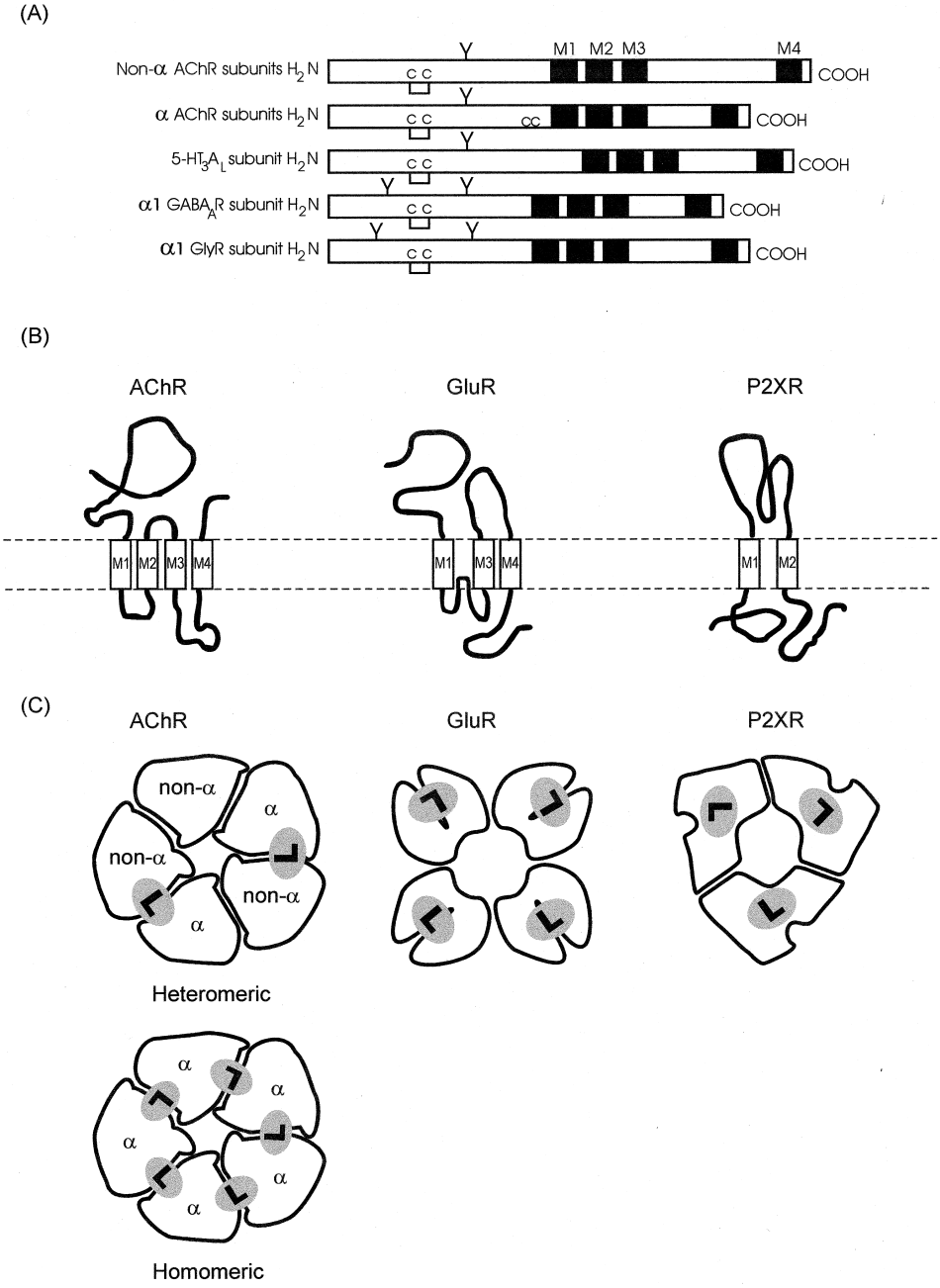

Fig. 1. Schematic representation of the structures of several ligand-gated ionotropic receptor families. (A) Schematic illustration of the primary sequence of several subunits from members of the ligand-gated ion channel superfamily which includes the α (α1–α9) and non-α (β1–β4, γ, ϵ, and δ) subunits of the AChR, the 5-HT_3A_L subunit of the 5-HT_3R, the α1 subunit from the $GABA_AR$, and the α1 subunit from the GlyR. M1–M4, transmembrane domains; C–C, Cys–Cys bridge found in the ion-channel superfamily (homologous to C^{128} and C^{148} of the α1 AChR subunit; CC, Cys–Cys pair found in the α subunits from both muscle- and neuronal-type AChRs) corresponding to C^{192}–C^{193} from the α1 AChR subunit; Y, oligosaccharide groups. (B) diagram of the tertiary organization of the AChR, the GluR, and the P2XR. Each AChR subunit, as well as the subunits from the other members of the ligand-gated ion channel superfamily, includes: (1) a long NH_2-terminal hydrophilic extracellular region; (2) four highly hydrophobic domains named M1, M2, M3, and M4. It is postulated that the intrinsic ion channel is composed by five M2 segments, one from each subunit. Moreover, M1–M2 and M2–M3 are connected by minor hydrophilic stretches; and (3) a major hydrophilic segment facing the cytoplasm. Additionally, the M4 domain orientates the COOH-terminus to the synaptic side of the membrane. On the contrary, the subunit of the GluR presents three transmembrane domains M1, M3 and M4, a reentrant loop, and a cytoplasmic orientation for the COOH-terminus; while the subunit of the P2XR has only two transmembrane domains (M1 and M2) and both NH_2- and COOH-terminus are oriented against the cytoplasm. (C) Schematic representation of the oligomeric organization of AChR, GluR and P2XR. The hypothetical pentameric AChR is formed by two α subunits and three non-α chains. The two ligand binding sites (L) are located at the interfaces of one α subunit and one non-α chain. For instance, the muscle-type AChR presents a high-affinity ACh binding site at the αδ subunit interface and another low-affinity ACh locus at the αγ subunit interface. Regarding homomeric AChRs (e.g. α7, α8, and α9), up to five ligand binding sites may putatively exist. On the contrary, GluR and P2XR present four and three ligand binding sites, respectively, each one located on only one subunit.

30–35 Å. The domains M1, M2, and M3 are separated from each other by short hydrophilic stretches. In particular, the portion between M2 and M3 of the AChR α1 subunit photoreacted with the potent local anesthetic analogue meproadifen mustard (Pedersen et al., 1992; reviewed in Arias, 1996, 1997, 1998a, 1999). The hydrophilic faces of the five M2 segments, one from each receptor subunit, form the wall of the ion channel. The ion channels from the $GABA_AR$, the $GABA_CR$, and the GlyR, are specific to anions (e.g. Cl^-), whereas the ion channels from the 5-HT_3R and AChRs allow for the passage of cations (e.g. Na^+, K^+, and Ca^{2+}). The ion channel itself is the target site for the pharmacological action of several NCIs that act by a steric blocking mechanism (reviewed in Arias, 1996, 1997, 1998a, 1999; Changeux and Edelstein, 1998; Hucho et al., 1996; Karlin and Akabas, 1995).

The M1, M3, and M4 transmembrane domains from the AChR, and probably from the other receptor members, are in contact with the lipid membrane. Although these transmembrane domains have traditionally been considered as α-helical, several lines of experimental research suggest a mixed α-helical/non-helical secondary structure (reviewed in Arias, 1998a; Hucho et al., 1996; Karlin and Akabas, 1995). Interestingly, the extracellular end of the M1 domain has been found to bear structural elements for the high-affinity binding site of the NCI quinacrine (reviewed in Arias, 1996, 1997, 1998a).

3. The hydrophilic cytoplasmic segment, approximately four-fold smaller than the extracellular one, is intercalated between domains M3 and M4. The M4 domain orientates the COOH-terminus to the synaptic side of the membrane. The cytoplasmic domain of these receptors carries several phosphorylation sites (reviewed in Huganir and Greengard, 1990; Swope et al., 1992). The process of phosphorylation-dephosphorylation has been found to be very important for the modulation of this ion channel superfamily (reviewed in Levitan, 1994). More particularly, the AChR cytoplasmic region bears the linking site for the nonreceptor 43 kDa protein, actually named rapsyn, which functions in receptor clustering and receptor-cytokeleston communication (Phillips et al., 1991).

The notion that each receptor can be structurally and functionally represented by three different but interacting domains (the extracellular, the transmembrane, and the cytoplasmic domain) is supported by the following experimental evidence. (a) The construction of a chimeric receptor formed by the NH_2-terminal portion of the α7 subunit and the remanent by the 5-HT_3A_L subunit yields functional chloride channels that are gated by ACh (Eiselé et al., 1993). (b) The α4/5-HT_3A_L receptor chimera was found to be activated by 5-HT and the Ca^{2+} flux was higher than the homomeric 5-HT_3R indicating that the α4 subunit contributes to the formation of the ion channel when expressed with the 5-HT_3A_L subunit (Kriegler et al., 1999; van Hooft et al., 1997).

The major structural information on this superfamily has been obtained from studies that use the muscle-type AChR. The muscle-type AChR is a pentamer structurally formed by two α subunits, one β, one δ and, one γ or one ϵ subunit depending on whether the receptor is in an embryonic or adult stage, respectively. Specific intersubunit contacts determine the formation of the agonist binding sites and a correct transport of the assembled AChR to the cell surface (Green and Wanamaker, 1998; Gu et al., 1991; Kreienkamp et al., 1995). Based on the existence or not of two adjacent cysteines in or close to the position 192 and 193 of the muscle-type α subunit, which are involved in the recognition and binding of agonist, the neuronal-type AChR subunit classes are designated α (when they contain both cysteines) and non-α or β (when they do not). Up to-date, eight α subunits (α2–α9) and three β subunits (β2–β4) have been identified in vertebrates. The α and β subunits of the muscle-type AChR are actually numbered α1 and β1. Interestingly, several AChR subunits have also been discovered in distinct invertebrate animals including nematodes (reviewed in Brownlee and Fairweather, 1999) and insects (Sgard et al., 1998 and references therein). In addition to the great variety of AChR subunits, biochemical and cDNA sequence data have established subunit diversity for the other members of the ion channel superfamily as well (reviewed in Boess and Martin, 1994; Brownlee and Fairweather, 1999; Langosch et al., 1990; Sieghart, 1995). From phylogenetic analysis, a gene duplication was postulated to be the main cause for the observed subunit diversity (Le Novère and Changeux, 1995; Ortells and Lunt, 1995). The existence of a high number of functional and pharmacological distinct receptor entities is a direct consequence from such genetic variety (reviewed in McGehee and Role, 1995).

The receptors comprising the ligand-gated ion channel superfamily are formed by five (but not necessarily distinct) subunits (Fig. 1(C)). Viewed from the synaptic cleft, these receptors appear as a rosette with a central depression. The five subunits are arranged pseudosymetrically around an axis that passes through the ion pore, perpendicular to the plane of the membrane. In homology with the muscle-type AChR, the neuronal AChRs are also considered to be oligomers composed of five subunits (Anand et al., 1991). However, depending on the kind of tissue involved, these chains

can be linked in several heteromeric combinations (e.g. one of the main brain AChRs is composed of two α4 subunits and three β2 subunits; see review by Role, 1992), and even in homomeric combinations of only one subunit (e.g. α7 and α8 receptors in chick retina (Keyser et al., 1993) and α9 in cochlear hair cells (Elgoyhen et al., 1994)) (see Fig. 1(C)). The other members of the ligand-gated ion channel superfamily basically present the same pentameric organization (Boess et al., 1995; Langosch et al., 1990; Nayeem et al., 1994).

Each member of this superfamily exhibits two neurotransmitter binding sites located at different subunit interfaces. Regarding the muscle-type AChR, each monomer contains two α subunits bearing nonequivalent binding sites which recognize the endogenous neu-

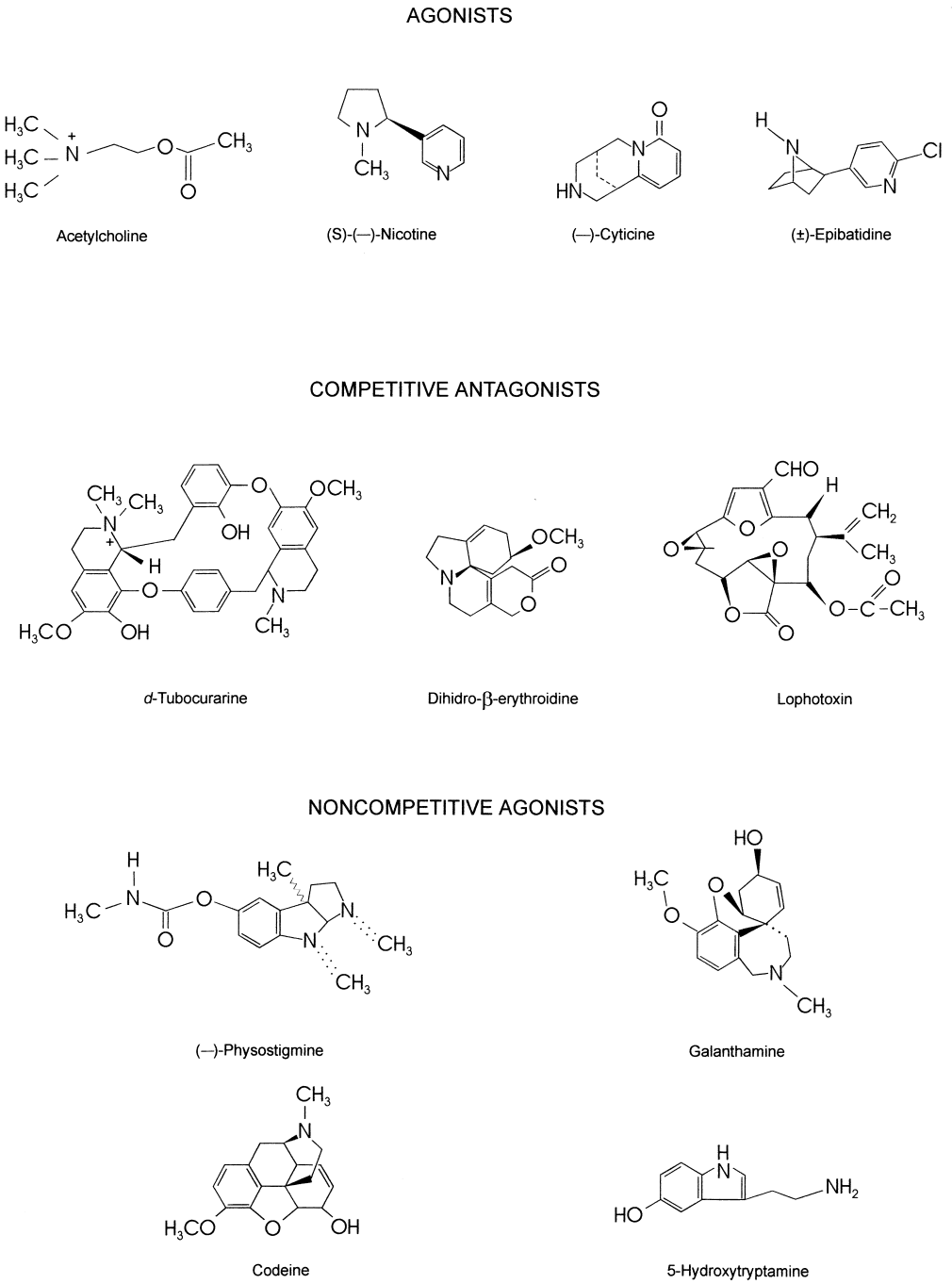

Fig. 2. Molecular structures of different agonists, competitive antagonists and noncompetitive antagonists. The structure of competitive antagonists such as the α-neurotoxin from *N. mossambica mossambica* and several α-CoTxs are shown in Fig. 7 and Table 6, respectively.

rotransmitter acetylcholine (ACh) (see molecular structure in Fig. 2). This specific binding produces a conformational change on the receptor that opens the ion channel to allow for the movement of monovalent and divalent cations in favour of the electrochemical gradient. A recent picture involving the change in configuration from the closed to the open-channel AChR by means of ACh binding has been determined by electron microscopy images at 9 Å resolution (Unwin, 1995).

In general, neuronal-type AChRs present higher Ca^{2+} permeability than muscle-type AChRs. In turn, this feature is physiologically modulated by extracellular Ca^{2+} levels (Mulle et al., 1992). At least in the particular case of the α7 receptor, this potentiation seems to be mediated by Ca^{2+} binding to several extracellular sites: one at the residue sequence 161–172 and two others at the level of E^{18} and E^{44} (Galzi et al., 1996).

Channel opening can be inhibited by diverse ligands that compete for the neurotransmitter binding site. This mechanism receives the general name of competitive antagonism. Fig. 2 shows the molecular structure of several cholinergic competitive antagonists. There also exists another process named desensitization in which the receptors, in a prolonged exposition to specific agonists, remain on the surface of the membrane but in a closed conformational state (reviewed in Jones and Westbrook, 1996). In this state, they do not respond to any further agonist addition.

In addition to binding sites for agonists and competitive antagonists, the ligand-gated ion channel receptors posses sites for a heterogeneous class of compounds named NCIs. These drugs inhibit agonist-evoked ion flux activity without inhibiting agonist binding. The NCIs are structurally and chemically very different from each other and, at least for the AChR, their binding sites are located at distinct luminal and nonluminal domains (reviewed in Arias, 1996, 1997, 1998a, 1999; Changeux and Edelstein, 1998; Hucho et al., 1996; Karlin and Akabas, 1995). Nevertheless, these molecules preserve certain common pharmacological properties such as the apparent blockade of the ion pore by a steric mechanism, or the channel inactivation by an allosteric process, and/or the enhancement of the desensitization rate. Interestingly, several local anesthetics that act as NCIs on the AChR behave as competitive antagonists on the 5-HT_3R (reviewed in Arias, 1999).

From a physiological point of view, an important characteristic of the ligand-gated ion channel receptor superfamily is that each member may be modulated by ligands other than the natural neurotransmitter. For example, either nicotinic agonists (Gurley and Lanthorn, 1998) or antagonists such as *d*-tubocurarine (*d*-TC) and their analogues (Yan et al., 1998, 1999) competitively antagonize the action of 5-HT on 5-HT_3Rs from different sources. In addition, 5-HT and analogues enhance the desensitization process (Cross et al., 1995), inhibit ion flux activity in the micromolar concentration range (Nakazawa and Ohno, 1999; reviewed in Arias, 1998a,b) as well as potentiate the agonist-activated currents in the submicromolar concentration magnitude (Schrattenholz et al., 1996) on both neuronal- and muscle-type AChRs. Finally, competitive antagonists of the ligand-gated ion channel superfamily such as bicuculline ($GABA_A$R), strychnine (GlyR), and ICS-205,930 (5-HT_3R) behave as competitive antagonists of the cochlear α9 (Rothlin et al., 1999), and the α7 and α4β2 AChRs (Matsubayashi et al., 1998).

In addition to this receptor superfamily, other neurotransmitter-gated ion channels such as the receptors for glutamate (GluR) (Bennett and Dingledine, 1995) and for ATP (P2XR) (Brake et al., 1994) have been found (reviewed in Barnard, 1996; Brake et al., 1994; Changeux and Edelstein, 1998; Paas, 1998; Sieghart, 1995). Nevertheless, both receptors present several structural characteristics that make them distinct from that comprising the AChR and their cousins. For comparative purposes, the tertiary structure and the oligomeric organization of both the GluR and the P2XR are shown in Fig. 1. From the tertiary structures shown in Fig. 1(B), it becomes evident that these receptors do not share a common hydrophobic segment pattern as the one previously described for the ion channel receptor superfamily. More specifically, the GluR presents three transmembrane domains (M1, M3, and M4) and a reentrant membrane loop with the ascending limb in an α-helical conformation and the descending limb in an extended orientation (Bennett and Dingledine, 1995; Kuner et al., 1996; Paas, 1998), whereas the P2XR has only two transmembrane domains (M1 and M2) (Newbolt et al., 1998; reviewed in Brake et al., 1994; Changeux and Edelstein, 1998; Paas, 1998). Thus, a cytoplasmic COOH-terminal location is expected for the former receptor, while both P2XR terminals are exposed to the intracellular side. Surprisingly, the ion-conducting pathway of P2XR seems to progressively dilate during prolonged (10–60 s) ATP activation (Virginio et al., 1999), and its ion selectivity changes in the second time regime (Khakh et al., 1999). These intrinsic properties are considered to be functionally related with the neuronal modulation elicited by these ion channel receptors.

From the subunit organization displayed in Fig. 1(C), it is possible to distinguish that the GluR and the P2XR are formed by four (Laube et al., 1998; Wu et al., 1996) and three subunits (Nicke et al., 1998), respectively. In addition, these receptors show neither the same number nor the same localization of neurotransmitter binding sites as that found on the AChR and its ionotropic receptor superfamily

(Fig. 1(C)). The heteromeric forms of the ligand-gated ion channel receptor superfamily show two neurotransmitter binding sites at the interfaces of two subunits (see Fig. 1(C)). Exceptions are the receptors formed by homologous subunits. For instance, the homomeric α7 nicotinic receptor has putatively five binding sites (Palma et al., 1996a) (see Fig. 1(C)). On the contrary, the GluR has four agonist binding sites, each one located at the interface of the two extracellular lobes provided by only one subunit (Paas et al., 1996;

Table 1
Photolabeling of the AChR by agonist, competitive antagonist, and noncompetitive agonist analogues

Ligands	Labeled subunits	Specific residues[a]	Loop[b]	References
Agonists				
[^{3}H]Bromoacetylcholine	αγ (low)[c]; αδ (high)[d]	αC^{192} and αC^{193}	C	(Damle et al., 1978; Dunn et al., 1993; Moore and Raftery, 1979)
[^{3}H]Nicotine	α and γ	αC^{192}, αC^{193}, αY^{198}, αY^{190}, and γW^{55}	C and E	(Middleton and Cohen, 1991; Chiara et al., 1998)
[^{3}H]ACh mustard	α	Y^{93}	A	(Cohen et al., 1986)
[^{3}H]AC_5	all	not determined	not determined	(Chatrenet et al., 1992)
[^{125}I]Azidoimidacloprid	66 kDa (to a lesser extent 61 kDa)	not determined	not determined	(Tomizawa and Casida, 1997)
Competitive antagonists				
[^{3}H]TDF	α	C^{192} and C^{193}	C	(Changeux et al., 1967)
[^{3}H]MBTA	αγ (high)[d]	αC^{192} and αC^{193}	C	(Damle and Karlin, 1978; Kao and Karlin, 1986; Martin and Karlin, 1997)
[^{3}H]MPTA	α	C^{192} and C^{193}	C	(Sobel et al., 1980)
[^{3}H]DAPA	all	αC^{192} and αC^{193}	C	(Witzemann and Raftery, 1977; Tine and Raftery, 1993)
[^{3}H]*d*-Tubocurarine	αγ (high); αδ (low)	αY^{190} (to a lesser extent αC^{192} and αY^{198}), δW^{57} and γW^{55} (to a lesser extent γY^{111} and γY^{117})	C, E, and F	(Pedersen and Cohen, 1990; Chiara and Cohen, 1997; Chiara et al., 1999)
[^{3}H]Lophotoxin	αγ (low); αδ (high)	αY^{190}	C	(Abramson et al., 1989)
[^{3}H]DDF	α	C^{192}, C^{193}, Y^{190}, Y^{198}, Y^{93} and W^{149} (to a lesser extent Y^{151} and W^{86})	A, B, and C	(Galzi et al., 1990; 1991a,b)
[^{3}H]4-Benzoylbenzoylcholine	γ	L^{109}	F	(Wang et al., 1996)
α-[^{125}I]CoTx MI[e]	all (βγ)	not determined	not determined	(Myers et al., 1991)
N^{ϵ}-ASA α-[^{125}I]-CoTx GIA[f]	γδ	not determined	not determined	(Myers et al., 1991)
N^{α}-ASA α-[^{125}I]-CoTx GIA[g]	βγ	residues γ121–183 and β149–255	G	(Myers et al., 1991)
p-Benzoylphenylalanyl-α-[^{125}I]-CoTx GI[h]	αγ	not determined	not determined	(Kasheverov et al., 1999)
ω-[^{125}I]CoTx GVIA[i]	α	not determined	not determined	(Horne et al., 1991)
[^{3}H]Azido ethidium derivatives[j]	αγ (high)	not determined	not determined	(Pedersen, 1995)
Noncompetitive agonist				
(−)-Physostigmine or eserine[k]	α	K^{125}		(Schrattenholz et al., 1993a,b)

[a] Labeling specificity for the agonist/competitive antagonist sites is defined by following the criteria: (1) the labeled site (e.g. subunits, domains, polypeptides, residues, loops, etc.) should be inhibited by agonists such as ACh and/or competitive antagonists such as α-BTx but (2) should not to be affected by the pharmacological action of high-affinity NCIs such as the hallucinogenic drug phencyclidine or histrionicotoxin.

[b] See Fig. 3 for details on specified loops.

[c] Site at which the used probe binds with low affinity.

[d] Site at which the used probe binds with high affinity.

[e] The labeling was relatively nonspecific (all subunits were labeled) by using ethylen glycol bis(succinimidyl succinate) as cross-linker which has 1.6 nm nominal radii. Subunits β and γ were labeled by using disuccinimidyl tartrate as cross-linker which has 0.65 nm nominal radii.

[f] N^{α}-ASA α-[^{125}I]-CoTx GIA, azidosalicylate α-[^{125}I]conotoxin GIA derivative labeled at amino terminal.

[g] N^{ϵ}-ASA α-[^{125}I]-CoTx GIA, azidosalicylate α-[^{125}I]conotoxin GIA derivative labeled at K^{15}.

[h] *p*-Benzoylphenylalanyl α-[^{125}I]conotoxin GI derivative labeled at Y^{11}.

[i] Specific crosslinking was reduced by Ca^{2+} in the millimolar concentration range but not by α- or κ-BTx, α-CoTx or CCh.

[j] [^{3}H]Azido ethidium derivatives, 3- and 8-[^{3}H]azido, and 3,8-[^{3}H]diazido ethidium, reacted with the high-affinity binding site of *d*-TC.

[k] The labeling of this site was not inhibited by classical agonists or antagonists and thus, this agonist noncompetitive site is considered a new pathway for AChR activation or co-agonistic action.

reviewed in Changeux and Edelstein, 1998; Paas, 1998), whereas the P2XR has three agonist binding sites, each one located at the large extracellular domain from every subunit (reviewed in Changeux and Edelstein, 1998).

The aim of this review is to discuss several recent findings on both structural and functional relevant aspects of ligand binding sites of the AChR. We will put special emphasis on the description of the localization of ligand binding sites for cholinergic agonists such as the native neurotransmitter ACh, for curariform drugs, for several α-neurotoxins and antibodies which specifically compete with agonists, as well as for those acetylcholinesterase inhibitors and the neurotransmitter 5-HT that activate the AChR in a noncompetitive manner. Fig. 2 shows the molecular structure of several agonists, competitive antagonists, and noncompetitive agonists. The information described herein has been mainly obtained by means of methods such as photolabeling, site-directed mutagenesis in combination with electrophysiological techniques, and by using biophysical approaches such as quantitative fluorescence spectroscopy and high resolution electron microscopy.

2. Principal component of the binding sites for agonists and competitive antagonists

2.1. Evidence from the photolabeling approach

The specific agonist binding sites are located at the extracellular portion of the AChR (Fairclough et al., 1993). A major insight into the structure of the agonist/competitive antagonist sites was provided, like for the study of the localization of NCI binding sites (reviewed in Arias, 1996, 1997, 1998a, 1999), by using affinity and photoaffinity labeling techniques. The collected information on agonist/competitive antagonist binding sites location by using different cholinergic probes is shown in Table 1. Among used probes we may cite, natural molecules that can be directly activated by simple ultraviolet (UV) irradiation, alkylating agents, and photoactivatable derivatives with specific photoreactive groups such as diazonium, azido, mustard, etc.

Early works demonstrated that the α1 subunit was labeled by affinity drugs that resemble the ACh molecule. Changeux's laboratory at Pasteur Institut (Paris, France) was one of the first groups that studied photoaffinity labeling of the agonist binding sites by using the probe trimethylammonium diazonium fluoroborate (TDF) (Changeux et al., 1967). Later, the competitive antagonist bis(3-azidopyridinium)-1,10-decane perchlorate (DAPA) was also used as a photoaffinity label (Tine and Raftery, 1993; Witzemann and Raftery, 1977).

Due to the existence of both C^{192} and C^{193} on the AChR, subsequent studies were performed by using different alkylating agents. Among them, there are agents that present competitive antagonist activity such as 4-(*N*-maleimido)benzyltrimethylammonium iodide (MBTA) (Damle and Karlin, 1978; Kao and Karlin, 1986; Martin and Karlin, 1997) and 4-(*N*-maleimido)phenyltrimethylammonium iodide (MPTA) (Sobel et al., 1980), others with agonist properties such as bromoacetylcholine (BrACh) (Damle et al., 1978; Dunn et al., 1993; Moore and Raftery, 1979) and an oxidizable dithiol carbamylcholine (CCh) analogue (Servent et al., 1995). These sulfhydryl-directed affinity ligands are far less chemically reactive than photoaffinity derivatives such as TDF and DAPA and require previous disulfide reduction of the AChR to be active. The obtained data indicate that the antagonists MBTA and MPTA and the agonist BrACh reacted with C^{192} or C^{193} upon disulfide reduction. The importance of both cysteines in ligand recognition and binding was supported by the fact that disulfide reduction causes a decrease in cholinergic agonist affinities (Walker et al., 1984), and vice versa, agonists and competitive antagonists affect the reactivity of the disulfide site (Damle and Karlin, 1980). In addition, reduction of α4β2 neuronal receptors with dithiothreitol inhibited the binding of the alkaloid [^{3}H]cytisine and the effect of this agonist was reversed upon reoxidation with dithiobisnitrobenzoic acid (Rossant et al., 1994). Opposite to this, under nonreducting conditions, alkylation of free sulfhydryl groups by using relatively nonpolar alkylating agents such as *N*-phenylmaleimide produced inhibition of ion channel activity without affecting ligand binding properties including ligand-induced transitions (Clark and Martínez-Carrión, 1986; Walker et al., 1984). This apparent contradiction was overcame by mutating the Cys residues and determining their effect on ACh binding properties, an issue that will be developed later.

In order to explore the recognition site of nonderivatized cholinomimetic drugs, Taylor's laboratory at the University of California (San Diego, USA) has used the covalent properties of the natural cyclic diterpenoid lophotoxin (see molecular structure in Fig. 2) found in gorgonian corals such as *Lophogorgia* and *Pseudopterogorgia* to label the AChR (Abramson et al., 1989). This marine neurotoxin acts inhibiting neuromuscular, peripheral, and neuronal AChRs (reviewed in Arias, 1997). Other drugs such as the alkaloid nicotine (Chiara et al., 1998; Middleton and Cohen, 1991) and the poison *d*-TC (Chiara and Cohen, 1997; Chiara et al., 1999; Pedersen and Cohen, 1990) were also utilized under UV irradiation as natural probes (see molecular structures in Fig. 2). From these experiments, an important difference between

alkylating and natural agents was found: alkylating agents mainly labeled $C^{192–193}$ whereas lophotoxin and *d*-TC primarily labeled Y^{190}, and nicotine labeled Y^{198} (Table 1). *d*-Tubocurarine also labeled $C^{192–193}$ and, to a lesser extent, Y^{198}. Another piece of evidence that supports the above location for nicotine is given for binding studies by using the synthetic peptide 181–200 from the α1 subunit (Lentz et al., 1998). [^{3}H]-Labeled nicotine bound with lesser affinity to peptides containing mutated residues at positions K^{185}, H^{186}, Y^{190}, C^{192}, C^{193}, T^{196}, or Y^{198}.

An improvement in the labeling was achieved by using the competitive antagonist *p*-*N*,*N*-(dimethylamino)phenyldiazonium fluoroborate (DDF) and by selecting the bound drug measuring the fluorescence resonance energy transfer (FRET) elicited from the protein (Galzi et al., 1990, 1991a; reviewed in Arias, 1997; Changeux and Edelstein, 1998; Hucho et al., 1996; Karlin and Akabas, 1995). Upon photolysis, this bisquaternary probe generates an extremely reactive aryl cation that irreversibly labeled fragment 179–207, specifically at Y^{198} and Y^{190}, in addition to C^{192} and C^{193}, in an agonist-protectable manner. These photolabeling data indicate that a stretch of amino acids comprising C^{192}, C^{193}, Y^{190}, and Y^{198} contribute to the binding of ACh (see loop C in Fig. 3). Interestingly, practically the same amino acids (i.e. Y^{190}, C^{192}, and C^{193}) were photolabeled by using [^{3}H]5-HT as a probe for the agonist/competitive antagonist binding sites on the *Torpedo* AChR (Blanton M. P., McCardy E. A., Fryer J. D., Liu M. and Lukas R. J., personal communication). Two additional loops have also been found by using DDF: one which includes residue Y^{93} (and perhaps W^{86}) (loop A in Fig. 3) and the other that includes amino acid W^{149} (and perhaps Y^{151}) (loop B in Fig. 3). In addition, the reactive azirinium ion derivative of 2-[(*N*-2′-chloroethyl)-*N*-methylamino]ethyl acetate (ACh mustard) labeled Y^{93}, which is the residue comprised by loop A (Cohen et al., 1991).

A structural and functional relationship was found on the labeling of loops A and B: the receptor in the desensitized state presents higher labeling than in the resting state (Galzi et al., 1991b). Significantly, the amino acids labeled with DDF are conserved in both the muscle and the neuronal α chains, but not in non-α subunits from neuronal AChRs.

Although the use of the photolabeling approach has provided important information for the localization of the agonist/competitive antagonist binding sites, a note of caution should be taken into account: this technique is limited in accuracy when only small populations of the receptor is labeled, as is often the case for secondary and/or low-affinity binding sites.

These data are consistent with the existence of a principal component for the agonist/competitive antagonist binding site on the α subunit which is formed by the structural contribution of loops A–C (Fig. 3).

2.2. Evidence from the combination of mutagenesis and electrophysiological approaches

In parallel to the above experimental evidence, site-directed mutagenesis in combination with patch-clamp techniques have confirmed that loops A–C (see Table 1 and Fig. 3) contribute to the agonist/competitive antagonist locus. The effect of α subunit residue-directed mutagenesis on agonist and competitive antagonist binding properties is summarized in Table 2. For example, when C^{192} and C^{193} were replaced by Ser the inhibition of α-bungarotoxin (α-BTx) binding elicited by 10 mM CCh reached only 34 and 66% of control, respectively (Mishina et al., 1985). However, the fact that the AChR channel response to ACh was not detectable might be due to a low receptor expression. The specificity of both $C^{192–193}$ in agonist binding is manifested by the fact that mutations of several cysteines located at positions other than 192–193 in different subunits have demonstrated no functional effect on binding properties (Lee et al., 1994; Li et al., 1990, 1992; Lo et al., 1991; Pradier et al., 1989). Nevertheless, these mutations affected the ion channel gating process. For instance, the mutation C222S located at αM1 from *Torpedo* AChR (Mishina et al., 1985), or its equivalent in murine AChR C^{230} (Lo et al., 1991), and the mutations of γC^{416} and γC^{420} to Ser or Phe located in between the M3 and M4 domains (Pradier et al., 1989).

In regards to amino acids other than C^{192} and C^{193}, when Y^{190} was replaced by Phe, a concentration of ACh 20–180 times higher than that for the nonmutated AChR was necessary for channel activation (Aylwin and White, 1994a,b; Chen et al., 1995; O'Leary and White, 1992; O'Leary et al., 1994; Sine et al., 1994; Tomaselli et al., 1991) (Table 2). This mutation also caused about 400-fold decreasing in dimethyl-*d*-tubocurarine (DMT) affinity (Sine et al., 1994). However, it is necessary to take into account that the increase in the apparent dissociation constant (K_d) for ligands does not only reflect changes in the recognition site but also in the allosteric coupling (Spivak, 1995). Additionally, the agonist concentration required for half-maximal current (EC_{50}) is a parameter that depends on the performance of both binding and gating processes. Thus, in order to determine whether mutations alter either (both) the binding or (and) the gating process, single channel kinetic analyses were performed on Y190F mutated AChRs. These experiments indicated that Y^{190} is involved in both binding and gating events (Chen et al., 1995). The observed reduced ACh affinity for the Y190F mutated AChR was more pronounced at the high-affinity binding site

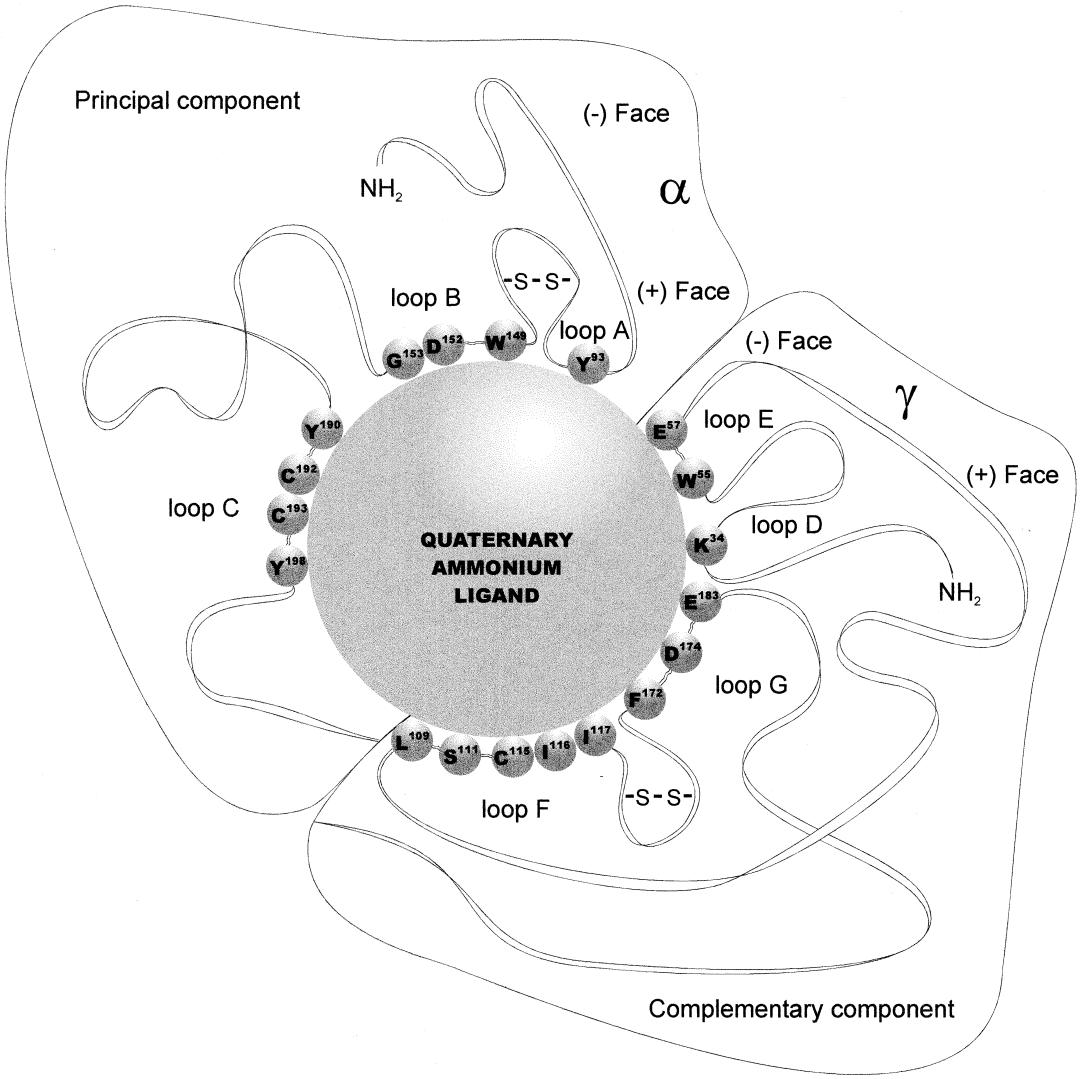

Fig. 3. Top view of a schematic model for the proposed folding of the extracellular domain involved in the binding site of several quaternary-ammonium compounds, including the native neurotransmitter ACh and the competitive antagonist curare. The high-affinity *d*-TC (and the low-affinity ACh) binding site is located in the αγ interface. Its counterpart, the low-affinity *d*-TC (and the high-affinity ACh) binding site, which is located in the αδ interface is not included in this model (but see Fig. 5). The large sphere represents a quaternary ammonium-containing molecule. The principal component of the ligand binding site is located in the α subunit which contributes with loops A, B, and C. The residues involved in the binding site are represented by small spheres in one letter code. Loop A is mainly formed by residue Y^{93}. Loop B is molded by amino acids W^{149}, Y^{152} and probably G^{153}. Loop C is shaped by residues Y^{190}, C^{192}, C^{193}, and Y^{198}. The disulfide bond indicated in the α subunit as —S—S— represents the link between C^{128} and C^{142}. The complementary component of the ligand binding site is located on either the γ or the δ subunit. We only show the complementary component corresponding to the γ subunit which probably contributes with loops D, E, F and G. Loop D is formed by residue K^{34}. Loop E is designed by W^{55} and E^{57}. Loop F is built by a stretch of amino acids comprising L^{109}, S^{111}, C^{115}, I^{116}, and Y^{117}. Loop G is shaped by F^{172} and by the negatively-charged amino acids D^{174} and E^{183}. In the γ subunit, —S—S— indicates the above mentioned disulfide bond. The used residue sequence number corresponds to the mouse AChR. The complementary component of the δ subunit (model not shown for simplicity) is instead formed by homologous loops. The observed complementarity between loops D and G suggests that these two loops come into close proximity at the non-α surface of the binding site (Sine et al., 1995b; reviewed by Prince and Sine, 1998b).

(αδ) and it was considered to be due to a 60 times lower association rate constant than the one of the wild-type AChR. However, the principal cause for the shifts in the macroscopic dose-response curves for either Y^{93} or Y^{198} to Phe mutation is a reduction in ACh affinity for the AChR resting state (Aylwin and White, 1994a,b).

The effect of the residue charge was evidenced since the mutation on Y^{190} to the basic amino acid His reduced DMT affinity by almost three orders of mag-

Table 2
Residue mutations on the AChR α subunit that strongly affect the binding of both agonists and competitive antagonists as well as the gating properties of agonists

Mutation	Source of AChR	Pharmacological effect[a]			References
		Reduction of competitive antagonist binding[b]	Reduction of agonist binding[c]	Reduction of agonist-induced channel activation[d]	
C192S	*Torpedo* receptor expressed in *Xenopus* oocytes		34 (CCh)	NCD	(Mishina et al., 1985)
C193S			66 (CCh)	NCD	
Y190F	BC_3H-1 receptor expressed in *Xenopus* oocytes		77 (ACh)	50	(Tomaselli et al., 1991)
W148F	α7 expressed in *Xenopus* oocytes			92 (ACh); 306 (nicotine)	(Galzi et al., 1991b)
Y92F				12	
Y187F				10	
Y190F	*Torpedo* receptor expressed in *Xenopus* oocytes	20 (curare)[e]		20	(O'Leary et al., 1994)
Y93F				8	
Y93F	mouse receptor expressed in HEK-293 cells		50 (ACh)		(Sine et al., 1994)
Y190F			402 (ACh)		
Y190W		34 (DMT)[f]	43 (CCh)		
Y93W			88 (CCh)		
Y198S		18 (DMT)[f]	270 (CCh)		
Y93S			137 (CCh)		
Y190S		167 (DMT)[f]	485 (CCh)		
Y198T		89 (DMT)[f]	588 (CCh)		
Y93T			164 (CCh)		
Y190T		156 (DMT)[f]	510 (CCh)		
Y198C		36 (DMT)[f]	306 (CCh)		
Y190C			254 (CCh)		
Y198H			882 (CCh)		
Y190H			907 (CCh)		
Y93I			127 (CCh)		
Y190F	*Torpedo* receptor expressed in *Xenopus* oocytes	no effect		20	(O'Leary and White, 1992)
Y190S		no effect		NCD	
Y198S		no effect		30	
Y190C	mouse receptor expressed in *Xenopus* oocytes			NCD	(McLaughlin et al., 1995)
Y198C				~140	
Y190F	mouse receptor expressed in HEK-293 cells		35 and 2 (ACh)[g]	184	(Chen et al., 1995)
Y93F	mouse receptor expressed in *Xenopus* oocytes			18	(Aylwin and White, 1994a)
Y93W				37	
Y93S				28	
Y190F				42	
Y190W				11	
Y190S				NCD	
Y198S				33	
Y198E	mouse $\alpha_2\beta\gamma_2$ expressed in HEK-293 cells	~50 (DMT)			(Fu and Sine, 1994)
Y198C		~15 (DMT)			
Y198S		~45 (DMT)			
Y198T		~45 (DMT)			
Y198R		~500 (DMT)			
D152N	mouse receptor expressed in HEK-293 cells	40 and 7 (DMT)[h]	124 (CCh)		(Sugiyama et al., 1996)
D152Q		162 and 99 (DMT)[h]	31 (CCh)		
D152N/ S154A		79 and 33 (DMT)[h]	28 (CCh)		

(continued on next page)

Table 2 (*continued*)

Mutation	Source of AChR	Pharmacological effect[a]			References
		Reduction of competitive antagonist binding[b]	Reduction of agonist binding[c]	Reduction of agonist-induced channel activation[d]	
D152Q	mouse receptor expressed in HEK-293 cells	37 and 22 (*d*-TC)[i]; 64 and 19 (DMT)[h]	16 (CCh); 16 (SubCh)		(Osaka et al., 1998)
D152Y		68 and 41 (*d*-TC)[i]	44 (CCh)		
G153S	mouse receptor expressed in HEK-293 cells		37 (ACh)[j]		(Sine et al., 1995a)
G152K	α7/5-HT_3 receptor chimera expressed in HEK-293 cells and *Xenopus* oocytes		22 (ACh)[j]; 50 (nicotine)[j]	11[j]	(Corringer et al., 1998)
W54H	α7/5-HT_3 receptor chimera expressed in HEK-293 cells and *Xenopus* oocytes		42 (ACh); 61 (nicotine)	188 (ACh); 47 (nicotine)	(Corringer et al., 1995)
W54A			10 (ACh)	6	
W54F			3 (ACh)	4	

[a] Pharmacological effect corresponds to the pharmacological properties of a ligand elicited on the mutated over the wild AChR. These values are expressed in times the pharmacological effect (fold). The only exception are the values obtained from Mishina et al. (1985) which are expressed in percentage of reduction.
[b] These values were obtained by measuring the inhibition of the initial rate of α-BTx binding elicited by competitive antagonists.
[c] As above for agonists.
[d] These values were obtained by measuring the agonist concentration required for half-maximal current (EC_{50}).
[e] This value was obtained by measuring the half-inhibitory curare concentration (IC_{50}).
[f] These values correspond to reduction of DMT binding to its high-affinity site.
[g] These values correspond to reduction of ACh binding to either the high- or the low-affinity site, respectively.
[h] These values correspond to reduction of DMT binding to either the high- or the low-affinity site, respectively.
[i] These values correspond to reduction of *d*-TC binding to either the high- or the low-affinity site, respectively.
[j] These values correspond to increase of both agonist binding and activation, respectively. NCD, no current detected.

nitude (Sine et al., 1994). Furthermore, a complete agonist insensitivity for channel activation was observed when this aromatic amino acid was replaced by Ser (O'Leary et al., 1994) or by Cys (McLaughlin et al., 1995). Mutations on Y^{93} and Y^{198} to aromatic amino acids showed a lower effect on agonist-induced channel activation than the Y190F mutation (Aylwin and White, 1994a; O'Leary et al., 1994; Tomaselli et al., 1991;). Nevertheless, the mutations on Y^{93} or Y^{198} caused a great effect on competitive antagonist binding (Sine et al., 1994). This effect was also found in receptors with stoichiometry $\alpha_2\beta\gamma_2$ (Fu and Sine, 1994). On the contrary, the Y198F mutation caused an increase in the affinity of curariform drugs (see Table 2). Since this increase in affinity may be due to an increase in the association rate and/or a decrease in the dissociation rate, the time course of recovery of ACh-elicited currents from *d*-TC blockade was studied (O'Leary and White, 1992). The recovery from *d*-TC preincubation in the mutant was found to be slower ($t_{1/2} \approx 65$ s) than the nonmutated AChR ($t_{1/2} \approx 3$–5 s), indicating a reduction in the rate of *d*-TC dissociation from the mutated AChR. The residue charge effect was also evidenced on Y^{198} when it was exchanged by charged amino acids such as Arg or His (Fu and Sine, 1994; Sine et al., 1994). Finally, 140 times higher ACh concentration was necessary for channel activation when Y^{198} was substituted by Cys (McLaughlin et al., 1995). These data suggest that cholinergic ligands interact with Y^{93} by a salt bridge whereas they bind Y^{198} through the aromatic moiety. The importance of the hydroxyl group on Y^{93} and of the aromatic ring on Y^{198} was also evidenced by using the nonsense codon suppression method to incorporate unnatural Tyr and Phe derivatives in intact cells and determining the dose-response relationship on each position by electrophysiological analysis (Nowak et al., 1995).

Practically the same reduction in affinity was described for the neuronal-type homooligomer α7 expressed in *Xenopus* oocytes (Table 2). Mutations on Y^{92}, Y^{187}, or W^{148} (which correspond to Y^{93}, Y^{190}, or W^{149} in the muscle-type AChR) by Phe residues, reduced 10–92 times the ACh EC_{50} (Galzi et al., 1991b). Additionally, this effect was less pronounced (two-fold) by using nicotine, except in the particular case of mutated W^{148} which showed an EC_{50} 300 times higher than that for control. This would indicate that both agonists interact differently with the three residues.

There is no experimental evidence from the site-directed mutagenesis approach confirming the meager labeling of W^{86} by DDF (Galzi et al., 1990) and thus,

supporting the possible contribution of this amino acid to the agonist/competitive antagonist binding sites on the muscle-type AChR. In this regard, recent mutational studies indicated that the residue at position 84 (L^{84} in chick and Q^{84} in rat) on the neuronal-type α7 AChR, which is located at the periphery of loop A, has been implicated in the specificity of piperazinium-derived cholinergic agonists (Vazquez and Oswald, 1999). However, these mutations had moderate effect on the ACh affinity.

In addition, no effect on agonist-induced channel activation was observed when Y^{151}, which was slightly labeled by DDF, was exchanged by Phe (O'Leary et al., 1994). Taking into account that mutation of aromatic amino acids such as Y^{93}, Y^{190}, and Y^{198} to Phe caused a great effect on agonist binding (Table 2), it is possible to suggest that Y^{151} is actually not involved in the agonist/competitive antagonist binding sites. Nevertheless, charge neutralization at the neighboring residue D^{152} markedly reduced agonist, partial agonist, and competitive antagonist affinities (Osaka et al., 1998; Sugiyama et al., 1996) (Table 2). Thus, it seems likely that the anionic residue D^{152}, in addition to other negatively-charged residues of both γ and δ subunits, plays an important role in the stabilization of quaternary ligands by means of long range electrostatic interactions. This idea was corroborated since the mutation to Asp of the homologous residue $\alpha7G^{151}$, which is uncharged, practically does not affect agonist activation (Corringer et al., 1998; Galzi et al., 1991b). The fact that the double mutation G151D/S154K produced no effect, whereas the sum of the effects of both single mutations is expected to display eight-fold decrease in the ACh affinity, suggests that both residue side chains interact each other (Corringer et al., 1998).

The natural mutation α1G153S increases agonist affinity for the resting closed state and prolongs activation episodes by allowing multiple reopenings before ACh can dissociate, suggesting a putative role on agonist binding (Croxen et al., 1997; Sine et al., 1995a). In this regard, the G153S mutation increases the rate of ACh association 17-fold, resulting in a 90 times increase in affinity for one of the two binding sites (Sine et al., 1995a). The substitution α7G152α4K on the α7/5-HT_3R chimera, which is homologous to $\alpha1G^{153}$, increased both ACh and nicotine affinities (Corringer et al., 1998). The use of several α4/α7 chimeras of the NH_2-terminal domain indicated that several segments individually contribute to the marked pharmacological differences existing between the α7 and the α4β2 receptor. In addition to α1G153S, the α1V156M mutation has been also considered to be related to a slow-channel congenital myasthenic syndrome (Croxen et al., 1997; reviewed in Vincent et al., 1997).

An important conclusion based on the preceding data is the significance of aromatic groups in the AChR binding sites for quaternary ammonium ligands such as cholinergic agonists and curariform antagonists. Interestingly, other members of the ligand-gated ion channel superfamily also present aromatic amino acids on their ligand binding sites. For example, F^{159}, Y^{161}, and Y^{202} of the GlyR α1 subunit have been shown to be important for the binding of both agonists (e.g. glycine) and competitive antagonists (e.g. strychnine) (Rajendra et al., 1995a). Additionally, $\alpha1F^{65}$ as well as residues Y^{157}, Y^{159}, and Y^{202} from the β2 subunit have been indicated as being significant determinants of GABA binding (reviewed in Darlison and Albrecht, 1995).

One possible binding mechanism that accounts for the ACh–AChR complex formation includes the interaction of π-electron systems from aromatic amino acids with the cholinium nitrogen from the quaternary compounds (Dougherty and Stauffer, 1990; reviewed in Dougherty, 1996). Recent high-resolution solid-state nuclear magnetic resonance (NMR) studies support this idea (Williamson et al., 1998). This binding force is also shared by other proteins and molecules that bind quaternary ammonium ions, in particular acetylcholinesterase (AChE) (Dougherty and Stauffer, 1990; Sussman et al., 1991; reviewed in Dougherty, 1996). However, spectroscopic evidence suggests that each ligand binding site (one from the AChR and the other from the AChE) presents a different environment (Bolger et al., 1984; reviewed in Arias, 1997). In this regard, the existence of hydrophobic interactions in the formation of AChR-cholinergic drug complexes has been suggested. For example, it has been found that the binding of DMT is stabilized by Y^{190} and Y^{198} residues through both aromatic-quaternary ammonium and hydrophobic interactions (Sine et al., 1994). This evidence also indicates certain Tyr-specificity for both agonists and curariform drugs. Whereas the binding of agonists receives contributions from all three conserved tyrosines with a strong requirement for the aromatic hydroxyl at positions 93 and 190, the binding of DMT only requires Y^{190} and Y^{198} without preference for the aromatic hydroxyl. It has been proposed that the observed residue-specificity may be due to different spatial orientations of both kinds of cholinergic ligands into the binding pocket (Sine et al., 1994).

Interestingly, loops homologous to the AChR have been found on the GlyR, the $GABA_AR$, and the 5-HT_3R as well. In particular, the principal component for the agonist/competitive antagonist binding site at the GlyR α1 subunit is formed by loop A which encompasses the residue I^{111}, by loop B that comprises D^{148} and the sequence F^{159}–G^{160}–Y^{161}, and by loop C which includes amino acids K^{200}, Y^{202}, T^{204}, and probably A^{212} (for a model see Rajendra et al., 1995b and

references therein). Instead, the principal component for GABA binding in the $GABA_AR$ is located on the β2 subunit. At least two homologous loops have been determined in this subunit: loop B which is shaped by the sequence Y^{157}–G^{158}–Y^{159}–T^{160} and loop C that is built by the fragment T^{202}–G^{203}–S^{204}–Y^{205} (mammalian sequence number) (reviewed in Darlison and Albrecht, 1995). Regarding the $5\text{-}HT_3R$, residues E^{106} (Boess et al., 1997) and perhaps W^{67} (Schulte et al., 1995) have been indicated as forming the homologous loop A on the main $5\text{-}HT_3A_L$ subunit (reviewed in Arias, 1999).

In conclusion, the principal component of the ligand binding site on the α1 AChR subunit comprises three amino acid loops, where loop A is mainly formed by residue Y^{93}, loop B is molded by amino acids W^{149}, Y^{152}, and probably G^{153}, and loop C is shaped by residues Y^{190}, C^{192}, C^{193}, and Y^{198} (see Fig. 3).

2.3. Spatial localization of the agonist binding sites

Another approach that has been successfully used to determine the location of the agonist/antagonist binding sites on the AChR is based on FRET measurements. Particularly, FRET between the agonist fluorescent derivative 6-(5-dimethylaminonaphtalene-1-sulfonamido) hexanoic acid-β-(*N*-trimethylammonium) ethyl ester (dansyl-C_6-choline) bound to the AChR and two membrane-partitioned fluorescent probes, octadecylrhodamine B (C_{18}-rhodamine) and 5-(*N*-dodecanoylamino)eosin (C_{12}-eosin), was used to measure the transverse distance between the agonist binding sites and the surface of the lipid membrane (Valenzuela et al., 1994a). Dansyl-C_6-choline, a well characterized ACh fluorescent derivative that binds with a K_d in the nanomolar range to the agonist binding sites (Heidmann and Changeux, 1979; Valenzuela et al., 1994a) was used as an electronic energy donor. The positively charged C_{18}-rhodamine and negatively charged C_{12}-eosin lipid probes were employed as energy acceptors. Both lipid probes are assumed to be located at the water-lipid interface upon partitioning into the membrane, as was experimentally evidenced for C_{18}-rhodamine (Arias et al., 1993). Transverse distances of 31 and 39 Å for C_{12}-eosin and C_{18}-rhodamine, respectively, were calculated by using the Off-Axis FRET model (Yguerabide, 1994).

The basic tenets of the Off-Axis FRET model, which is illustrated in Fig. 4, are as follows. (a) The donor is attached at a distance δ from the major axis of symmetry of a cylindrical protein embedded into a planar–lipid membrane. (b) The symmetry axis of this protein is perpendicular to the membrane surface. (c) R_p is the transverse distance from the protein-bound donor to acceptors positioned in the plane of the water–lipid interface. (d) α is the distance of closest approach between the acceptors and the central axis of the protein in the acceptor plane, and (e) α is greater than or equal to δ.

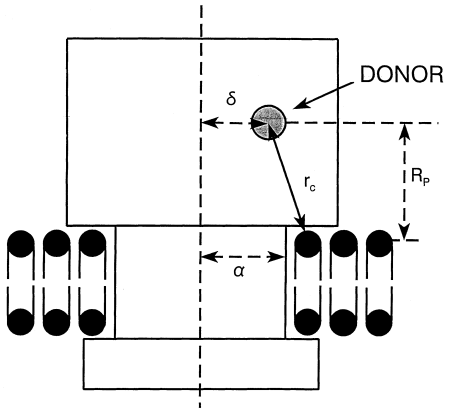

Fig. 4. Schematic representation of the Off-Axis membrane fluorescence resonance energy transfer (FRET) model (modified from Valenzuela et al., 1994a,b; Yguerabide, 1994). r_c is the distance of closest approach between the donor (represented here as a grey circle) and an acceptor (not shown) in the surface of the membrane (the head-groups and the acyl chains of the bilayer-forming lipids are represented here as black circles with two tails). The donor is attached at a distance δ from the major axis of symmetry of a cylindrical protein. Membrane-partitioned acceptors are assumed to be distributed randomly in a planar array at a transverse distance R_p from the plane of the protein-bound donor. α is the distance of closest approach between the acceptor and the central axis of the protein in the acceptor plane and this distance is greater than or equal to δ.

Therefore, given that the receptor protrudes 55–65 Å out of the extracellular side of the membrane (Toyoshima and Unwin 1990; Unwin, 1993), the agonist binding sites are located significantly below the extracellular apex of the AChR (Fig. 5). The finding that the agonist binding sites are located ~35 Å above the membrane surface (Valenzuela et al., 1994a) is consistent with a structural analysis of the AChR at 9 Å resolution (Unwin, 1993), where a pocket approximately at the center of each α-subunit at ~30 Å above the surface of the membrane is shown. The observed distances for the location of the ACh binding sites agree with the ones assumed by Herz et al. (1989) for the steady-state and lifetime FRET measurements between the agonist dansyl-C_6-choline (22–40 Å) or the competitive antagonist bis(choline)-*N*-(4-nitrobenzo-2-oxa-1,3-diazol-7-yl)-iminodiproprionate (BCNI; 21–35 Å) as energy donors and the fluorescent acceptor ethidium bromide as a probe for the high-affinity NCI binding site.

The observed water-filled cavities are formed by three rods running approximately normal to the plane of the bilayer, two of them next to the entrance of the channel and the third, which is tilted radially out-

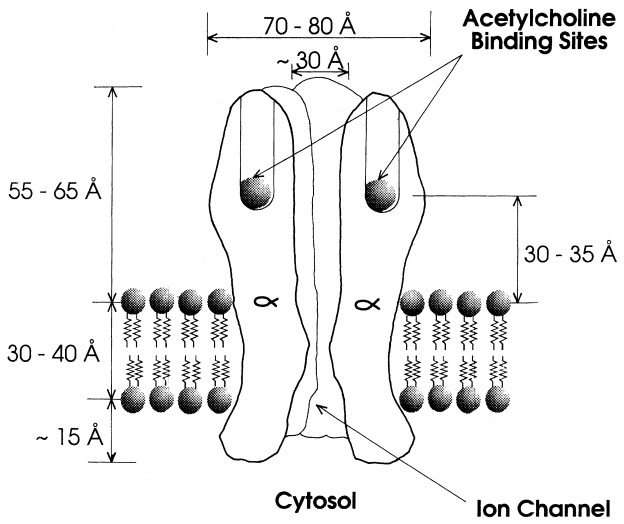

Fig. 5. Transverse schematic representation of the muscle-type AChR showing the possible locations of the acetylcholine binding sites. The value of 30–35 Å corresponds to the transversal distance between the agonist binding site and the membrane surface obtained by using FRET (Valenzuela et al., 1994a) and electron microscopy at 9 Å resolution (Unwin, 1993).

wards, lies outside (Unwin, 1993) (Fig. 6). This direct evidence is in agreement with the observation of Changeux's laboratory indicating three loops in the α subunit as the principal component of the ACh binding region (see photoaffinity evidence described in Table 1 and loops A–C in Fig. 3). The rods twist around each other as in a left-handed coil and are associated with a hollowed-out region on the surface. This cleft may represent a difuseable region for the free access of ACh molecules to their binding sites.

In general, this model resembles that of the binding site for ACh on the AChE, where there is a pocket of about 20 Å located halfway into the enzyme (Sussman et al., 1991). Additionally, the cavity previously found on the α subunit located next to the δ chain has been considered to be functionally important (Unwin, 1995). The hollow, which presumably forms the ACh binding pocket in this particular α subunit, disappeared by the effect of ACh released onto tubular vesicles containing AChRs. More recently, the projection structure of the inactivated AChR at 7.5 Å resolution indicated that the two α subunits, more precisely the putative α-helices encir-

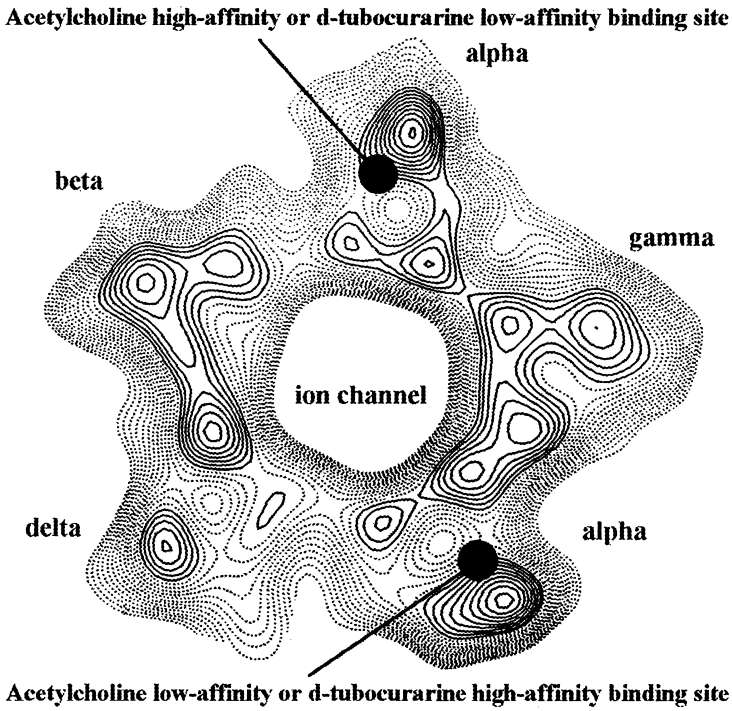

Fig. 6. Normal section of the muscle-type AChR at approximately 30 Å above the membrane surface (modified from Unwin, 1993). There are three density peacks in each subunit arising from three rods running approximately normal to the plane of the section. The black circles indicate the possible localization of the binding sites for the neurotransmitter ACh. The high-affinity ACh binding site (and the low-affinity *d*-TC binding site) is tentatively located in the α subunit with the γ subunit to the right. The low-affinity ACh binding site (and the high-affinity *d*-TC binding site) is tentively located in the α subunit with the γ subunit to the left. Although an αβαγδ arrangement was suggested by Unwin's laboratory (Unwin, 1996 and references therein), the muscle-type AChR subunits are disposed according to Hucho's data (reviewed in Hucho et al., 1996).

cling the assumed agonist cavities, are unequally inclined (Unwin, 1996).

In conclusion, the most probable transverse distance between both agonist binding sites (average) and the lipid membrane surface is 30–35 Å.

3. Secondary component of the binding sites for agonists and competitive antagonists

Two molecules of agonist are required to be bound on the receptor oligomer, one to each α subunit, for channel activation. The binding of agonists to the high-affinity site rapidly activates the AChR, whereas the binding to the low-affinity site abruptly closes the channel following a stimulus (Jackson, 1989). One characteristic of agonist activation is the existence of positive cooperativity (Hill coefficient of 1.5–3.0). This means that upon the proper positioning of one ACh molecule to a first α subunit, the agonist induces certain conformational change on the structure of the receptor that finally enhances the probability for another molecule of ACh to be bound at a second α subunit. Probably, all receptor subunits are involved in the overall conformational change in a concerted manner to permit the binding of two ACh molecules and mediate channel opening.

Evidence that supports the existence of two nonequivalent agonist/competitive antagonist binding sites is the fact that several agonists and competitive antagonists present differences in binding affinities for each specific site (reviewed in Arias, 1997). For instance, distinct agonist binding affinities in *Torpedo* AChR expressed in mouse fibroblasts were revealed by single channel current kinetic studies (Sine et al., 1990). Similar results were also obtained on mouse embryonic AChRs (Zhang et al., 1995).

Since the two α subunits are encoded for by a single gene (e.g. in the mouse the gene coding for both α subunits of the muscle-type AChR are located on chromosome 17) and they are not nearest neighbors on the AChR (reviewed in Changeux and Edelstein, 1998; Hucho et al., 1996; Karlin and Akabas, 1995), the differences in cholinergic binding properties between subunits are probably due to the asymmetric microenvironment surrounding each particular α subunit corresponding to the structural contribution of other non-α subunits.

3.1. Photolabeling and crosslinking evidence

In addition to the experimental evidence indicating the α subunit as the main target labeling site, different cholinergic derivatives labeled both γ and δ receptor-forming subunits in AChR-enriched membranes (reviewed in Arias, 1997). Interestingly, the [^{125}I]azidonicotinoid derivative labeled two (the 66 kDa subunit and, to a lesser extent, the 61 kDa subunit) of the three subunits (the other is the 69 kDa subunit) of the *Drosophila* AChR (Tomizawa and Casida, 1997).

On the basis of photoaffinity labeling experiments, there exists consensus for the preference of certain competitive antagonists such as *d*-TC (Pedersen and Cohen, 1990) and MBTA (Martin and Karlin, 1997) as well as agonists such as nicotine (Middleton and Cohen, 1991) and the derivative BrACh (Dunn et al., 1993) for the αγ interface which displays the low-affinity ACh binding site. It seems that substituents at positions 12′ and 13′ of the phenyl ring and the stereocenter at carbon 1 of the fused ring of *d*-TC (see molecular structure in Fig. 2) are important in discriminating both binding sites (Pedersen and Papineni, 1995). The same basic results were obtained for the 5-HT_3R (Yan et al., 1998). Bipinnatins that belong to the family of lophotoxins (Groebe et al., 1994) prefer the αδ pair which displays the high-affinity ACh binding site. Surprisingly, three azido derivatives of the NCI ethidium labeled both α and γ subunits in a *d*-TC protectable manner, indicating that ethidium preferably binds to the high-affinity *d*-TC locus (Pedersen, 1995). The case of α-conotoxins (α-CoTxs) is special because different toxin subtypes bind with high affinity to distinct subunit interfaces (see Table 6).

On the basis of crosslinking experiments by using *S*-(2-[^{3}H]glycylamidoethyl)dithio-2-pyridine ([^{3}H]GCP) in the presence of 1-ethyl-3-(3′-dimethylamino-propyl)carbodiimide to induce formation of an amide bound between a carboxyl and a primary amine, residues 164–257 of the δ subunit have been identified to cross-react with the α1 subunit (Czajkowski and Karlin, 1991, 1995) (Table 1). In particular, D^{165}, D^{180}, and E^{182} from the δ subunit remained attached by an amide bond to the crosslinking moiety after reduction of the disulfide bond of the α subunit. Taking into consideration the extended conformation of GCP, a distance of ~9 Å was calculated between the cysteamine thio group in the α1 subunit and the glycyl amino group in the δ subunit (Czajkowski and Karlin, 1991, 1995).

Other amino acids than these acidic residues have been shown to be labeled by *d*-TC (Table 2). The primary site of incorporation in the γ subunit is found on W^{55} (see loop E in Fig. 3). While γY^{111} and γY^{117} (see loop F in Fig. 3) incorporated with an efficiency of 5 and 1% from that observed for γW^{55}, respectively (Chiara and Cohen, 1997; Chiara et al., 1999). The γW^{55} residue was also labeled by [^{3}H]nicotine (see loop E in Fig. 3) (Chiara et al., 1998). Interestingly, γL^{109}, the neighbour residue of γY^{117}, was specifically photolabeled with the competitive antagonist [^{3}H]-4-benzoylbenzoylcholine (see loop F in Fig. 3) (Wang et al., 1996).

The homologous counterparts on the δ subunit were also labeled. For instance, δW^{57}, the homologous residue of γW^{55}, was labeled with relatively high efficiency (Chiara and Cohen, 1997). In addition, the positive charge of δR^{113}, the homologous residue of γY^{111}, seems to be one of the structural causes that account for the observed *d*-TC selectivity on *Torpedo* AChR. These and other structural studies suggest that the region comprising residues 108–120 presents an antiparallel β-sheet orientation with a γ-turn around the highly conserved residue G^{114} with the side chains of amino acids L^{109}, Y^{111}, S^{115}, Y^{117}, and L^{119} from the *Torpedo* γ subunit (and their homologous on the δ and ϵ subunits) facing the subunit interfaces that bear the agonist binding sites (Chiara et al., 1999 and references therein).

The above data indicate that: (1) different ligands bind with distinct specificity to either the αδ or the αγ subunit interface; and (2) the amino acid W^{55} is forming loop E whereas residues L^{109}, Y^{111}, S^{115}, Y^{117}, and L^{119} are constituting loop F (see Fig. 3).

3.2. Expression of AChRs containing different subunit compositions and site-directed mutated subunits

The expression of AChR pentamers with different subunit composition made it possible to account for the two affinities seen in native subunit composition. By cell coexpression of mouse αγ, αδ, or αβ pairs, complexes formed either by δ or γ, but not by β, with the α subunit, were detected (Blount and Merlie, 1989). The presence of the α subunit in the cell is not sufficient by itself to bind CCh and *d*-TC (Blount and Merlie, 1988). However, αδ and αγ complexes can bind agonists such as CCh and epibatidine (an alkaloid originally isolated from the skin of the Ecuadorian poison arrow frog *Epipedobates tricolor*; see molecular structure in Fig. 2) as well as competitive antagonists such as *d*-TC and α-toxins (Blount and Merlie, 1989; Gershoni et al., 1983; Gu et al., 1991; Pedersen and Cohen, 1990; Sine, 1993; Sine and Claudio, 1991). This is in agreement with the observed 1000 to 10,000 times lower affinity of α-BTx to isolated *Torpedo* α subunits than to native AChRs (Gershoni et al., 1983). In the same context, by expressing chimeric subunits in HEK-293 cells in the presence of wild-type chains, the sequence 21–131 of the γ subunit (and not homologue residues on the β subunit) was found to be sufficient for association with its respective neighboring α subunit and to form agonist-displaceable toxin binding sites (Kreienkamp et al., 1995). These studies indicated that the αγ and αδ pairs present high and low affinity for *d*-TC and low and high affinity for ACh, respectively (Blount and Merlie, 1989) (Figs. 3 and 6). The αβγ- and αβδ-containing receptors bind *d*-TC with high and low affinities, respectively, which is opposite to the case of lophotoxin binding (Sine and Claudio, 1991). Interestingly, epibatidine, a very potent analgesic, was found to preferably bind to the αγ or the αϵ subunit interface when the receptor is in the desensitized state (Prince and Sine, 1998a). In contrast to epibatidine selectivity, CCh was shown to display little site selectivity for desensitized fetal or adult AChRs. Thus, further studies using epibatidine as a probe for the agonist binding site might yield important evidence for the elements that confer state-dependent selectivities of the binding sites.

Coexpressing several δγ chimeras of different length with both α and β subunits, and by comparing the binding properties of the curariform drug DMT on $\alpha_2\beta\gamma_2$ and $\alpha_2\beta\delta_2$ AChRs, Sine's laboratory at Mayo Clinic (Rochester, Minnesota, USA) found that homologous residues of δ and γ subunits are responsible for the ~100 times decrement in curare affinity (Sine, 1993; reviewed in Prince and Sine, 1998b). These extracellular sites are flanking a disulfide loop formed by C^{132}–C^{148} which is found throughout the ligand-gated ion channel superfamily (Le Novère and Changeux, 1995; Ortells and Lunt, 1996) (see Fig. 1(A)) but which does not structurally participate in the neurotransmitter binding site (Amin et al., 1994; Criado et al., 1986).

In the predisulfide region of the γ and δ subunits, residues γY^{116} and γY^{117} (see loop F in Fig. 3), in addition to amino acids δV^{118} and δT^{119} have been shown to be responsible for curare selectivity (Sine, 1993). In addition, only one amino acid was found in the postdisulfide region (S^{161} in the γ subunit, and K^{163} in the δ subunit). However, these latter residues appear to interact with DMT allosterically (Fu and Sine, 1994).

The studies developed by Sine's laboratory using a combination of chimeric and site-directed mutated receptors helped to elucidate the structural components that interact with cholinergic ligands (reviewed in Prince and Sine, 1998b). Exchanging the residues of the γ subunit with the corresponding δ residues one at each time, the importance of γY^{117} for DMT binding was evidenced. For instance, different mutations enhanced (Fu and Sine, 1994) or diminished (Sine, 1997) the affinity of DMT (Table 3). The highest effect was observed on Arg, probably by the repulsion elicited between the positively charged guanidinium side chain and the quaternary ammonium group of DMT. These data are consistent with a model where, in addition to the stabilization of one of the quaternary ammonium groups of DMT by Y^{198} from the α1 subunit, the second quaternary nitrogen of DMT is more tightly associated with the γ subunit by means of Y^{117}. In this context, the effect of αY^{198} mutations on DMT site-specificity may arise from changes in the α1 subunit that affect the bridging of the drug to the other δ and γ subunits (Sine et al., 1994).

Table 3
Residue mutations on non-α subunits that affect the binding of both agonists and competitive antagonists as well as agonist gating

Mutation	Source of AChR	Times the pharmacological effect			Reference
		Reduction of competitive antagonist binding[a]	Reduction of agonist binding[b]	Reduction of agonist-induced channel activation[c]	
γ Subunit					
F172δI178	mouse $\alpha_2\beta\gamma_2$ receptor expressed in HEK-293 cells	16[d] (α-CoTx M1)			(Sine et al., 1995b)
S111δY113		60[d] (α-CoTx M1)			
K34δS36/F172δI178		45[d] (α-CoTx M1)			
K34δS36/S111δY113/F172δI178		~ 1000[d] (α-CoTx M1)			
K34δS36/F172δI178	human αγ subunits expressed in HEK-293 cells		9 (CCh)[d]		(Prince and Sine, 1996)
K34δS36/C115δY117/F12δI178			13 (CCh)[d]		
K34δS36/S129δP131/F172δI178			10 (CCh)[d]		
K34δS36/F172δI178	mouse receptor expressed in HEK-293 cells		11 (CCh)[d]		(Prince and Sine, 1996)
W55L	*Torpedo* receptor expressed in *Xenopus* oocytes	8 (*d*-TC)[e]		7	(O'Leary et al., 1994)
Y117δT119	mouse $\alpha_2\beta\gamma_2$ receptor expressed in HEK-293 cells	~ 16 (DMT)			(Sine, 1993)
Y117δT119/S161δK163		~ 56 (DMT)			
Y117T	mouse $\alpha_2\beta\gamma_2$ receptor expressed in HEK-293 cells	~ 25 (DMT)			(Fu and Sine, 1994)
Y117I		~ 10 (DMT)			
Y117R		~ 250 (DMT)			
Y111δR113	*Torpedo* receptor expressed in *Xenopus* oocytes	11 (*d*-TC)[e]; 11, 4 (*d*-TC)[f]			(Chiara et al., 1999)
L119K	mouse receptor expressed in HEK-293 cells	1085 (DMT)[g]			(Sine, 1997)
D174N	mouse receptor expressed in *Xenopus* oocytes		26 (ACh)[h]	6 (ACh)	(Martin et al., 1996)
D174N	mouse $\alpha_2\beta\gamma_2$ receptor expressed in *Xenopus* oocytes	10 (*d*-TC)[g]	167 (ACh)		
D174N	mouse $\alpha_2\beta\gamma_2$ receptor expressed in HEK-293 cells	7 (*d*-TC)[g]	85 (CCh)		(Osaka et al., 1998)
D174N/δD180N	mouse $\alpha_2\beta\gamma\delta$ receptor expressed in HEK-293 cells	5, 3 (*d*-TC)[f]	120 (CCh)		
D174N/δD180N		4, 4 (DMT)[f]	130 (SubCh)		

Table 3 (*continued*)

Mutation	Source of AChR	Times the pharmacological effect			Reference
		Reduction of competitive antagonist binding[a]	Reduction of agonist binding[b]	Reduction of agonist-induced channel activation[c]	
D174T	mouse $\alpha_2\beta\gamma_2$ receptor expressed in *Xenopus* oocytes	2 (*d*-TC)	30 (ACh)		(Martin and Karlin, 1997)
D174C		16 (*d*-TC)	42 (ACh)		
D174V		18 (*d*-TC)	48 (ACh)		
D174A		18 (*d*-TC)	89 (ACh)		
D174N		10 (*d*-TC)	117 (ACh)		
D174K		29 (*d*-TC)	197 (ACh)		
D174Y		10 (*d*-TC)	616 (ACh)		
D174H		6 (*d*-TC)	no effect		
D174E/δD180E	mouse $\alpha_2\beta\gamma\delta$ receptor expressed in *Xenopus* oocytes			22 (ACh)	
D174T/δD180T				61 (ACh)	
D174A/δD180A				64 (ACh)	
D174C/δD180C				72 (ACh)	
D174N/δD180N				137 (ACh)	
D174H/δD180H				140 (ACh)	
D174V/δD180V				146 (ACh)	
D174K/δD180K				656 (ACh)	
ϵ *Subunit*					
I58δH60	mouse $\alpha_2\beta\epsilon\delta$ receptor expressed in HEK-293 cells	17 (DMT)[g]			(Bren and Sine, 1997)
D59δA61		25 (DMT)[g]			
I58δH60/D59δA61		47 (DMT)[g]			
S117R		42 (DMT)[g]			
L119K	mouse $\alpha_2\beta\epsilon\delta$ receptor expressed in HEK-293 cells	12 (DMT)[g]			(Sine, 1997)
D175N	mouse $\alpha_2\beta\epsilon\delta$ receptor expressed in HEK-293 cells			8 (ACh)[i]	(Zhang et al., 1995)
P121L	human receptor expressed in HEK-293 cells		66 (ACh)[j]	41 (ACh)[i]	(Ohno et al., 1996)
δ *Subunit*					
S36γK34	mouse $\alpha_2\beta\delta_2$ receptor expressed in HEK-293 cells	5 (α-CoTx M1)			(Sine et al., 1995b)
S36γK34/I178γF172		~1000 (α-CoTx M1)			
S36γK34/I178γF172	human αγ subunits expressed in HEK-293 cells		50 (CCh)		(Prince and Sine, 1996)
S36γK34/D59γE57/I178γF172			20 (CCh)		
S36γK34/Y117γC115/I178γF172		54 (CCh)			
S36γK34/P131γS129/I178γF172		54 (CCh)			
S36γK34/D59γE57/Y117γC115/I178γF172		26 (CCh)			

(continued on next page)

Table 3 (*continued*)

Mutation	Source of AChR	Times the pharmacological effect			Reference
		Reduction of competitive antagonist binding[a]	Reduction of agonist binding[b]	Reduction of agonist-induced channel activation[c]	
S36γK34/I178γF172	mouse $\alpha_2\beta\delta_2$ receptor expressed in HEK-293 cells		8 (CCh)		(Prince and Sine, 1996)
S36γK34/D59γE57/I178γF172			4 (CCh)		
S36γK34/Y117γC115/I178γF172		6 (CCh)			
S36γK34/D59γE57/Y117γC115/I178γF172			5 (CCh)		
L121K	mouse $\alpha_2\beta\epsilon\delta$ receptor expressed in HEK-293 cells	43 (DMT)[k]			(Sine, 1997)
D180N	mouse $\alpha_2\beta\delta_2$ receptor expressed in *Xenopus* oocytes	2 (*d*-TC)[k]	200 (ACh)	84 (ACh)	(Czajkowski et al., 1993; Martin et al., 1996)
E189Q		no effect	7 (ACh)	13 (ACh)	
D180N	mouse $\alpha_2\beta\gamma\delta$ receptor expressed in *Xenopus* oocytes			2 (ACh)	(Martin and Karlin, 1997)
D180N	mouse $\alpha_2\beta\delta_2$ receptor expressed in HEK-293 cells			84 (ACh)	
D180N	mouse $\alpha_2\beta\delta_2$ receptor expressed in HEK-293 cells	no effect	74 (CCh)		(Osaka et al., 1998)
D180N	mouse $\alpha_2\beta\delta_2$ receptor expressed in *Xenopus* oocytes	2 (*d*-TC)	248 (CCh)		(Martin and Karlin, 1997)
D180C		3 (*d*-TC)	294 (CCh)		
D180A		6 (*d*-TC)	402 (CCh)		
D180H		no effect	484 (CCh)		
D180V		4 (*d*-TC)	832 (CCh)		
D180T		5 (*d*-TC)	1016 (CCh)		
D180K		16 (*d*-TC)	3712 (CCh)		

[a] These values were obtained measuring the inhibition of the initial rate of α-BTx binding elicited by competitive antagonists.
[b] As above for agonists.
[c] These values were obtained measuring the agonist concentration required for half-maximal current (EC_{50}).
[d] In these cases an enhancement of ligand binding is observed.
[e] This value was obtained measuring the inhibition of *d*-TC on the currents elicited by ACh (IC_{50}).
[f] The observed competitive antagonist binding inhibition corresponds to the high- (αγ) and the low-affinity (αδ) site, respectively.
[g] The observed competitive antagonist binding inhibition is restricted to the high-affinity (αε or αγ) site.
[h] The observed ACh binding inhibition is restricted to the low-affinity (αγ) site.
[i] The observed effect on the dissociation constant for ACh binding to the opening state was calculated by using kinetic parameters.
[j] The observed ACh binding inhibition is restricted to the low-affinity (αε) site when the receptor is in the desensitized state.
[k] The observed competitive antagonist binding inhibition is restricted to the low-affinity (αδ) site.

Interestingly, Tyr residues in a position homologous to γY^{117} on the muscle-type AChR were found in several subunits of other neurotransmitter-gated ion channel receptors, suggesting the existence of a structural motif for the binding site of different ligands. However, when ϵS^{117}, the homologous residue of γY^{117}, was exchanged by different residues on the adult receptor, a small effect on DMT binding was found (Bren and Sine, 1997). Although the εS117R mutation produced the highest decrease in the K_d for DMT (10-

fold), the extent of this effect is not comparable with the effect elicited by the γY117R mutation (~250-fold; Table 3) (Fu and Sine, 1994). Thus, ϵS^{117} is probably close to the DMT binding site of the mature AChR but it does not provide high affinity for DMT.

The residue γY^{111} has been considered to be important for *d*-TC binding but not for ACh binding (Chiara et al., 1999) (Table 3). Interestingly, amino acids $\gamma C^{115}/\delta Y^{117}$, which are positioned on the primary sequence two residues before the pair $\gamma Y^{117}/\delta T^{119}$, have been considered as secondary determinants for CCh selectivity by means of site-directed mutagenesis studies on chimeric receptors (Table 3) (Prince and Sine, 1998a).

The natural mutation ϵP121L, which is also found at the predisulfide region, was detected to reduce the affinity of one of the two binding sites for ACh, presumably the αϵ subunit interface, when the AChR is either in the open or in the desensitized state (Ohno et al., 1996). Considering that P^{121} is conserved in the γ subunit, it is probable that this residue is involved in the low-affinity ACh binding site.

The question of whether the contribution of non-α subunits in neuronal AChRs is or not important for ligand specificity has been presently answered by taking into account the relative sensitivity of cholinergic ligands on receptors containing different subunits. For example, β4-containing AChRs generally present larger responses to the ganglionic stimulants such as nicotine and cytisine (an alkaloid extracted from the seeds of *Cytisus laburnum*; see molecular structure in Fig. 2) than β2-containing AChR subtypes (Wheeler et al., 1993), whereas the opposite is true for ACh (Cohen et al., 1995). In addition, α3β2 receptors are more sensitive to blockade by dihydro-β-erythroidine (DHβE) and κ-bungarotoxin (κ-BTx) than the α2β4 complex (Harvey and Luetje, 1996). In this regard, chimeras where the ligand-sensitive sequence segment of one subunit is replaced by another (e.g. the α4 subunit with β4/β2 chimeras consisting of COOH- or NH_2-terminal sequences of appropriate lengths from β2 and β4, respectively) were constructed, then expressed in *Xenopus* oocytes, and subsequently studied by pharmacological methods. The results indicated that the region of β4 and β2 that contributes to agonist and competitive antagonist selectivity as well as neurotoxin inhibition is localized at residues 1–80 from the NH_2-terminal (Harvey and Luetje, 1996; Papke et al., 1993). Particularly, the major determinant of specificity for both DHβE and κ-BTx is located between residues 56 and 63 (Harvey and Luetje, 1996). The fact that the mutation $\beta 2T^{59} \rightarrow \beta 4K^{59}$ decreased both DHβE (ninefold) and κ-BTx (71-fold) sensitivity supports the conjecture that this residue is the primary element that modulates the observed differences in competitive antagonist susceptibility between β2- and β4-containing neuronal receptors. Additionally, a minor determinant is observed on sequence 1–54 for both competitive antagonists, and between residues 74–80 for the particular case of κ-BTx (Harvey and Luetje, 1996). However, the significance of these components is uncertain.

Based on this kind of studies it was also possible to discriminate residues within sequence 1–120 in the extracellular NH_2-terminal of the β2 subunit as responsible for the relative ACh selectivity (Cohen et al., 1995; Figl et al., 1992). For example, substituting sequence 104–120 from the β2 subunit for sequence 106–122 from the β4 chain, reduced the EC_{50}s but did not restore the β4-like values (Figl et al., 1992). Interestingly, residues I^{118} and F^{119} both found within sequence 104–120 of the neuronal β2 subunit are homologous to residues γI^{116} and γY^{117} which are considered to be important for DMT binding (Sine, 1993) (Table 3 and Fig. 3). In addition, residues γS^{111} and γY^{117}, homologous to $\beta 2S^{113}$ and $\beta 2F^{119}$ within the sequence 104–120, were found to be labeled with *d*-TC (Chiara and Cohen, 1997; Chiara et al., 1999) (Table 1). In this regard, it is plausible that sequence 104–120 from the β2 subunit contributes to a ligand binding site on neuronal AChRs. From the physiological point of view, studies with β2 subunit-knockout mice indicated that this subunit is implicated in the behavioral effect of nicotine (Picciotto et al., 1995, 1997).

In conclusion, both the γ and the δ subunit from muscle-type AChRs as well as different β subunits from neuronal-type AChRs bear several residues (complementary component) involved in the interaction of distinct cholinergic ligands with the AChR.

3.3. Evidence from the site-directed mutagenesis approach

The suggested participation of γW^{55} and δW^{57} in additional interactions for the stabilization of *d*-TC (Chiara and Cohen, 1997) or nicotine (Chiara et al., 1998) with the AChR has received experimental support (O'Leary et al., 1994) (see Table 2). These Trp residues were substituted for Leu, which maintains a large hydrophobic group but without the aromatic character. The γW55L mutation resulted in an 8.3-fold decrease in *d*-TC affinity (Table 3). The exchange of δW^{57} for Leu did not affect *d*-TC binding which is consistent with the fact that the δ chain is related to the low-affinity *d*-TC binding site. Concomitantly, the ACh half-maximal activation (EC_{50}) value changed from 136.7 ± 7.4 μM in the γW55L mutated AChR to 20.3 ± 0.4 μM in the wild AChR, while this latter value was not changed by the δW57L mutation. These findings support the previous evidence indicating the αγ interface as the high-affinity binding site for *d*-TC.

The importance of W^{54} for ligand binding on the α7

neuronal-subtype AChR, which is homologous to residues δW^{57} and γW^{55} from the muscle-type AChR, was also demonstrated (Corringer et al., 1995). The residue W^{54} was mutated to Phe, Ala, or His, on the α7/5-HT_3R chimera (Eiselé et al., 1993). These mutations diminished both the affinity and the pharmacological response of agonists such as ACh and nicotine (see Table 2) as well as the antagonist DHβE, whereas α-BTx binding kinetic constants were not affected.

Homologous residues of γW^{55} and δW^{57} on other receptor members of the ligand-gated ion channel superfamily may be also important for the agonist binding site formation. For example, exchanging F^{64} for Leu on the α1 subunit of the α1β2γ2 $GABA_AR$, a 200-fold decrease in agonist sensitivity was observed (Sigel et al., 1992). Homologous mutations on the other subunits did not show the same effect. However, mutation on F^{77} from the γ2 subunit altered the binding of benzodiazepine ligands (Buhr et al., 1997). In addition, the residue I^{121} from the α1 subunit is a determinant of GABA binding and gating. This residue aligns with *Torpedo* γV^{110} which is close to γY^{111}. Regarding the 5-HT_3R, mutations on W^{89} markedly diminished the affinity of the competitive antagonist curare, whereas the affinity of the agonist 5-HT was reduced by substituting only R^{91} (Yan et al., 1999). The affinity of the competitive antagonist granisetron was also reduced by the same mutations in addition to the Y^{93} exchange.

Other neighbor amino acids to the pair $\delta W^{57}/\gamma W^{55}$ have also been considered to be involved in the DMT binding sites from the adult mouse AChR (Bren and Sine, 1997). Exchange of one ($I^{58} \rightarrow H^{60}$ or $D^{59} \rightarrow A^{61}$) or two ($I^{58}/D^{59} \rightarrow H^{60}/A^{61}$) residues from the ϵ subunit with the equivalent amino acids on the δ chain decreased the apparent K_d of DMT only on the high (αϵ) binding site (Table 3). The double mutation on residues from the γ subunit ($M^{58}/Q^{59} \rightarrow \delta H^{60}/A^{61}$), which are equivalent to the ones previously exchanged in the ϵ chain, does not affect DMT affinity. This indicates that these determinants are not essential for the binding of DMT to the high-affinity αγ interface. In conclusion, one of the two quaternary DMT ammonium groups may electrostatically interact with ϵD^{59} and/or ϵI^{58}. The fact that the equivalent position of γY^{117} (the residue that interacts with one of the two DMT ammonium groups) on the ϵ subunit is occupied by Ser supports such possibility. Depending on the environmental pH, His may be positively charged and thus, electrostatic repulsion between His and DMT in its low-affinity binding site may exist.

In addition to $\gamma C^{115}/\delta Y^{117}$ (loop F in Fig. 3), amino acids $\gamma E^{57}/\delta D^{59}$ (loop E in Fig. 3), which are positioned two residues following the pair $\gamma W^{55}/\delta W^{57}$, have been considered to be secondary determinants for CCh selectivity (see Table 3) (Prince and Sine, 1998a). The importance of $\alpha 7Q^{56}$, the homologous residue of pair $\gamma E^{57}/\delta D^{59}$, in ligand binding was also corroborated since the mutation of this specific residue, but neither M^{57} or Y^{58}, decreased ACh and nicotine affinities two to four times (Corringer et al., 1995). In addition to pairs $\gamma E^{57}/\delta D^{59}$ and $\gamma C^{115}/\delta Y^{117}$, a primary set of determinants of agonist selectivity comprising pairs $\gamma K^{34}/\delta S^{36}$ (loop D in Fig. 3) and $\gamma F^{172}/\delta I^{178}$ (loop G in Fig. 3) has been detected (Prince and Sine, 1998a) (Table 3). The region between residues 118 and 171 of the δ subunit does not contain major determinant of agonist selectivity. Furthermore, the agonist selectivity was found to depend on the receptor conformational state: whereas pairs $\gamma K^{34}/\delta S^{36}$ and $\gamma F^{172}/\delta I^{178}$ contribute with agonist selectivity when the AChR is in the resting state, γE^{57} is responsible for the selectivity on desensitized receptors (Prince and Sine, 1998a). Interestingly, similar high affinity and degree of selectivity were observed for the αδ subunit interface in human receptors. The position 36 on the human δ subunit is replaced by Ala. Thus, the CCh affinity change conferred by the mutual exchange of γK^{34} and δS^{36} seems to be more likely produced by steric occlusion or/and electrostatic repulsion from the positively charged Lys than by polar interaction with the hydroxyl group of Ser.

In an attempt to demonstrate whether the aspartates and the glutamates found in the 164–224 residue segment of the mouse muscle δ and γ subunits contribute to agonist binding, each amino acid was site-directed mutated and the receptor expressed in *Xenopus* oocytes (Table 3). When δD^{180} and δE^{189} were, respectively, mutated to Asn and Gln, an enhancement of 84 and 15 times the ACh EC_{50} in αβδ-containing oocytes, and a 200 and seven times lesser ACh affinity than the non-mutated was found (Czajkowski et al., 1993) (Table 3). Other exhaustive mutational analyses indicated that both δD^{180} and γD^{174} are involved in agonist binding (see Table 3) (Martin and Karlin, 1997; Martin et al., 1996; Osaka et al., 1999). The highest effects (ACh and *d*-TC binding decrease) where found on mutations that exchange the side chain charge (from a positive to a negative charge; i.e. D174K and D180K) (Martin and Karlin, 1997). An eight-fold increase in ACh EC_{50} was observed when the homologous residue ϵD^{175} was mutated to Asn (Zhang et al., 1995). Most of this effect seems to be accounted for by a decrease in the channel opening rate. Results from mutational studies also suggest that the charged residues $\gamma D^{174}/\delta D^{180}$ and αD^{152} confer independent, noninteracting electrostatic contributions to the cholinergic agonist binding sites (Osaka et al., 1999).

The same mutations diminished the binding of competitive antagonists such as *d*-TC, hexamethonium, and DHβE, but to a lesser extent than that found for agonists (Martin and Karlin, 1997; Martin et al., 1996;

Osaka et al., 1999). This difference may be ascribed to distinct points of contact of agonists and competitive antagonists within overlapping loci. Another explanation, is that a dominant part of the mutational effects are on isomerization steps elicited upon agonist binding but not upon antagonist binding (Martin and Karlin, 1997). Mutations to Gln on each Glu or Asp residue located at different positions on both δ and γ subunits only decreased ACh-induced current by approximately two to five times, and mutations δE166Q, γE183Q, δD202N, or δD208N, practically made no change (Czajkowski et al., 1993).

Concerning ACh selectivity, the involved determinants on the δ subunit comprise a primary set of components including residues S^{36} (which is located on a region homologous to loop D), D^{59} (which is located on a region homologous to loop E), Y^{178}, D^{180}, and E^{189} (which are located on a region homologous to loop G), and a secondary set of determinants comprising residues Y^{117} and P^{121} (which are located on a region homologous to loop F). Thus, both ACh and curare share at least loops E and F.

The final conclusion is that although each cholinergic ligand binds to different AChR residues, these residues are forming an overlapping domain at the α/non-α subunit interface that account for their pharmacological activity. In this regard, the complementary component at the γ subunit is probably formed by four loops: loop D (K^{34}), loop E (W^{55} and E^{57}), loop F (L^{109}, S^{111}, C^{115}, I^{116}, and Y^{117}), and loop G (F^{172}, D^{174}, and E^{183}).

3.4. Interfacial ligand-binding model

Based on the above results and taking into consideration: (a) that residues identical to D^{180} and E^{189} in the δ subunit are also present in α, ϵ, and γ (i.e. D^{174} and E^{183}, respectively) subunits, but not in the β subunit, (b) that the tertiary structure of all subunits are very similar, and (c) the existence of a quasi-fivefold symmetry for the pentameric complex, Karlin's laboratory at Columbia University (New York, USA) developed a model where the positively charged ACh ammonium group electrostatically interacts with δD^{180} or γD^{174} (or ϵD^{175}) (see loop G in Fig. 3) at either the high- or the low-affinity binding site (Czajkowski and Karlin, 1991, 1995; Czajkowski et al., 1993; Martin and Karlin, 1997; Martin et al., 1996; reviewed in Karlin and Akabas, 1995). In this regard, two to three charges and an effective electrostatic potential of about −30 mV were calculated to exist in the ACh locus (Stauffer and Karlin, 1994). However, a potential of -15 ± 3 mV at one of the agonist binding sites was obtained using a MBTA nitroxide analogue and continuous wave power saturation electron paramagnetic resonance (EPR) spectroscopy (Addona et al., 1997). Regardless of the absolute value, the observed potential at the ligand binding site may account for long-range electrostatic interactions with the quaternary ammonium group of ACh.

Regarding neuronal AChRs, acidic side residues are lacking in non-α subunits. Thus, they do not posses the electronegative subsite found in muscle-type AChR δ and γ subunits to complement the positive charge carried by the quaternary amine present in cholinergic agonists. In the special case of neuronal-type α subunits capable of forming homooligomeric AChRs such as α7, α8, and α9, the putative disposition of the agonist/competitive antagonist binding site at the α/α subunit interface would implicate that both the principal and the complementary component showed in Fig. 3 for the muscle-type AChR is carried by the same α7 (or α8 or α9) subunit (see Fig. 1(C)).

Karlin and his group also postulated that, upon ACh binding to the α subunit, the negatively charged residue Asp from each δ, or γ (or ϵ) subunit, moves closer to the agonist quaternary group. In turn, this movement may conduct other residues into more advantageous positions enhancing the interaction of the agonist molecule with its site. Finally, this contraction could impel the sliding of neighboring chains, propagating the structural changes from the extracellular domain across the transmembrane portion to the gate which is close to the cytoplasmic end of the ion channel (Pascual and Karlin, 1998; Wilson and Karlin, 1998).

The interfacial location for cholinergic ligands on the AChR is consistent with the extracellular model of the muscle-type AChR developed by Taylor and coworkers at the University of California (San Diego, USA) using sequence homology with copper binding proteins, plastocyanin, and pseudoazurin, together with data from mutagenesis and labeling studies (Tsigelny et al., 1997). An interesting concept is that equivalent residues in the linear sequence of each subunit map the same spatial position at one of the two faces of the subunit. Thus, the ligand binding site at the subunit interface is formed by a positive (+) face (also called counterclockwise face) provided by the α subunit and a negative (−) face (also called clockwise face) provided by the non-α chain (δ, ϵ, or γ) (see Fig. 3) (see Machold et al., 1995a; Sine et al., 1995b). These (interfacial) models are not strictly consistent with that proposed by Unwin at the MRC Laboratory of Molecular Biology (Cambridge, UK), where the binding site for agonists are topologically localized in pockets, one on each α subunit, and there is no evidence for these pockets to be located at any subunit interface (Unwin, 1993). However, a model of the extracellular portion based on novel secondary structure predictions where the pentameric arrangement is not rod-shaped but more flattened allows the agonist binding sites to

be placed at the interfaces between two subunits (Le Novère et al., 1999). In addition, a distinct conformation for each α subunits was observed on nonactivated *Torpedo* AChRs at 7.5 Å resolution (Unwin, 1996). The rods encircling the cavities where the agonist binding sites have been putatively located are tilted at different degrees with respect to the major axis of symmetry of the AChR.

The most probable location of cholinergic ligands is at the α/non-α subunit interface of AChRs.

4. α-Neurotoxin binding sites

4.1. Snake neurotoxins

The family of toxins from the snake venom of *Elapidae* and *Hydrophidae* species are important competitive antagonists of both muscle- and neuronal-type AChRs. To date, approximately 100 α-neurotoxins and 4 κ-toxins have been isolated and sequenced. α-Neurotoxins are polypeptides with molecular weights ranging from 7 to 8 kDa that bind quasi-irreversibly to the muscle-type AChR with K_ds between 10 pM and 1 nM (reviewed in Endo and Tamiya, 1991). Depending on the number of amino acids, these toxins can be classified as long or short α-neurotoxins. Short α-neurotoxins contain 60–62 amino acids and four disulfide bridges in common positions. Fig. 7 shows a scheme of the tertiary structure of the short α-neurotoxin from *Naja mossambica mossambica*. Long α-neurotoxins are formed by 66–74 residues and contain another fifth disulfide bond. Long toxins associate and dissociate much more slowly than short α-neurotoxins. In the muscle-type AChR (in addition to α7, α8, and α9 neuronal subtypes), the most profusely used long α-neurotoxin is the α-BTx. κ-Neurotoxins are designed by 66 amino acids which contain five disulfide bonds. In the α3- or α4-containing neuronal-subtypes, the most widely employed is the κ-BTx (reviewed in Chiappinelli et al., 1996). Both α- and κ-BTxs are obtained from fractioning the venom of the Taiwanese krait *Bungarus multicinctus*. Analysis of the three-dimensional structure has revealed that α-neurotoxins are relatively flat molecules with three loops (I, II, and III; see Fig. 7) forming a large β-pleated sheet which protrudes from a hydrophobic core stabilized by four or five disulfide bridges.

Early studies by using electron microscopy techniques evidenced that α-BTx binds to two sites (Bon et al., 1984; Holtzman et al., 1982) on the top or outer perimeter of the protein (Fairclough et al., 1983). The photolabeling approach has been useful to obtain more information on the exact localization of the α-neurotoxin binding sites on the AChR. Depending on the type of neurotoxin, on the kind of crosslinker

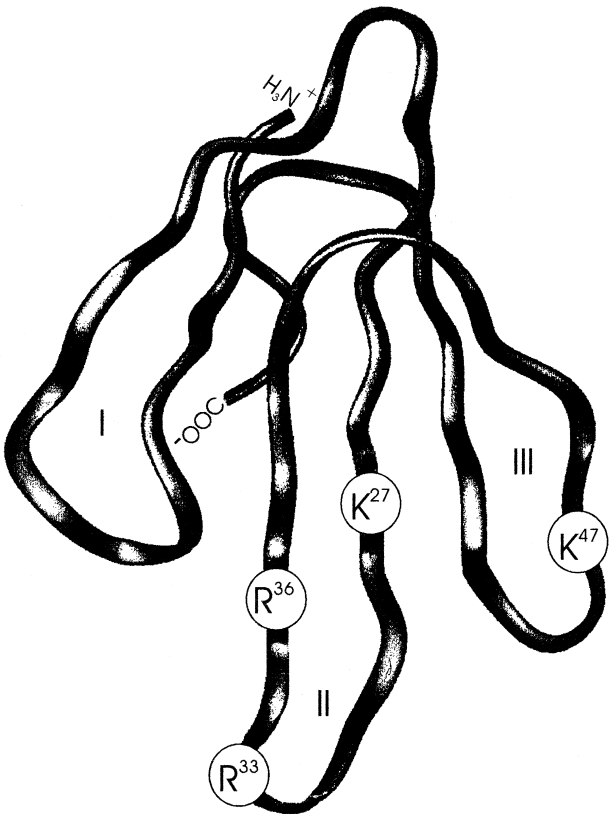

Fig. 7. Scheme of the tertiary structure of the α-neurotoxin from *N. mossambica mossambica* (taken from Osaka et al., 1999). The concave face of the toxin is facing the viewer. The localization of the mutated residues are also included. Residue R^{33} is near the tip of loop II, whereas K^{27} is closer to the top and opposite side of loop II. Amino acid R^{36} is on loop II, whereas K^{47} is located on an exposed surface of loop III.

group (e.g. size, reactivity. etc.), and on the location of the reacting group in the toxin molecule, different subunits were labeled. Table 4 summarizes the updated information obtained by means of the photolabeling approach. All subunits were labeled, albeit to different extent, by using different α-neurotoxin derivatives. The α1 subunit was mainly labeled by using α-neurotoxin derivatives from *N. naja oxiana* with the photoactivatable group attached at K^{46} (Kreienkamp et al., 1992) and from *N. naja nigricollis* with the group attached at the analogue residue K^{47} (Chatrenet et al., 1990). Both residues are located on the concave side of loop III of the toxin structure (see Fig. 7). In addition, using the [^{125}I]-neurotoxin II derivative carrying the photoactivatable group at K^{26} (Kreienkamp et al., 1992), toxin 3 from *N. naja siamensis* with the azidogroup attached at K^{23} (Utkin et al., 1998), or α-BTx under simple UV irradiation (Oswald and Changeux, 1982), practically only the δ and γ subunits were labeled. Moreover, α-cobratoxin (α-CTx) derivatives with photoactivatable groups at either position K^{25} (*N. naja oxiana*) (Mac-

Table 4
Localization of α-neurotoxin binding sites on the AChR by the photolabeling approach

α-Neurotoxin derivative	α-Neurotoxin species	Position of the activatable group (Loop)	Labeled subunits[a]	References
Long α-neurotoxins				
Arylazido-[^{125}I]αBTx	*B. multicinctus*	unidentified	αδ[b]; δ[b]	(Chaturvedi et al., 1992)
N-[(5-Azido-2-nitrobenzoyl)amino]sacetimidate-[^{125}I]αBTx	*B. multicinctus*	unidentified	all	(Nathanson and Hall, 1980)
[^{125}I]αBTx	*B. multicinctus*	direct UV activation	α, γ, and δ	(Oswald and Changeux, 1982)
Dithiobis(succinimidylpropionate)-activated [^{3}H]methyl-α-CTx	*N. naja siamensis*	unidentified	βγ (high)[c]; αδ (low)[d]	(Hamilton et al., 1985)
p-Azidobenzoyl-[^{125}I]αCTx	*N. naja siamensis*	K^{23} (Loop II)	γ and δ	(Utkin et al., 1998)
Tetrafluoroazidobenzoyl-[^{125}I]αCTx	*N. naja siamensis*	K^{23} (Loop II)	γ and δ	(Utkin et al., 1998)
Trifluoromethyldiazyrinilbenzoyl-[^{125}I]αCTx	*N. naja siamensis*	K^{23} (Loop II)	α, γ, and δ	(Utkin et al., 1998)
Benzoylbenzoyl-[^{125}I]αCTx	*N. naja siamensis*	K^{23} (Loop II)	α and δ	(Utkin et al., 1998)
Short α-neurotoxins				
p-Azidobenzoyl-[^{3}H]αCTx	*N. naja nigricollis*	K^{15} (Loop I); K^{47} (Loop III); K^{51} (Loop III)	αδ (high)[e]; αδ (high)[e]; δ (high)[e]	(Chatrenet et al., 1990)
p-Azidobenzoyl-[^{125}I]-neurotoxin II	*N. naja oxiana*	K^{46} (Loop III); K^{26} (Loop II)	α; γ (high)[c]; δ (low)[d]	(Kreienkamp et al., 1992)
p-Azidobenzoyl-[^{125}I]-neurotoxin II	*N. naja oxiana*	K^{26} (Loop II)	δ (starting at F^{148})	(Utkin et al., 1994a)
p-Benzoylbenzoyl-[^{125}I]-neurotoxin II	*N. naja oxiana*	different Lysines	α	(Kasheverov et al., 1999)
p-Azidosalicylamidoethyl-1,3′-dithiopropyl-[^{125}I]-neurotoxin II	*N. naja oxiana*	K^{25} (Loop II); K^{15} (Loop I); K^{46} (Loop III)	δ (at A^{268}); αβ (low)[d]; δ and γ	(Machold et al., 1995a,b)

[a] The criteria to demonstrate specificity is based on the inhibition of labeling elicited by nonderivatized α-neurotoxins.
[b] Both α and δ subunits were covalently linked by the arylazido-[^{125}I]αBTx derivative containing a 14 Å side chain, whereas only the δ subunit was labeled by the derivative containing a 33 Å side chain.
[c] Site at which *d*-TC competes with high-affinity.
[d] Site at which *d*-TC competes with low-affinity.
[e] Site at which native α-neurotoxin competes with high-affinity.

hold et al., 1995a,b) or K^{27} (*N. naja nigricollis*) (Hervé et al., 1992) reacted almost exclusively with the δ subunit.

From EPR spectroscopy (Rousselet et al., 1984) as well as chemical modification and site-directed mutagenesis studies (Ackermann and Taylor, 1997; Hervé et al., 1992; Pillet et al., 1993; Trémeau et al., 1995) there is consensus in that residues homologous to the conserved amino acid K^{26} which is located on the concave side of loop II are involved in the specific neurotoxin binding to the AChR (see Fig. 7). Opposite to this, the residue K^{47} and homologous amino acids located on loop III (see Fig. 7) do not interact with the AChR residues implicated in α-neurotoxin binding (Ackermann et al., 1998). Evidence from fluorescence spectroscopy has questioned the contribution of the homologous Lys residue on AChR binding specificity (Johnson et al., 1990). For example, K^{23}-labeled α-CTx from *N. naja siamensis*, a long α-neurotoxin, did not diminish binding affinity and the fluorescence of the attached fluorophore group (fluorescein) was quenched by iodide, demonstrating accessibility of the aqueous solute to the fluorophore. A possible explanation for this is that K^{23}, as observed for its homologous residue K^{26}, is located on the concave side of loop II (see Fig. 7). Thus, K^{23} would be oriented towards the AChR ion channel. Therefore, the labeled residue might be accessible to aqueous solutes.

There is also evidence that other invariant residues are important for neurotoxin binding (Ackermann and Taylor, 1997; Ackermann et al., 1998; Pillet et al., 1993; Trémeau et al., 1995). In this regard, a strong energetic coupling between residue R^{33} of *N. mossambica mossambica* α-neurotoxin (which is located at the tip of loop II; see Fig. 7) and αV^{188} (2.6 kcal/mol; Ackermann et al., 1998) or γE^{176} (−2.7 kcal/mol; Osaka et al., 1999) on the mouse AChR has been calculated. This is in accord with the observation that the charge reversal of Arg reduces 350-fold the erabutoxin *a* binding (another short neurotoxin) (Trémeau et al., 1995) and 16,000-fold the *N. mossambica mossambica* binding to the αγ site (Osaka et al., 1999). A high

coupling (−2.2 kcal/mol) was also observed between R^{36} (which is located on loop II; see Fig. 7) of *N. mossambica mossambica* α-neurotoxin and γE^{176} (Osaka et al., 1999). The R36A mutation, the homologous residue of α-BTx, also reduced ~90-fold the α-BTx affinity to wild-type receptors (Spura et al., 1999 and references therein). Smaller but significant linkage of 2.1 kcal/mol was also observed between α-neurotoxin-K^{27} (which is located closer to the top and opposite side of loop II; see Fig. 7) and the receptor residue αV^{188} (Ackermann et al., 1998). In addition, a strong energetic coupling (−5.9 kcal/mol) was found between the same α-neurotoxin residue and γE^{176} (Osaka et al., 1999). Thus, the electrostatic force between γE^{176} and K^{27} is a primary factor in stabilizing the toxin-AChR complex. In addition, a lower energetic coupling (1.5–1.9 kcal/mol) was determined between α-neurotoxin-K^{27} and residues $\alpha 1Y^{190}$, $\alpha 1P^{197}$, or $\alpha 1D^{200}$ at the αδ subunit interface (Ackermann et al., 1998). Regarding the D^{200} residue, interesting information was obtained by using small ligands. Although the D200N mutation practically did not change the affinity of either the full agonist ACh (O'Leary and White, 1992) or the competitive antagonist *d*-TC (O'Leary et al., 1994) obtained by permeability response, the D200Q mutation decreased the affinity for both the agonist (30-fold) and the high-affinity *d*-TC (13-fold) binding site but increased the association of *d*-TC for its low-affinity binding site (Osaka et al., 1999). The transitions to the desensitized state and the subsequent conversion to the high affinity state is probably the main cause that account for the difference between the two studies. Thus, these findings support the conclusion that the conserved Asp in this region is not very important in small agonist/competitive antagonist-AChR interactions but it may affect gating, desensitization, and α-neurotoxin binding.

From photolabeling experiments with the K^{26}-*p*-azidobenzoyl derivative of neurotoxin II from *N. naja oxiana*, a fragment starting on δF^{148} was found to be labeled (Utkin et al., 1994a). More precisely, the azidosalicylamidoethyl derivative of neurotoxin II labeled A^{268} (Machold et al., 1995a). Taking into consideration the position of this residue and the AChR dimensions, the center of the α-neurotoxin binding site is located at ~40 Å from the receptor top surface (or ~20 Å from the lipid membrane surface), close to the channel axis (Machold et al., 1995a; reviewed in Hucho et al., 1996). The scheme of Fig. 8(A) shows such localization.

The neurotoxin II derivative with the activatable group at position K^{15} crosslinked both α and β chains (Machold et al., 1995b) (Table 4). In addition, the α-toxin from *N. naja nigricollis* with the activatable group at K^{51} labeled both δ and β subunits (Chatrenet et al., 1990) (Table 4). However, these residues, which

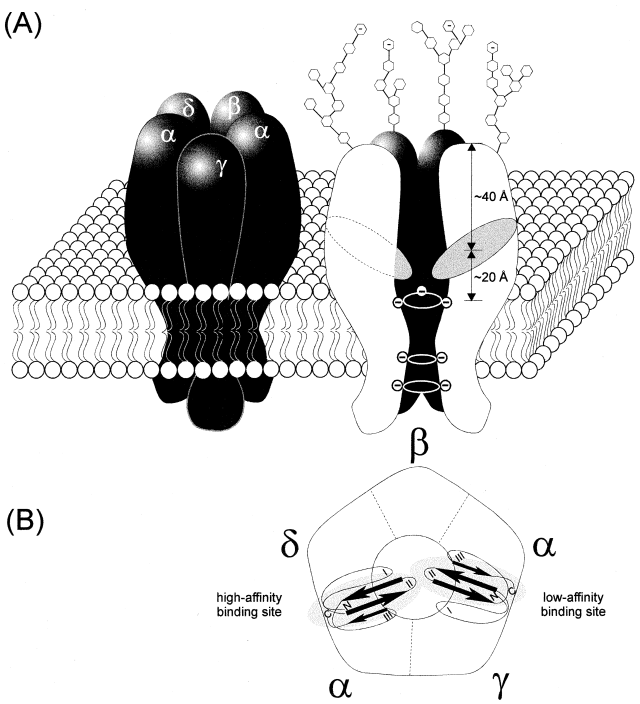

Fig. 8. Schematic model for the location of the *Elapidae* α-neurotoxin binding sites on the muscle-type AChR (modified from Hucho et al., 1996). (A) Transverse representation of the muscle-type AChR showing two α-neurotoxin molecules (grey oval), each one located at the αγ and the αδ subunit interface. It is noteworthy that the bottom part of the α-neurotoxin molecule reaches the ion channel's mouth that is negatively-charged. (B) Top view of the quaternary structure of the muscle-type AChR showing the localization of either α-neurotoxin molecule at the respective subunit interface. Taking into account the quaternary structure of the α-neurotoxin molecule, it becames evident that the second (II) loop (see Fig. 7) is oriented to the ion channel.

are located at the convex side of loop I and loop III, respectively (see Fig. 7), have been considered by mutational experiments to be unimportant for neurotoxin binding (Trémeau et al., 1995).

Interestingly, several α-neurotoxin derivatives with the photoactivatable group at K^{26} (*N. naja oxiana*) (Kreienkamp et al., 1992) or at the homologue residue K^{23} (*N. naja siamensis*) (Utkin et al., 1998) reacted with both γ and δ subunits in a *d*-TC-sensitive fashion (Table 4). In addition, the crosslinking on γ and β subunits was affected by low *d*-TC concentration more strongly than on α and δ chains (Hamilton et al., 1985). Thus, these data indicate the existence of nonequivalence between the two α-neurotoxin binding sites. Fig. 8(B) shows the most probable location for the α-neurotoxin sites: the high-affinity locus coincides with the *d*-TC low-affinity and the ACh high-affinity binding site (αδ interface), and vice versa.

From these studies a structural model to explain how the α-neurotoxins bind to the AChR is proposed. Fig. 8 shows the basic tenets of this model. (1) The

concave sides of loops II and III (see Fig. 7) form the main region by which the neurotoxin contacts the AChR. (2) The concave side of the central loop II (e.g. through residue K^{27}) makes contact with the α1 subunit (e.g. through residue sequence V^{188}–D^{200}) at the αδ (high-affinity) or the αγ (low-affinity) subunit interfaces. The portion of loop II proximal to loop III has been suggested to be closer to the γ subunit where the residue E^{176} is found (Osaka et al., 1999). (3) Additional contacts between α-neurotoxin-R^{33} and -R^{36} (and perhaps also loop III) and receptor residues αY^{190}, αV^{188}, and γE^{176} may stabilize the neurotoxin complex.

A distance of ~0.8 nm was suggested to exist between carbon β from residues W^{187}, V^{188}, F^{189}, Y^{190}, and P^{194} forming the putative negative subsite on the α1 AChR subunit and the large net positive charge (+4) observed on the α-BTx molecule on the basis of the size of the MTSET modification (Spura et al., 1999). The experimental data showing that spatially separated loops of the toxin (e.g. loop II which carries K^{27} and loop III containing K^{47}; sequence number from *N. mossambica mossambica*; see Fig. 7) interact with different AChR subunits or different chain domains (Table 4) support the idea of multipoint contact on a rather extended area of the AChR-toxin complex.

The venom of the Southeast Asian snake *Trimeresurus wagleri* presents four peptides (22–24 residues) with just one Cys bridge and high Pro content (Sellin et al., 1996). These toxins, namely waglerins, also inhibit the postsynaptic AChR at the neuromuscular junction (Aiken et al., 1992). Either the single substitution H10Y, or mutations C9S or/and C13S, which are involved in disulfide bonds, significantly reduces toxicity. The observed specificity of waglerin-1 to inhibit mature AChRs (but not to inhibit neonatal AChRs; ~2000-fold preference) was found to be mediated by the ϵ chain (McArdle et al., 1999) by binding at the αϵ subunit interface (Taylor et al., 1998).

The observed strong correlation between labeling and site-directed mutation studies indicates that at least residues V^{188}, Y^{190} (see loop C), P^{197}, and D^{200} from the α1 subunit and amino acid γE^{176} (close to loop G) are leading the binding of snake α-neurotoxins through the interaction with (at least) residues K^{27}, R^{33}, and R^{36}.

4.2. Snake α-neurotoxin binding-polypeptides

Synthetic peptides have been useful to study the location of the binding site for α-neurotoxins on the α subunit. Peptides with different sequences can be compared with each other by determining their ability to bind α-BTx. Moreover, the role of binding site-determining individual residues can be resolved by substituting certain amino acids of the peptide. A disadvantage of this approach is that the peptide binds α-BTx with an affinity two to four orders of magnitude lower than the native receptor. However, this affinity is similar to that found in denatured or intact α subunits, indicating that the polypeptides preserve the principal determinant for toxin binding. By using this approach, the region comprising the sequence segment 170–210 from both the AChR native α1 subunit and synthetic polypeptides corresponding to homologous sequences from several sources of AChR α1 subunits has been demonstrated to be involved in the α-neurotoxin binding site (reviewed in Arias, 1997). In addition, α-BTx binds to human AChR α1 subunit peptide 185–199 but not to peptides 125–147 or 389–409 (Greismann et al., 1990). However the 183–204 peptide from human α1 subunit binds α-BTx with lower affinity than other assorted animal species (Ohana and Gershoni, 1990). The α-BTx K_ds (in the μM range) follow the sequence: *Torpedo californica* (0.06) < chick (0.15) < *Xenopus* (0.54) < *Drosophila* (1.7) < mouse (3.2) < calf (6.2) ~ human (6.5). In addition, the human sequence α185–196 has virtually no toxin binding ability (Neumann et al., 1986). Opposite to this, the native human AChR binds toxin with affinities in the same order as *Torpedo* AChR (K_d ~ 0.5 nM; Lukas et al., 1981). Based on this experimental evidence and in particular on the works of Neumann et al. (1986) and Lentz (1995) it can be concluded that sequence 185–196 from the α1 subunit is the shortest required for α-BTx binding. This is in agreement with studies using fluorescence (Pearce and Hawrot, 1990) and NMR (Basus et al., 1993) spectroscopy where it was found that the α-BTx molecule undergoes a conformational change upon binding to the synthetic dodecapeptide α185–196.

Similar segments containing the Cys pair, for instance 181–200 from both α7 and α8 subunits and 180–199 from α5, were recognized as important for α-BTx binding (reviewed in Conti-Fine et al., 1995). Whether the sequence 180–199 in fact contributes in the cognate native neuronal α5-containing AChR to a site able to bind α-BTx is unclear. Taking into account that α5-containing receptors do not bind α-BTx, the most reasonable feasibility is that the binding of α-BTx to the native receptor is impeded by surrounding structural elements. Additional polypeptide studies indicated that two clusters of amino acids positioned at V^{188}–Y^{189}–Y^{190} and C^{192}–C^{193}–P^{194} are necessary for α-BTx binding (reviewed in Conti-Fine et al., 1995; Conti-Tronconi et al., 1994).

Several laboratories have suggested the importance of aromatic residues at positions homologous to Y^{189} and Y^{190}, in addition to C^{192} and C^{193}, for α-BTx binding to different α-BTx-sensitive AChRs (e.g. muscle-type and α7 receptors) (Balass et al., 1997;

Lentz, 1995; Scherf et al., 1997). This was corroborated by substituting Y^{189} and Y^{190} for Phe and His, and $C^{192–193}$ for Ser, His, or Val, which affected, at different extents, the binding of α-BTx on the α181–200 peptide (McLane et al., 1994). Structural changes on the peptide α181–200 by substituting P^{194} or P^{197} with two adjacent Gly residues or by inserting Gly in between of C^{192} and C^{193} were incompatible with α-BTx binding (McLane et al., 1994). The same was observed by replacement of Y^{189} by either Ala or Gly (Tzartos and Remoundos, 1990). Other substitutions such as V188I or V188T, and K^{185} or D^{195} to residues that maintain or change the charge distribution of the peptide produced only minor effects on α-BTx binding (McLane et al., 1994). On the contrary, different mutations on AChR-V^{188} greatly affected the binding of the *N. mossambica mossambica* short α-neurotoxin (Ackerman and Taylor, 1997) (see Table 5). However, these mutations did not strongly reduce α-BTx binding (a long α-neurotoxin). In this regard, only long α-neurotoxins have been found to bind with high affinity to the neuronal-subtype α7 receptor (Servent et al., 1998).

A sequence other than α185–196 has been also suggested to be involved in α-neurotoxin binding. Specifically, the residues within segment 55–74 of the α1 subunit were also identified by the binding of α-BTx and by antibodies that specifically compete with cholinergic ligand binding sites (Conti-Tronconi et al., 1990; Wahlsten et al., 1993). It is interesting to denote that this sequence also bears the main immunogenic region 67–76 (reviewed in Conti-Tronconi et al., 1994). In addition, residue sequence 122–138 of both human and *Torpedo* AChRs possess the components for long and short α-neurotoxin binding (Ruan et al., 1991). For instance, His^{134} has been involved in the binding of α-BTx to either *Torpedo* or human AChRs (Venera et al., 1997).

The evidence by using snake α-neurotoxin binding-polypeptides indicates that both long and short toxins bind to overlapping but not identical areas on the AChR.

4.3. Evidence from the mutagenesis approach

Substitutions of several residues on the α1 subunit from the whole receptor also demonstrated the importance of several segments in α-neurotoxin binding (Table 5). For instance, the F189N mutation in mouse AChR expressed in fibroblasts caused a 100-fold loss in α-BTx affinity, whereas the double mutation W187N/F189T caused a higher effect (Keller et al., 1995; Kreienkamp et al., 1994). In particular, the latter mutation diminished between 580 and 2900 times the α-BTx affinity for the high-affinity binding site and between 15 and 180 times for the low-affinity binding site. In addition, several mutations on either V^{188}, Y^{190}, P^{197}, or D^{200} decreased α-neurotoxin (*N. mossambica mossambica*) binding affinity at the αγ subunit interface (low-affinity site) (Ackermann and Taylor, 1997). The fact that mutation α1Y198F did not inhibit α-BTx binding (Tomaselli et al., 1991) is consistent with the possible role of this residue on agonist binding (see loop C in Fig. 3) but not on α-BTx binding.

Although Cys mutagenesis is well tolerated in region 183–197, BrACh or [2-(trimethylammonium)ethyl]-methanetiosulfonate (MTSET) modification of W187C, V188C, and F189C, decreased α-BTx binding by 55–70% (Spura et al., 1999). Furthermore, studies involving α1/α3 chimeric receptors expressed in *Xenopus* oocytes indicated that substitution of *Torpedo* α1 residues for their α3 homologous (i.e. W184Y, W187E, V188I, Y189K, and T191N) confers significant α-BTx sensitivity to the intact chimeric receptor (Spura et al., 1999 and references therein).

Regarding other subunits, each mutation L119C from either γ or ϵ subunit or δL121C following methanethiosulfonate treatment reduced in 50% the number of α-BTx binding sites, suggesting that these residues (one from each subunit) are involved in the α-BTx binding site (Sine, 1997). In addition, the exchange of γL119 by Lys, which resembles the thioethylamine moiety of MTSET, slowed the intrinsic rate of α-BTx binding to the αγ site. Recent results indicate that both P^{175} and E^{176} have been considered to confer high affinity ($K_d \sim 0.1$ nM) to the γ subunit-containing site in the fetal AChR, while their homologous residues T^{175} and A^{176} impart relatively low affinity ($K_d \sim$ 100 nM) to the ϵ subunit-containing site in the adult AChR (Osaka et al., 1999).

Although other mutations such as H186F and P194S on the muscle-type AChR (Tomaselli et al., 1991) as well as S94N, G82E, and W153F on the α-BTx-sensitive neuronal-type α7 receptor (Galzi et al., 1991a) also inhibited α-BTx binding, the nature of these changes remains unclear.

These data support the concept that: (1) the α-neurotoxin molecule interacts with the AChR at multipoint attachments on a rather large area; and (2) the residue sequence W^{187}–D^{200}, which partially overlaps with loop C (see Fig. 3), is forming the principal component of the snake α-neurotoxin binding site.

4.4. Snake α-neurotoxin-resistant AChRs

Taking advantage of the observed naturally-occurring mutations in AChRs from lizards, snakes, mongooses, and hedgehog which are resistant to the action of α-BTx, a short stretch of 11 residues (187–197) was proposed to be important in α-BTx binding (Barchan et al., 1992, 1995; Chaturvedi et al., 1992; Kachalsky et al., 1995; Kreienkamp et al., 1994). In particular, Y^{187}, Y^{189}, and P^{194} from *Torpedo* α1 subunit were

Table 5
Residue mutations on the AChR affecting the binding properties of different α-neurotoxins

Mutation	Source of AChR	Times the pharmacological effect		References
		Inhibition of α-neurotoxin binding[a]	Reduction of agonist-induced channel activation[b]	
α1 *Subunit*				
C192S	*Torpedo* receptor expressed in *Xenopus* oocytes	60[c]		(Mishina et al., 1985)
C193S		70[c]		
F189N	mouse receptor expressed in HEK-293 cells	105		(Kreienkamp et al., 1994)
W187N/F189T		576 and 15[d]		
F189N/S191A		no effect		
P197H		no effect		
F189N	mouse receptor expressed in HEK-293 cells	106		(Keller et al., 1995)
F189N/P194L		6875 and 225[d]		
W187N/F189T		2875 and 181[d]		
D111N/F189N/P194L		15,625 and 625[d]		
W187N/F189T/P194L		2188 and 381[d]		
P194L	166–211 α *Torpedo*/TrpE protein expressed in *E. coli*	high effect[e]		(Chaturvedi et al., 1992
Y189N		high effect[e]		
T191S/P194L		high effect[e]		
W187E/Y189K/T19N		high effect[e]		
Y190F	mouse receptor expressed in HEK-293 cells	500[f] and 25[g]		(Ackermann and Taylor, 1997)
Y190T		490[f] and 49[g]		
V188K		390[f] and 20[g]		
P197I		69[f] and 3[g]		
D200Q		66[f] and 2[g]		
Y93S	mouse receptor expressed in HEK-293 cells	6[h,i]		(Sugiyama et al., 1998)
Y93F		12[h,i,b]		
D152N		6[h,b]		
V188K		7[h,i]		
Y190T		32[h,b] and 3[h,i]		
Y198T		2480[h,b] and 16[h,i]		
α3 *Subunit*				
K185Y	α3β2 receptor expressed in *Xenopus* oocytes		3	(Harvey et al., 1997)
I188K			11	
α7 *Subunit*				
W55R	α7/5-HT_3 homooligomeric chimera expressed in HEK-293 cells	3[i]		(Quiram and Sine, 1998a)
S59Q		3[i]		
T77K		10[i]		
W55R/S59Q		9[i]		
W55R/T77K		19[i]		
S59Q/T77K		18[i]		
W55R/S59Q/T77K		48[i]		
β2 *Subunit*				
T59K	α3β2 receptor expressed in *Xenopus* oocytes		4	(Harvey et al., 1997)
γ *Subunit*				
Y111δR113	$\alpha_2\beta\gamma_2$ *Torpedo* receptor expressed in *Xenopus* oocytes	13,000[i]		(Chiara et al., 1999)
L119K	mouse receptor expressed in HEK-293 cells	> 8[i]		(Sine, 1997)
P175εT176	$\alpha_2\beta\gamma\delta$ mouse receptor expressed in HEK-293 cells	36[f]		(Osaka et al., 1999)
E176εA177		16[f]		
E176K		660[f]		
P175εT176/E176K		290[f]		
ε *Subunit*				

(continued on next page)

Table 5 (*continued*)

Mutation	Source of AChR	Times the pharmacological effect		References
		Inhibition of α-neurotoxin binding[a]	Reduction of agonist-induced channel activation[b]	
T176γP175/ A177γE176	$\alpha_2\beta\epsilon\delta$ mouse receptor expressed in HEK-293 cells	1180[f,j]		(Osaka et al., 1999)
δ *Subunit*				
R113γY111	$\alpha_2\beta\delta_2$ *Torpedo* receptor expressed in *Xenopus* oocytes	750[g,h]		(Chiara et al., 1999)
S36K/I178F	$\alpha_2\beta\delta_2$ mouse receptor expressed in HEK-293 cells	1000		(Sine et al., 1995a)
Y113γS111		10		

[a] Values determined by α-neurotoxin equilibrium binding.
[b] Mutation effect elicited at the low-affinity (αγ) binding site of α-CoTx MI on mammalian AChRs.
[c] In these mutations the reduction of α-BTx binding is expressed in percentage.
[d] Reduction of α-BTx affinity determined by association kinetics at the αγ (low-affinity site) and αδ (high-affinity site) subunit interfaces, respectively.
[e] High effect means that α-BTx binding is abolished.
[f] Reduction of α-neurotoxin binding at the low-affinity site (αγ or αϵ subunit interface).
[g] Reduction of α-neurotoxin binding at the αδ subunit interface (high-affinity site).
[h] In these cases an enhancement of α-CoTx MI binding is observed.
[i] These values were obtained by measuring the inhibition of the initial rate of α-BTx binding elicited by the used α-CoTx.
[j] In this case an enhancement of
α-neurotoxin *N. mossambica mossambica* binding is observed.

found to be substituted in snake and mongoose AChRs.

Binding experiments by using the fragment 122–205 expressed in *Escherichia coli* corresponding to the α subunit of several species showed that: (a) the hedgehog fragment does not bind α-BTx; (b) the human fragment is a partial binder; and (c) the shrew and the cat fragment bind α-BTx (Barchan et al., 1995). Since residues at positions 187 and 189 from both hedgehog and human AChRs are not aromatic, it seems likely that aromatic amino acids at these particular positions are required for full α-BTx binding. In fact, α-BTx binding is affected by mutations on the α subunit to residues found in toxin-resistant animals. For instance, the results by using a fusion protein consisting on residues 166–211 of the *Torpedo* α1 with the TrpE protein which is further expressed in *E. coli* indicated that, single mutations on the *Torpedo* α1 P^{194} and Y^{189} to the respective Leu and Asn residues found in snake AChR abolished toxin binding (Chaturvedi et al., 1992). The same result was found on the triple exchange of *Torpedo* α1 W^{187}, Y^{189}, and T^{191} to the corresponding α3 amino acids Glu, Lys, and Asn. Regarding P^{194}, which putatively induces a β-bend or turn, its substitution might produce a major conformational change on the α-BTx binding site.

Since these studies were performed in bacteria-expressed peptides, the role of *N*-glycosylation has not been determined. Thus, in order to resolve whether glycosylation signals (i.e. N-X-S/T) influence or not toxin binding, different mutations were produced on fibroblast-expressing muscle-type AChRs (Keller et al., 1995; Kreienkamp et al., 1994). The introduction of a glycosylation signal (e.g. F189N) on the α1 subunit resembling the cobra AChR subunit, expressed in the presence of wild-type β1, γ, and δ subunits, showed a 100-fold decrease in α-BTx affinity (Kreienkamp et al., 1994) (Table 5). However, the nonglycosylatable F189N/S191A double mutation only decreased α-BTx affinity in two times. In addition, the single substitution W187N, which is present in the mongoose, only produced a three times less affinity for α-BTx, whereas the double mutation W187N/F189T, that introduces a glycosylation signal, inhibited in 580 and 2900 times the high-affinity binding site and between 15 and 180 times the low-affinity binding site for α-BTx (Table 5). In conclusion, it has been proposed that glycosylation signals at residues N^{187} (mongoose) and N^{189} (snakes) is one of the principal causes of α-BTx resistance by affecting the conformation and stability of AChR-bound α-BTx (Keller et al., 1995). Indeed, the residue N^{187} on the mongoose α1 subunit can be glycosylated (Asher et al., 1998).

These results are in agreement with the fact that the mutation of three *Torpedo* residues to snake amino acids (i.e. W184F, K185W, and W187S) had no effect on toxin binding (Kreienkamp et al., 1994). Interestingly, the P194L mutation did not produce an appreciable effect on α-BTx binding to mouse AChR-expressing fibroblasts (Kreienkamp et al., 1994). However, double or triple mutations containing the glycosylation signal provoked a high effect on both α-BTx

binding sites (Keller et al., 1995). This latter datum is in favor of a synergistic effect elicited by L^{194} on toxin-resistance. Finally, experimental evidence suggests that other *N*-glycosylation conserved sites such as $\alpha 1T^{143}$, γS^{143} and δS^{145}, but not $\beta 1T^{143}$, contribute to the formation of the α-BTx binding site (Gehle et al., 1997).

Several animals have developed different degrees of α-BTx resistance during evolution. Nature's strategy includes the introduction of a glycosylation site and mutations on the α subunit at residues specific for α-neurotoxin binding but not crucial for the pharmacological action of small ligands such as the neurotransmitter ACh (e.g. exchange of aromatic residues by different non-aromatic ones and mutation on Pro).

4.5. Spatial location of snake α-neurotoxin binding sites

The localization of the binding site for α-CTx on the AChR was determined by means of FRET measurements. By using α-CTx labeled at K^{23} and K^{49} with an appropriate donor/acceptor pair (fluorescein/rhodamine), an intramolecular distance between toxins of about 67 Å in solubilized AChRs was found (Johnson et al., 1984). Interestingly, a higher FRET efficiency was observed in membrane-associated than in solubilized AChRs, indicating that intermolecular energy transfer also occurs. Additionally, by using the same fluorescein-labeled K^{23}-α-CTx as energy donor and the membrane-partitioned C_{18}-rhodamine and C_{12}-eosin probes as acceptors, distances between 39 and 45 Å from the toxin binding sites and the membrane surface were determined (Johnson et al., 1990). Taking into account the AChR dimensions provided by electron microscopy at 9 Å resolution (Unwin, 1993), and the size (20 × 30 × 40 Å; Walkinshaw et al., 1980) and orientation (Johnson et al., 1990) of the α-toxin, the α-toxin molecules should be located close to the outer perimeter of the AChR at a distance of ~42 Å above the membrane surface. Interestingly, this distance is almost double than that proposed by Hucho's laboratory (~20 Å above the membrane surface; see Fig. 8(A)) at the Freie Universität Berlin (Berlin, Germany) (Machold et al., 1995a; reviewed in Hucho et al., 1996), and longer than the transverse distance for the agonist binding sites (30–35 Å) (Unwin, 1993, 1996) (see Fig. 5). The observed difference in the position of the α-toxin binding site by using either the FRET or the photolabeling approach may be due to the fact that the fluorescein-labeled K^{23} residue of *N. naja siamensis* (a long α-neurotoxin) is located at a site opposite from the one for the labeled residue at position K^{25} of *N. naja oxiana* (a short α-neurotoxin) (Betzel et al., 1991). It is also possible for the labeled residue of the toxin to be located, according to the Off-Axis FRET model (see Fig. 4), at a certain distance δ from the major axis of symmetry of the AChR (Yguerabide, 1994).

These data underline the importance of the position of the probe (photoactivatable, fluorescent, etc.) attached to the α-neurotoxin molecule to determine the position of the α-neurotoxin binding sites on the AChR.

4.6. Structural components of the neuronal bungarotoxin binding site

κ-Neurotoxins comprising κ-, κ2- and κ3-BTx from *B. multicinctus* and κ-flavitoxin (κ-FTx) from *B. flaviceps* are competitive antagonists of the AChR but present a different receptor subtype specificity than that for α-neurotoxins (reviewed in Chiappinelli et al., 1996). The overall structure of κ-neurotoxins is very similar to that for α-neurotoxins. Nevertheless, κ-neurotoxins differ from α-neurotoxins in their native aggregation state: while the α-neurotoxin molecule is monomeric, the κ-neurotoxins occur as homodimers (Dewan et al., 1994). Interactions between F^{49} and I^{20} are essential for dimer formation (Grant et al., 1997). The remotion of only one of the five disulfide bonds, namely the C^{27}–C^{31} disulfide, reduces 47-fold the activity of the toxin (Grant et al., 1998). Mutagenesis studies indicated that R^{34}, located near the tip of loop II, is the most critical residue for AChR binding and for inhibition of neuronal transmission (Fiordalisi et al., 1994; Pillet et al., 1993; reviewed in Chiappinelli et al., 1996).

From the point of view of neuronal AChR sensitivities to κ-BTx, α3β2 is 10 times more sensitive ($IC_{50} \leq 0.1$ μM) than α4β2 whereas α3β4 is insensitive (reviewed in Conti-Tronconi et al., 1994). Taking into account this difference, Luetje et al. (1993) co-expressed distinct α3/α4 chimeras with the β2 subunit to demonstrate which residues are related to the κ-BTx binding site. They showed that residue sequences 84–121, 121–181 and 195–215, but not amino acids 1–84, from the α3 subunit are involved in κ-BTx binding. Specifically, E^{198} corresponding to the α3 subunit (which is exchanged to P^{198} in α2) is the residue forming the κ-BTx binding site. This residue has also been found to be related to the nicotinic binding site in the chicken α neuronal subunit (Hussy et al., 1994). However, in addition to the preceding evidence, peptides 51–70 and 1–18 from the α3 NH_2-terminal sequence were demonstrated to bind κ-BTx with high affinity and to inhibit the binding of κ-BTx to neuronal-type AChRs expressed in the rat pheochromocytoma cell line PC12 (McLane et al., 1990). In addition, peptides homologous to sequences that bind α-BTx (180–199 and 183–201) also inhibited 50% of the κ-BTx binding to PC12 cells. Interestingly, none of the peptides from the α3 subunit bound α-BTx. The 51–70 peptide

reduced four times the apparent rate of κ-BTx association to PC12 cells. More particulary, several substitutions (but not single substitutions) on two negatively charged residues E^{51} and D^{62} and on several aliphatic and aromatic amino acids comprising L^{54}, L^{56}, and Y^{63}, lowered the κ-BTx affinity for this peptide (reviewed in Conti-Fine et al., 1995). The same basic requirements have been demonstrated for the κ-FTx. However, the electrostatic interactions between the κ-flavotoxin and the AChR seem to be mediated by positively rather than negatively charged amino acids at positions 57, 64, 66, and 68 (reviewed in Conti-Fine et al., 1995). In this regard, the natural substitution of residue E^{48} from the κ-FTx molecule by Gln in κ-BTx which are located on loop II might produce a different overall charge and differences in the spatial arrangement of charged groups. The observed different spatial arrangement between R^{50} from κ-BTx and R^{52} from κ-FTx supports such conjecture.

In addition to the components on the α3 subunit, the amino terminal half portion (residues 1–121) of the nicotinic β subunit also regulates the kinetics of inhibition of κ-BTx (Papke et al., 1993). In this regard, changing T^{59} to Asp on the β2 subunit, and thus introducing a negative charge, an increase in κ-BTx sensitivity was found (Harvey and Luetje, 1996). On the contrary, the same mutation does not affect α-conotoxin MII binding indicating that $\beta2T^{59}$ is not shared by both peptidic antagonists (Harvey et al., 1997).

Taking into account these results together with the data described in previous sections, we suggest the existence of homologous but different components for each α- or κ-neurotoxin binding site.

4.7. *Conus toxins*

The family of small neuropeptides called α-conotoxins (α-CoTxs) has become one of the most powerful tools to support the observed nonequivalence between both agonist/competitive antagonist binding sites on the AChR. Conotoxins are a mixture of different neuroactive compounds found in the venom of several *Conus* marine snail mollusk species (for reviews see Adams and Olivera, 1994; Myers et al., 1993; Olivera et al., 1990). The principal structural features of α-CoTxs are shown in Table 6. Most of them exhibit four Cys residues in the following conservative arrangements: CCX_3CX_5C (the $\alpha_{3/5}$ subclass), CCX_4CX_3C (the $\alpha_{4/3}$ subclass), and CCX_4CX_7C (the $\alpha_{4/7}$ subclass), where each alterned Cys pair forms a disulfide loop (i.e. loops I and II, respectively) (Table 6). The three-dimensional structures of α-CoTx PnIA (Hu et al., 1996), MII (Shon et al., 1997), MI (Gouda et al., 1997), CnIA and CnIB (Favreau et al., 1999), ImI (Maslennikov et al., 1999), and GI (Gehrmann et al., 1998; Guddat et al., 1996; Maslennikov et al., 1998) were determined by using either X-ray crystallography or NMR spectroscopy. These studies have provided support for the idea that these small triangular polypeptides achieve their wedge-like structure and conformational stability by means of disulfide bonding. This and other conformational restraints have been found to be necessary for effective α-CoTx interactions with the AChR (Ashcom and Stiles, 1997).

Another conformational characteristic is the number of non-Cys amino acids (X) between cysteines. There are three and five residues (the $\alpha_{3/5}$ subclass), four and three residues (the $\alpha_{4/3}$ subclass), or alternatively four and seven residues CCX_4CX_7C (the $\alpha_{4/7}$ subclass) forming the first and the second loop, respectively (Table 6). The only representative of the $\alpha_{3/5/3}$ subclass, which has three Cys bonds, is α-CoTx SII. Additionally, a conserved Pro residue is found between the second and the third Cys on almost all studied α-CoTxs. The exception is the αA–CoTx family (e.g. αA-PIVA and αA-EIVA; see Table 6) which has a core sequence very different to the other subtypes (Han et al., 1997; Hopkins et al., 1995; Jacobsen et al., 1997).

Most of the characterized α-CoTxs inhibit muscle-type AChRs (Table 6). Particularly, GI, MI, and SIA subtypes actively bind to vertebrates including mammals, whereas SI and SII subtypes are more specific for *Torpedo* than for mammalian AChRs. For instance, α-CoTx GI produces tetanic fade at the rat neuromuscular junction (Blount et al., 1992) and α-CoTx CnIA blocks the miniature endplate potentials of a phrenic nerve hemidiaphragm preparation (Favreau et al., 1999). α-Conotoxin-induced displacement of [^{125}I]α-BTx binding to the *Torpedo* AChR presented the same potency for subtypes SI, MI, and GI. Subtype SI appears to bind to a homogeneous population of α-BTx sites on the *Torpedo* AChR (Hann et al., 1994). However, whereas both GI and MI subtypes bind with high affinity to the *d*-TC site (αγ interface) of the *Torpedo* receptor (Groebe et al., 1995; Hann et al., 1994; Myers et al., 1991; Utkin et al., 1994b), α-CoTx EI binds to the low-affinity *d*-TC site (αδ interface) (Martínez et al., 1995). Additionally, α-CoTxs of the subtypes MI, EI, GI, SI, and SIA have high affinity, albeit at different potencies, for the αδ site of BC_3-H1 cells containing the $\alpha1_2\beta1\gamma\delta$ receptor (Groebe et al., 1995; Kreienkamp et al., 1994; Martínez et al., 1995; Sine et al., 1995b). On the other hand, α-CoTx ImI (Broxton et al., 1999; Johnson et al., 1995; McIntosh et al., 1994; Pereira et al., 1996; Tavazoie et al., 1996), both PnIA and PnIB (Fainzilber et al., 1994), MII (Cartier et al., 1996; Harvey et al., 1997; Tavazoie et al., 1996), EpI (Loughnan et al., 1998), and AuIA–C (Lester et al., 1998; Luo et al., 1998) block different neuronal-type AChRs (see Table 6). In this regard, α-CoTx ImI inhibits both nicotine-evoked mitogenic hormones (e.g. 5-HT) release and human small cell lung

Table 6
Secondary structure of α-conotoxins and nicotinic acetylcholine receptor type specificity

α-Conotoxin (*Conus* species)	Primary[a] and secondary[b] structure	AChR source	IC_{50}[c] (subunit interface)		References
			high-affinity binding site (nM)	low-affinity binding site (μM)	
$\alpha_{3/5}$ *Subclass*					
MI (*C. magus*)	GRCCHPACGKNYSC[d]	BC_3H-1	$1.50 \pm 0.24(\alpha\delta)$; $0.42 \pm 0.15(\alpha\delta)$	22.0 ± 1.1 ($\alpha\gamma$); 23.0 ± 4.1 ($\alpha\gamma$)	(Hann et al., 1994; Zafaralla et al., 1988; Sine et al., 1995b; Utkin et al., 1994b; Martinez et al., 1995; Kreienkamp et al., 1994; Johnson et al., 1995; Groebe et al., 1995; Sugiyama et al., 1998; Quiram and Since, 1998b; Spura et al., 1999; Chiara et al., 1999)
		mouse	$0.55 \pm 0.06(\alpha\delta)$; 0.3 ($\alpha\delta$); 12*	$18.3 \pm 0.93(\alpha\gamma)$; 15 ($\alpha\gamma$)	
		Torpedo	2.6 ± 1.0 ($\alpha\gamma$); 0.12 ± 1.0 ($\alpha\gamma$); 4.5 ± 1.6 ($\alpha\gamma$); 8 ($\alpha\gamma$); 300	2.3 ± 0.7 ($\alpha\delta$); 21 ± 1 ($\alpha\delta$); $0.48 \pm 0.10(\alpha\delta)$; 1 ($\alpha\delta$)	
		human: α7/5-HT_3R; $\alpha_2\beta\epsilon\delta$	30 ± 1 ($\alpha\delta$)[c]	86 ± 4.3 ($\alpha\gamma$)[c]	
GI (*C. geographus*)	ECCNPACGRHYSC[d]	BC_3H-1	4.9 ± 1.9 ($\alpha\delta$); 20*	58 ± 12 ($\alpha\gamma$)	(Zafaralla et al., 1988; Utkin et al., 1994b; Kreienkamp et al., 1994; Groebe et al., 1995; Hann et al., 1994; 1997; McIntosh et al., 1994; Johnson et al., 1995; Quiram and Sine, 1998b)
		mouse	360 ± 40 ($\alpha\gamma$)	24 ± 2 ($\alpha\delta$)	
		Torpedo	39 ± 4 ($\alpha\gamma$); 550	3.3 ± 0.4 ($\alpha\delta$)	
		human: α7/5-HT_3R; $\alpha_2\beta\epsilon\delta$	20 ± 3 ($\alpha\delta$)[c]	685 ± 37 ($\alpha\gamma$)[c]	
		frog		2–4*	
		Eigenmannia (fish)	50–100*		
GIA (*C. geographus*)	ECCNPACGRHYSCGK[d]				
GII (*C. geographus*)	ECCHPACGKHFSC[d]				
CnIA (*C. consors*)	GRCCHPACGKYYSC[d]	*Torpedo*	190		(Favreau et al., 1999)
		α7	14.8		
CnIB (*C. consors*)	CCHPACGKYYSC[d]				
SI (*C. striatus*)	ICCNPACGPKYSC[d]	BC_3H-1	680 ± 160 ($\alpha\delta$)	220 ± 45 ($\alpha\gamma$)	(Ramilo et al., 1992; Zafaralla et al., 1988; Hann et al., 1994; Groebe et al., 1995; Quiram and Sine, 1998b)
		Torpedo	1600 ± 100 ($\alpha\gamma$); 1000; 420	16 ± 1 ($\alpha\delta$)	

(continued on next page)

Table 6 (*continued*)

α-Conotoxin (*Conus* species)	Primary[a] and secondary[b] structure	AChR source	IC_{50}[c] (subunit interface)		References
			high-affinity binding site (nM)	low-affinity binding site (μM)	
		human: α7/5-HT_3R; $\alpha_2\beta\epsilon\delta$	700 ± 70 (αδ)	634 ± 22 (αγ)	
SIA (*C. striatus*)	YCCHPACGKNFDC[d]	BC_3H-1	7.70 ± 0.14(αδ)	200 ± 8.6 (αγ)	(Myers et al., 1991; Zafaralla et al., 1988; Hann et al., 1994; Groebe et al., 1995)
		Torpedo	590 ± 40 (αγ); 420	> 260 (αδ)	
$\alpha_{4/7}$ *Subclass*					
MII (*C. magus*)	GCCSNPVCHLEHSNLC[d]	α3β2	0.5*; 3.5*; 8.0 ± 1.1*; 24.3 ± 2.9; 17.3 ± 0.1		(Cartier et al., 1996; Harvey et al., 1997; Kaiser et al., 1998)
		α4β2		0.4*	
EpI (*C. episcopatus*)	GCCSDPRCNMNNPDYEC[d]	α3β4	84 ± 19*; 210 ± 30*		(Loughnan et al., 1998)
		α3β2 (or β4)	1.6*		
EI (*C. ermineus*)	RDOCCYHPTCNMSNPQIC[d]	BC_3H-1	9.4 ± 1.2 (αδ)	0.28 ± 0.03 (αγ)	(Martinez et al., 1995)
		Torpedo	0.41 ± 0.09(αδ)	0.19 ± 0.02(αγ)	
PnIA (*C. pennaceus*)	GCCSLPPCAANNPDYC[d]	*Patella* (mollusc)	0.15 pmol/mg of body mass**		(Fainzilber et al., 1994; Groebe et al., 1995)
		BC_3H-1		> 5	
PnIB (*C. pennaceus*)	GCCSLPPCALSNPDYC[d]	*Patella* (mollusc)	0.18 pmol/mg of body mass**		(Fainzilber et al., 1994; Groebe et al., 1995; Loughnan et al., 1998)
		BC_3H-1		> 5	
		α3β4	700		
AuIB (*C. aulicus*)	GCCSYPPCFATNPD–C[d]	α3β4	500 ± 140*; 750*		(Luo et al., 1998)
		α7		> 7*	
AuIA (*C. aulicus*)	GCCSYPPCFATNSDYC[d]				
AuIC (*C. aulicus*)	GCCSYPPCFATNSGYC[d]				
$\alpha_{4/3}$ *Subclass*					
ImI (*C. imperialis*)	GCCSDPRCAWRC[d]	α7	200*; 300*		(McIntosh et al., 1994; Johnson et al., 1995; Groebe et al., 1995; Codignola et al., 1996; Pereira et al., 1996; Kehoe and McIntosh, 1998; Quiram and Sine, 1998b; Lopez et al., 1998; Broxton et al., 1999)
		α9		1.8*	
		α3β3/α3β4α5		2.5 ± 1.2	
		human: α7/5-HT_3R; $\alpha_2\beta\epsilon\delta$	2380 ± 500[c]	119 ± 4.0[c]	
		mouse		51*	
		BC_3H-1		> 2	

		rat	> 20		
		frog			
			250–500*		
		Eigenmannia (fish)		25–50*	
		Aplysia: Cl^- response; Na^+ response	47*; 150 ± 22*		
$\alpha_{3/5/3}$ *Subclass*					
SII (*C. striatus*)	GCCCNPACGPNYGCGTSCS[d]	BC_3H-1		18 ± 6.6	(Ramilo et al., 1992; Groebe et al., 1995)
		Torpedo		8	
αA *Subclass*					
αA-EIVA (*C. ermineus*)	GCCGPYONAACHOCGCKVGROOYCDROSGG[d]	*Torpedo*	17*		(Jacobsen et al., 1997)
		mouse	11 ($\alpha_2\beta\gamma\delta$)*; 32, 11* ($\alpha\beta\gamma$); 37, 15* ($\alpha\beta\delta$)		
		BC_3H-1	150 ± 10		
αA-EIVB (*C. ermineus*)	GCCGKYONAACHOCGCTVGROOYCDROSGG[d]	*Torpedo*	18*		(Jacobsen et al., 1997)
αA-PIVA (*C.purpurascens*)	GCCGSYONAACHOCSCKDROSYCG[d]	*Torpedo*	1–10		(Hopkins et al., 1995)

[a] The sequence alignment of the different α-CoTxs is shown in the standard one-letter amino acid code. The letter O represents *trans*-4-hydroxyproline.
[b] α-Conotoxin subclasses $\alpha_{3/5}$, $\alpha_{4/7}$, and $\alpha_{3/7}$ are formed by two disulfide bonds, while αA-CoTx subclass and α-CoTx SII ($\alpha_{3/5/3}$ subclass) have three disulfide bonds.
[c] These values were obtained by inhibition of [^{125}I]α-BTx binding except those determined *electrophysiologically or by **bioassays.
[d] Amidated COOH-terminus. Instead, α-CoTx SII presents a free COOH-terminus.
[e] Sulfated residue.

carcinoma proliferation (Codignola et al., 1996), nicotinic synapses on B neurons in frog sympathetic ganglia (Tavazoie et al., 1996), and the α-BTx-resistant nicotinic response in bovine adrenal chromaffin cells (Broxton et al., 1999). This toxin has been also found to discriminate between either the desensitizing or the sustained Cl^--dependent response in *Aplysia* neurons (Kehoe and McIntosh, 1998). The MII subtype blocks nicotine-stimulated dopamine release in rat striatal synaptosomes (Kaiser et al., 1998; Kulak et al., 1997), nicotinic synapses on C neurons in frog sympathetic ganglia (Tavazoie et al., 1996), and the slow component of embryonic avian ciliary ganglion neurons (Ullian et al., 1997). The AuIB type is the only α-CoTx from four related peptides tested that blocks nicotine-evoked norepinephrine release (Luo et al., 1998). The ability of α-CoTxs to discriminate between diverse AChR types may have potential significance for designing drugs for clinical use.

In order to determine which subunits from the *Torpedo* AChR are involved in the α-CoTx binding site, the purified α-CoTx MI was crosslinked with the AChR by using several bivalent succinimide reagents (Myers et al., 1991). In addition, two azidosalicylate α-CoTx GIA derivatives were used for photoaffinity labeling of the AChR (Myers et al., 1991). These studies showed that depending on the α-CoTx derivative used, the specifically labeled AChR subunits were βγ or δγ (Table 1). More precisely, the labeled sites on the γ and β subunits were located between residues 121 and 183 and between residues 149 and 225, respectively. In addition, the *p*-benzoylphenylalanyl derivative of α-CoTx GI labeled the α subunit-containing interfaces (Kasheverov et al., 1999).

In order to identify the determinants of α-CoTx MI selectivity, Sine's laboratory used different δ/γ chimeras and site-directed mutagenesis (Sine, 1997; Sine et al., 1995b). From these studies it was found that the elicited high affinity of subtype MI for the αδ subunit interface of mammalian AChRs is determined by amino acids S^{36}, Y^{113}, and I^{178} from the δ subunit, while the elicited low affinity for the αγ interface is determined by residues K^{34}, S^{111}, L^{119}, and F^{172} corresponding to the γ chain. Since δY^{113} and γS^{111} are exchanged by Arg and Tyr in the *Torpedo* AChR, these two natural mutations may account for the observed site-specificity between both species. This idea was corroborated by the fact that the mutation $\delta R113Y$ on $\alpha_2\beta\delta_2$ or the exchange $\gamma Y111R$ on $\alpha_2\beta\gamma_2$ *Torpedo* AChRs resulted either in an enhancement or a decrease in α-CoTx MI affinity, respectively (Chiara et al., 1999) (Table 5).

By using the same approach, Prince and Sine (1996) identified pairs $\gamma K^{34}/\delta S^{36}$ and $\gamma F^{172}/\delta I^{178}$ (loops D and G in Fig. 3) as primary determinants for CCh selectivity in mouse AChRs (see Table 3). This result co-

incides with that for the α-CoTx MI selectivity. On the contrary, neither mutation γS111Y nor δY113S affected CCh affinity, suggesting that agonists and at least the α-CoTx MI subtype do not share all the same selectivity determinants.

Since other residues from the α subunit have been considered to be involved in the agonist/competitive antagonist binding sites (see Table 2), Sugiyama et al. (1998) examined the contribution of some of these residues to the binding of α-CoTx MI. Mutations αY190F and αY189F do not affect α-CoTx MI affinity whereas the removal of aromaticity by exchanging these residues for Thr has a marked influence on α-CoTx association (Table 5). This suggests that aromaticity may be required to stabilize the cationic peptide. The effect elicited by mutations on residues Y^{93} (loop A in Fig. 3) and D^{152} (loop B in Fig. 3) (Table 5) indicates that both peptidic and nonpeptidic ligands bind to the same regional segments of sequence but not to identical residues.

In order to determine the existence of linkage relationship between mutations from α and δ/γ subunits, a mutant cycle analysis was used (Sugiyama et al., 1998). From this study, a high coupling energy (2.9 kcal/mol) between S^{36} and I^{178} from the δ subunit is demonstrated. On the contrary, a relatively low linkage ($\leq$0.35 kcal/mol) between residues $\alpha Y^{93}/V^{188}$ and pairs $\gamma K^{34}/\delta S^{36}$, $\gamma S^{111}/\delta Y^{113}$, and $\gamma F^{172}/\delta I^{178}$ is evident. Taking into account that the energetic contributions to α-CoTx MI association of amino acids in the α chain seem to be independent from the ones at the δ/γ subunits, it is postulated that one of the surface of the neurotoxin molecule interacts with the α subunit whereas the other surface interacts with the δ or the γ chain. In this regard, recent conformational studies by [H^1]-NMR spectroscopy suggest that both faces of the α-CoTx GI are involved in the orientation of the molecule within the αδ subunit interface (Gehrmann et al., 1998). The binding face of α-CoTx GI, a toxin closely related to the MI subtype structure, interacts by means of residues C^2, N^4, P^5, A^6, and C^7 (from loop I) with the α1 subunit, whereas the selectivity face comprising amino acids R^9 and H^{10} (from loop II) is oriented towards the δ subunit (the subunit forming the high-affinity α-CoTx GI locus in mammalian AChRs). Residues R^9 and H^{10} were found to be responsible for the high differential selectivity and affinity between both cholinergic ligand binding sites (Groebe et al., 1997; Hann et al., 1997). More precisely, the mutation R9P diminished by 330- and five-fold the elicited α-CoTx GI inhibition of [^{125}I]α-BTx binding to either the high (αγ) or the low (αδ) affinity site, respectively, on detergent-solubilized *Torpedo* AChRs (Hann et al., 1997). In addition, the mutation P9R (Hann et al., 1997) or P9K (Groebe et al., 1997) on the α-CoTx SI, a toxin that does not discriminate between both *Torpedo* ligand binding sites (see Table 6), restores the selectivity for the αγ interface. The lack of effect of the mutation P^9 to the neutral residue Ala on the α-CoTx SI suggests that the cationic group of A^9 on the α-CoTx GI plays a major role in αγ selectivity on the *Torpedo* receptor. The critical difference between α-CoTx GI and SI has been ascribed to position 9 (reviewed in Guddat et al., 1996). For instance, the affinity and selectivity of α-CoTx SI resembled to that of α-CoTx GI when the single residue substitution P9K in α-CoTx SI was performed. The mutation increased the α-CoTx affinity for the mouse AChR by two orders of magnitude. The importance of a cationic group conducting high selectivity is remarked by the fact that mutations on α-CoTx MI K^{10}, the homologous residue of A^9, produced loss of selectivity (Hann et al., 1997).

Taking into account that neuronal receptors containing the subunit pattern α4β2, α2β2, or α3β4 are more than 200-fold less sensitive to α-CoTx MII than α3β2, the determinants of α-CoTx selectivity were identified by using chimeric and mutant subunits (Harvey et al., 1997). Sequence segments 121–181 and 181–195 from the α3 subunit and 1–54, 54–63, and 63–80 from the β2 subunit were found to be the most important ones for α-CoTx MII selectivity. More specifically, residues $\beta 2T^{59}$, $\alpha 3K^{185}$, and $\alpha 3I^{188}$ were identified as determinants for α-CoTx MII sensitivity (see Table 5). Amino acid $\alpha 3K^{185}$ may be electrostatically interacting with E^{11} from α-CoTx MII. An important difference is that the β2T59D mutation does not affect α-CoTx MII sensitivity as was determined on κ-BTx (Harvey and Luetje, 1996), indicating that the interaction of α-CoTx with $\beta 2T^{59}$ is not charge-dependent.

Regarding α-CoTx ImI specificity, pairs $\alpha 7W^{55}$/$\alpha 1R^{55}$, $\alpha 7S^{59}$/$\alpha 1Q^{59}$, and $\alpha 7T^{77}$/$\alpha 1K^{77}$ have been considered as components conferring high affinity for α7/5-HT_3R over α1/5-HT_3R homooligomeric chimera (Quiram and Sine, 1998a) (Table 5). The third pair has not been previously described as a ligand component and may represent a new loop or an allosterically coupled loop. Experiments performed in parallel evidenced that two regions in the α-CoTx ImI molecule are essential for binding to the α7/5-HT_3R chimera (Quiram and Sine, 1998b): a region comprising residues D^5–P^6–R^7 in the first loop and a second region in loop II formed by W^{10}. Since P^6 is highly conserved among α-CoTxs, it seems likely that this residue, in addition to the two disulfide bridges, contributes to structural rigidity. The charge and side chain length of both D^5 and R^7 residues as well as the aromatic property of W^{10} seem to be important for the interaction with the α7 AChR. An important feature of α-CoTx ImI is that the cationic residue R^{11} is not important for binding as it is observed for MI and SI α-CoTx subtypes which are specific for muscle-type AChRs (Groebe et al., 1997; Hann et al., 1997; Sine et al., 1998).

In addition to the above expounded evidence, crosslinking the AChR with radiolabeled ω-CoTx GVIA, which has been extensively used as a probe for N-type neuronal presynaptic Ca^{2+} channels (see review by Adams and Olivera, 1994; Olivera et al., 1990), the mainly labeled subunit was α1 (Horne et al., 1991). Since this crosslinking was reduced by Ca^{2+} in the millimolar concentration range but not by α- or κ-BTx, α-CoTx, or CCh, we would be in the presence of a novel binding site for ω-CoTxs on the AChR α1 subunit that is structurally related to the Ca^{2+} locus. A specific site that recognizes Ca^{2+} with a K_d of 1 mM has been found on the AChR α1 subunit (Rübsamen et al., 1978). In accordance with the possibility that AChR is in fact affected by this particular CoTx, the nicotine-induced inward current in chromaffin cells was partially blocked by 1 μM ω-CoTx GVIA (Fernández et al., 1995; Villarroya et al., 1997). In addition, other Ca^{2+} channel blockers such as ω-CoTx MVIIA and MVIIC subtype, partially inhibited $^{45}Ca^{2+}$ entry-induced dimethylphenylpiperazinium in chromaffin cells (Villarroya et al., 1997).

From these results it is evident that: (1) α-CoTxs are peptides able to discriminate among distinct AChR subtypes and thus, may be used in combination with other selective cholinergic ligands to "fingerprint" AChR subtypes in different cells and tissues; and (2) specific residues in the cholinergic binding site are energetically coupled with their corresponding pairs in the toxin stabilizing the α-CoTx-AChR complex.

5. Arrangement of the nicotinic acetylcholine receptor subunits

Depending on which non-α subunit is located between both α subunits, the α subunit could be framed by a combination of γβ, δβ, or γδ pairs (for models of subunit organization see review by Fairclough et al., 1993). One model where γδ is inserted between both α subunits was proposed on the basis of crosslinking of subunits image reconstruction technique (Kistler et al., 1982), image analysis of tubular crystals from *T. marmorata* (Toyoshima and Unwin, 1990), and cholinergic agonist-dependent toxin crosslinking to AChR subunits (Hamilton et al., 1985). With the same basic approach, the high-affinity ACh binding site was located at the αδ pair and the low-affinity site at the αγ pair, in an arrangement where the β subunit is in between the two α subunits, and the high- and low-affinity ACh binding site-containing α subunits are in front of the γ and δ subunits, respectively (Chatrenet et al., 1990). The localization of the β subunit in between the α chains received support by the use of electron microscopy and the antibody 247G which is considered to be a possible marker of the *d*-TC high-affinity binding site (i.e. the αγ interface) (Fairclough et al., 1993). However, it is necessary to take into consideration that specific antibodies against the agonist high-affinity binding site provoke a great conformational change on the overall AChR structure and particulary on the agonist low-affinity binding site (Valenzuela et al., 1994b). Thus, we should be very careful in generating models based on the interpretation of experiments by using monoclonal or polyclonal antibodies.

By using *d*-TC as a probe to label the competitive antagonist binding sites on the AChR, either the δ or the γ subunit were inferred to reside between both α subunits (Pedersen and Cohen, 1990). By means of other experimental evidence, Hucho's group has proposed that the γ subunit is located between the two α chains in an arrangement αγαδβ (Machold et al., 1995c; reviewed in Arias, 1997; Hucho et al., 1996). In Fig. 6, we show the most plausible arrangement of the muscle-type AChR subunits.

For the case of neuronal-type AChRs where the existent subunits are α and β (or non-α), one of the most abundant receptors in the brain has the stoichiometry $\alpha_2\beta_3$ (reviewed in Arias, 1997, 1999). In almost all cases the AChR-forming α subunit subtype is the same but eventually, two different α chains coexist in the same receptor. In this context and by analogy with the muscle-type AChR, we can assume that neuronal-type AChRs possess a pseudo-five-fold symmetry with one of the β subunits in between both α chains. This picture is not valid for α7 and probably for α8 and α9 subunits since each one of them yielded functional channels when they were expressed in *Xenopus* oocytes. Nevertheless, in vivo they might be assembled with unidentified subunits. In this regard, α7 and α8 subunits have been found to coassemble to form heteromers in chick retina (Keyser et al., 1993).

In conclusion, the most probable subunit arrangement for the muscle-type AChR is αγαδβ in a clockwise manner.

6. Agonist binding sites–directed antibodies

6.1. Polyclonal and monoclonal antibodies

Since agonists bind to the α subunit and compete with the binding of neurotoxins, both agonists and neurotoxins are considered to bind at overlapping sites (for a review see Conti-Tronconi et al., 1994). One alternative approach to study this issue is the use of polyclonal and monoclonal antibodies raised against the AChR to characterize the binding site for agonists and neurotoxins. Monoclonal antibodies have been of fundamental importance in the elucidation of the following. (1) The synthesis, assembly, and transmem-

brane topology of AChR subunits (e.g. Watters and Maelicke, 1983; reviewed in Conti-Fine et al., 1996). (2) The localization, structure, and pharmacological properties of agonist binding sites (e.g. Fairclough et al., 1993). (3) The differences between neuronal AChR subtypes (for a review see Lindstrom, 1986); (4) AChR ion channel activation (Bufler et al., 1996, 1998). (5) The AChR conformational changes elicited by the same antibodies (Tamamizu et al., 1996; Valenzuela et al., 1994b). For example, monoclonal antibodies raised against native *Torpedo* (Conti-Tronconi et al., 1990; Watters and Maelicke, 1983) and mouse (Goldberg et al., 1983; Mochly-Rosen and Fuchs, 1981) AChRs, as well as polyclonal antibodies raised against native human AChRs, are mutually exclusive with α-BTx and cholinergic ligand binding. In addition, monoclonal antibodies directed against *Torpedo* AChR, on both solubilized and bound states, partially overlap with agonist and competitive antagonist binding sites (Watters and Maelicke, 1983).

Interestingly, WF6, a monoclonal antibody directed against the agonist binding sites, activates the AChR ion channel in the nanomolar concentration range (Bufler et al., 1996). Antibodies purified from myasthenic patients blocked the peak ACh current amplitude (Bufler et al., 1998). Functionally, rat antisera directed against a synthetic peptide corresponding to α183–200 from *Torpedo* AChR, decreased the amplitude of miniature endplate potential in rat skeletal muscle. This is in agreement with the fact that the monoclonal antibody 247 inhibits the opening of the AChR ion channel (Tamamizu et al., 1996). Opposite to this, monoclonal antibodies, directed against a synthetic peptide corresponding to the sequence 173–204 of the α1 subunit from *T. californica,* did not interfere with α-BTx binding and vice versa (Preston-Hurlburt et al., 1990). Probably, this divergence is due to the necessity of an appropriate tertiary folding of the α chain for the obtention of specific antibodies. The fact that the affinity of α-BTx for denatured, proteolized, or synthetic α segments is several orders of magnitude lower than that for native AChR is in agreement with this idea (Gershoni, 1987; Neumann et al., 1986).

It is known that the region flanking loop $C^{192–193}$ is specifically involved in agonist binding. For example, reduction of disulfide (Criado et al., 1986; Walker et al., 1984) or mutation of C^{192} or C^{193} (Mishina et al., 1985) affected cholinergic binding but did not significantly affect [^{125}I]α-BTx binding (see Tables 2 and 5). In addition, the labeling of AChR by high concentration of BrACh for a long period after sodium borohydride reduction was not affected by α-BTx treatment (Dunn et al., 1993). Thus, in order to localize this important region, Fairclough et al. (1993) used the monoclonal antibody 383C. This antibody presents a stoichiometry of one binding site per AChR, completely inhibits α-BTx binding, blocks CCh binding to only one site, does not produce significant changes on *d*-TC affinity, and binds to peptide α187–199. The results from X-ray diffraction analysis are in agreement with the location of 383C at the top of the extracellular region of the AChR.

The regions bordering the $C^{192–193}$ pair contain the major elements of the binding site for the monoclonal antibody WF6 (Conti-Tronconi et al., 1991; reviewed in Conti-Fine et al., 1996). In particular, residues W^{187}, T^{191}, P^{194}, D^{195}, and Y^{198} have been identified. Interestingly, WF6 competes with agonist binding on the AChR but not with the binding of small antagonist molecules (Conti-Tronconi et al., 1990). The locus for this antibody and for FK1, were recently found to be neighbors on the α subunit of the *Torpedo* AChR (Schröder et al., 1994). More precisely, the sequence regions 118–145 and 181–200 are the epitopes for the FK1 antibody. The synthetic polypeptide encoding residues 118–137 displayed the highest FK1 binding affinity. The attachment points for both FK1 and WF6 antibodies were considered to be distinct by using analogues of the 181–200 sequence containing one substituted residue.

Different interactions between the monoclonal antibody 5.5 and α-BTx on agonist binding to mouse and mongoose α subunits were also demonstrated (Kachalsky et al., 1993). This indicates that these two polypeptides recognize different moieties within the agonist binding site. This concept is in agreement with the accelerated dissociation of toxin-AChR complexes elicited by large concentrations of small cholinergic ligands (Kang and Maelicke, 1980 and references therein) and with the observed partial competence between antibodies from the serum of myasthenic patients and nicotinic ligands on chicken embryo myogenic cultures (Fulpius et al., 1980).

In conclusion, the use of antibodies directed to the agonist/competitive antagonist binding sites has allowed to elucidate the existence of either separate loci for small cholinergic agents and toxins or additional agonist sites (noncompetitive agonist) that interact allosterically with the agonist binding sites.

6.2. Antibody-induced global conformational changes in the AChR

Pharmacological and biochemical evidence indicate that monoclonal antibodies would induce significant structural changes in the AChR. For example, a monoclonal antibody raised against the α subunit blocked ligand interaction to the ACh binding sites (Fels et al., 1986). In this regard, we have studied the effect of two monoclonal antibodies, A6 and B1, that specifically recognize the high- and the low-affinity ACh binding site on the AChR, respectively (Valen-

zuela et al., 1994b) (see Fig. 5). These antibodies were used to direct the binding of dansyl-C_6-choline to the unblocked ACh binding site. Then, FRET and quenching techniques were used to assess the antibody-induced changes in the distance between AChR-bound dansyl-C_6-choline and the membrane surface. By using the Off-Axis FRET model (see Fig. 4), transverse distances of 39 and 31 Å were obtained between the two dansyl-C_6-choline binding sites (without antibodies) and the respective membrane-partitioned lipid probes C_{18}-rhodamine and C_{12}-eosin (Valenzuela et al., 1994a). In the presence of the antibody that recognizes the high-affinity ACh binding site (A6), the determined transverse distance between the low-affinity ACh binding site and the surface membrane was nearly nil. On the contrary, in the presence of the antibody that specifically binds to the low-affinity ACh binding site (B1), the distance between the high-affinity ACh binding site and the surface membrane was practically the same as the one found without antibodies: 31 and 40 Å by using C_{18}-rhodamine or C_{12}-eosin, respectively. This dramatic difference suggests that the A6 antibody induced the unblocked site move in close proximity to the lipid membrane.

This effect was corroborated by using the relative ability of 5-doxylstearate (5-SASL), a short-range lipophilic quencher, to reduce the emission of AChR-bound dansyl-C_6-choline fluorescence (Valenzuela et al., 1994b). In the absence of antibodies, 5-SASL quenching effectiveness was 160-fold lesser for the specifically bound dansyl-C_6-choline fluorescence than for membrane-partitioned C_{18}-rhodamine fluorescence. In the presence of A6, an increase of 45-fold in the dansyl-C_6-choline quenching constant was found after correction for the A6-induced adsorption of 5-SASL. In addition, the increase in the dansyl-C_6-choline quenching constant was seven times in the presence of B1. However, whereas the magnitude of the 5-SASL accessibility to AChR-bound dansyl-C_6-choline in the presence of A6 was within a factor of two of its accessibility to the membrane-partitioned C_{18}-rhodamine probe, the 5-SASL accessibility to AChR-bound dansyl-C_6-choline in the presence of B1 was still 27-fold lower than that for the same lipid probe. Although the results clearly showed that A6 induced proximity of the antibody-free agonist binding site to the membrane surface, the mechanism by which A6-induced structural changes on the AChR is unknown.

A possible model where there is either a (1) full or (2) partial movement of the AChR is illustrated in Fig. 9.

1. A full movement of the AChR would imply either (a) a specific rotation of its major symmetry axis or (b) a transverse motion of its extracellular domain into the lipid membrane. Both possibilities would shift extracellular and perhaps cytoplasmic domains into the lipid membrane concomitantly with exposure of AChR transmembrane domains to extracellular and cytoplasmic space (Fig. 9(A)). In this case, very large areas of normally hydrophilic surfaces would have to be converted into hydrophobic surfaces, and vice versa.
2. A partial movement would involve a folding or peeling back, like a flower petal, of a portion of the AChR into the lipid membrane (Fig. 9(B)). Viewed thermodynamically, case (1) would appear to be energetically more expensive than case (2). Thus, the more plausible physical interpretation of the results is that the monoclonal antibody A6 induced a partial motion of the AChR. An additional conclusion is the significant flexibility of the AChR protein or at least of the area of the receptor that forms the low-affinity ACh binding site. This distinctive flexibility between both ACh binding sites

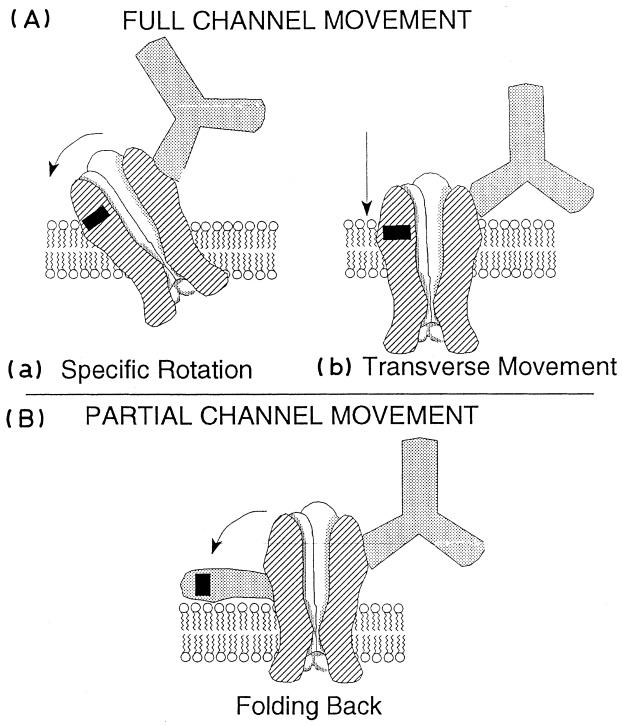

Fig. 9. Schematic representation of the possible effect of the monoclonal antibody A6 on the AChR (modified from Valenzuela et al., 1994b). (A) Two types of possible full movements of the AChR that would result in the motion of the low-affinity ACh binding site (represented here with a filled rectangle) in close proximity to the lipid membrane are despicted: (a) A specific rotation of the AChR about its major symmetry axis that would make it appear tilted. (b) A transverse movement of the AChR as if the protein had been pushed into the lipid membrane. (B) Possible partial movement of the AChR induced by A6. In this case, only a portion of the AChR, which includes the low-affinity ACh binding site, folds back like a flower petal into the lipid membrane.

might be, at least partially, responsible for the observed differences in agonist affinities.

In agreement with the monoclonal antibody A6-induced movement, both the monoclonal antibody 387 which inhibits 20% the AChR single-channel amplitude, and the monoclonal antibody 247, which binds to the αγ subunit interface and blocks ion channel activity, elicits the transition between the resting and desensitized states as monitored by the extent of decreased labeling by the photoreactive probe and high-affinity NCI 3-(trifluoromethyl)-3-(*m*-[^{125}I]iodophenyl)diazirine (Tamamizu et al., 1996). These antibodies would serve as valuable tools because they are able to decouple agonist binding from channel opening. Opposite to this, the monoclonal antibody 370, which binds to both agonist sites, neither alters single-channel behavior nor produces any AChR structural transition.

These studies indicate that the binding of monoclonal antibodies to the agonist binding sites induces a major conformational change in the AChR. Thus, precaution in the use of monoclonal antibodies for structural studies should be considered.

7. Noncompetitive agonists

7.1. Localization of the noncompetitive agonist binding site

Experimental evidence by using pharmacological and electrophysiological approaches indicated that neuromuscular transmission is affected by AChE inhibitors. Definitive evidence supports a direct interaction of classical AChE inhibitors such as carbamates and oximes with sites on the AChR (reviewed in Arias, 1997). At high concentrations (i.e. ≥100 μM), these compounds affect the kinetics of the AChR by acting as NCIs. The principal site of action of these drugs on the AChR seems to be the ion channel and the binding site would be located half-way across the membrane. Other cholinergic properties elicited by different AChEIs were also observed (reviewed in Arias, 1997). For instance, ecothiopate, soman, sarin, *O*-ethyl *S*-[2-(diisopropylamino)ethyl]methyl phosphoenolthiolate, edrophonium, and diisopropylfluorophosphate seem to enhance the rate of AChR desensitization in the micromolar concentration range. Whereas paraoxon, phospholine, diisopropylfluorophosphate, aminocarb, aldicarb, monocrotophos, dicrotophos, azinphos-methyl, and dichlorvos compete for the agonist binding sites at higher concentrations.

Despite the above description of the cholinergic properties elicited by reversible and irreversible AChE inhibitors on the AChR, a more complex picture was observed for certain compounds that activate the AChR by means of a weak agonist cholinergic activity (reviewed in Alburquerque et al., 1997; Arias, 1997; Maelicke et al., 1995a). For instance, the major alkaloid of the calabar bean *Physostigma venenosum* Balfour, (−)-physostigmine (also named eserine; see molecular structure in Fig. 2), in addition to its noncompetitive inhibitory property (Canti et al., 1998; Clarke et al., 1994), has been reported to induce at low concentrations (i.e. 0.1–10 μM) cation flux on both muscle (Pascuzzo et al., 1984) and *Torpedo* (Okonjo et al., 1991) receptors, and to enhance 4-[*N*-[(acetoxyethyl]-*N*-methylamino]-7-nitrobenz-2-oxa-1,3-diazole (NBD)-labeled AChR fluorescence (Dunn and Raftery, 1993). Such effects were observed even in the presence of saturating concentrations of ACh or competitive antagonists such as *d*-TC, α-BTx, α-CTx, DHβE, methyllycaconitine, and mecamylamine (Alkondon and Alburquerque, 1991; Dunn and Raftery, 1993; Kuhlmann et al., 1991; Okonjo et al., 1991). Interestingly, the agonist-like features of these molecules was inhibited by the monoclonal antibody FK1 (Okonjo et al., 1991). The same basic results were obtained on both *Torpedo* and neuronal receptors by using electrophysiological techniques (Pereira et al., 1993, 1994; Schrattenholz et al., 1993a,b; Shaw et al., 1985; Sung et al., 1998; Van den Beukel et al., 1998). This pharmacological property was found in several AChR-containing tissues and cells (Schrattenholz et al., 1993a and references therein). In addition, the same pharmacological characteristics as the ones of eserine were found for the classical antagonist benzoquinonium on neuronal AChRs (Pereira et al., 1993; Schrattenholz et al., 1993a), for the snowdrops plant alkaloid galanthamine in the α4β2 subtype (Pereira et al., 1994; Schrattenholz et al., 1993a), and for the morphine derivative codeine which does not bind to the AChE (Storch et al., 1995) (see molecular structures in Fig. 2).

Other carbamates with tertiary amines such as pyridostigmine and neostigmine, and the noncarbamate edrophonium also have the capability of AChR activation but at higher concentration ranges than (−)-physostigmine (Akaike et al., 1984; Alburquerque et al., 1985). However, earlier evidence indicated that these compounds blocked ACh binding to AChR (Seifert and Eldefrawi, 1974). Interestingly, benzoquinonium enhanced the binding of the high-affinity NCI histrionicotoxin to the AChR ion channel in the absence of agonists, indicating that benzoquinonium may activate and subsequently desensitize the receptor (Pereira et al., 1993). The noncompetitive agonists desensitize the AChR much weaker than classical agonists (Pereira et al., 1993, 1994; Storch et al., 1995). Moreover, (−)-physostigmine protects the AChR from

the desensitizing properties of cholinergic agonists (Maelicke et al., 1997).

The stoichiometry of the (−)-physostigmine binding site was found to be two per receptor by photoaffinity labeling and equilibrium binding experiments (Maelicke et al., 1995a,b; Schrattenholz et al., 1993a). Regarding the specific localization of this novel noncompetitive agonist binding site, (−)-physostigmine has been shown to label to residue K^{125} from the sequence 109–151 of the α1 subunit (Schrattenholz et al., 1993a) (Table 1). The noncompetitive agonist site overlaps, at least partially, with the binding site for the monoclonal antibody FK1 (Pereira et al., 1994; Schrattenholz et al., 1993b; Storch et al., 1995). This binding site is located, by means of hydrophobicity profile, in an amphipathic domain at the extracellular region of the AChR which may form a β-pleated sheet domain (Stroud et al., 1990). A similar secondary structure using newer and better prediction methods was also obtained (Le Novère et al., 1999). Taking into account that these agonist noncompetitive molecules are relatively hydrophobic, their binding sites are assumed to be located at the bottom of a gorge in between of the hydrophobic segments 118–124 and 130–137 of the α1 subunit. In addition, a nitrogen that is charged at physiological pH and that is located at an appropriate distance from the phenolic hydroxyl seems to be a structural requirement for these molecules (see Fig. 2). It has been suggested that the binding sites for the monoclonal antibodies FK1 and WF6, (−)-physostigmine, and ACh are located in neighboring domains (Schröder et al., 1994). Interestingly, the residues around K^{125} are conserved in most α subunits but are absent in non-α subunits (Pereira et al., 1993a,b).

The labeling results suggest that noncompetitive agonist molecules interact with residue K^{125} located on the α1 AChR subunit.

7.2. Physiological function of noncompetitive agonists

The physiological role of the noncompetitive agonist binding site is still unknown. An important question is whether these compounds may activate macroscopic currents as ACh or other cholinergic agonists do. In this regard, (−)-physostigmine (or galanthamine or codeine)-evoked macroscopic currents were found neither in muscle nor in neuronal cells even when applied at relatively high concentrations (Maelicke et al., 1997; Storch et al., 1995). A reasonable explanation is that the AChR activation mediated by (−)-physostigmine is produced at concentrations such that they also block ion channel flux. Additional evidence suggests that the inability to produce sizable whole-cell currents is due to both very short mean open times (fractions of milliseconds) and very low frequencies of channel openings.

Another question still remains: is there synergism between classical agonists and noncompetitive agonists to activate the AChR? Indeed, noncompetitive agonists seem to increase both the frequency of single-channel episodes and the amplitude of submaximal whole-cell currents activated by classical cholinergic agonists (Schrattenholz et al., 1996). In other words, the binding of noncompetitive agonists induces a conformational change on the AChR that facilitates the conversion from the resting to the open channel state elicited by ACh. An attractive hypothesis is the existence of an endogenous molecule that modulates the pharmacological action of ACh on AChRs upon binding to this unique site. Searching for such endogenous noncompetitive agonist indicated 5-HT (see molecular structure in Fig. 2), which has been recognized as an endogenous NCI (reviewed in Arias, 1998a,b), as a possible candidate. 5-Hydroxytryptamine was shown not to be able to directly activate AChRs but to inhibit the effect of (−)-physostigmine as well as to potentiate the pharmacological effect of ACh (Maelicke et al., 1997; Schrattenholz et al., 1996). Moreover, the mutated M2T247L α7 receptor was found to be activated by 5-HT in the submicromolar concentration range without the presence of any other agonist (Palma et al., 1996b, 1997). This pharmacological attribute resembles to that found for the co-agonistic property of both glycine on aspartate-activated *N*-methyl-D-aspartate subtype of GluR (reviewed in McBain and Mayer, 1994) and benzodiazepines on $GABA_A$Rs (reviewed in McDonald and Twyman, 1992). This evidence supports the conjecture that certain neurotransmitters specific for one receptor class may behave as modulating ligands for another receptor category (reviewed in Arias, 1998b). This could be a general mode of control in the nervous system.

The suggested AChR activation by means of another pathway distinct from those for the classical agonist ACh has been presently considered to be unlikely. Nevertheless, the mode by which noncompetitive agonists inhibit the AChR desensitization process might have the putative function of regulating the stability of desensitized AChRs thereby protecting the synapse activity from pathological situations where a long lasting pulse of high ACh concentration exists and thus, the transmutation from the desensitized to the resting state is very slow. The most convincing hypothesis for the function of a putatively endogenous noncompetitive agonist is to elicit an allosteric modulation by means of the co-activating properties of this molecule on agonist-stimulated AChRs.

An important consequence of the interaction of eserine with neuronal AChRs is the observed enhancement in memory in Alzheimer's disease (Thal et al., 1983) and cognition (Starter, 1991). More recently, the increase in the number of α4β2 receptors elicited by

chronic treatment with 1,2,3,4-tetrahydro-9-aminoacridine (tacrine), a reversible AChE inhibitor used to improve cognitive function in Alzheimer patients, has been considered to be achieved through interaction with a binding site on the AChR different to that for nicotine (Svensson and Nordberg, 1996). In addition, tacrine has been also demonstrated to behave as a NCI (Canti et al., 1998; Clarke et al., 1994). The observed high efficacy of heptylphysostigmine and phenserine, both (−)-physostigmine derivatives, to enhance learning performance on aged animals (Ikari et al., 1995 and references therein) might be mediated, in addition to its inhibitory effect on AChE, by the interaction of these drugs with the noncompetitive agonist binding site. In this regard, the synthesis and chemical characterization of new molecules acting at this particular locus will be of therapeutic importance for the treatment of neurodegenerative diseases such as Parkinson's paralysis, myasthenia gravis, several myasthenic syndromes, and Alzheimer's dementia (reviewed in Maelicke and Alburquerque, 1996).

The above results suggest that 5-HT may act as co-agonist of several AChRs to enhance the elicited pharmacological action of cholinergic agonists.

8. Conclusions

The expounded information of this review supports the concept that the AChR is an allosteric protein with multiple overlapping ligand binding sites. Several models for the localization and organization of different binding sites were depicted. Since these model were developed mostly from biochemical data, additional quantitative structural studies such as X-ray crystallography and NMR will be necessary to corroborate the correctness of these models.

The agonist and competitive antagonist binding sites are found at the interfaces of two AChR subunits. The link between specific subunits by means of the binding of ACh molecules might play a pivotal role in the relative shift among receptor subunits. This conformational change would allow the opening of the intrinsic receptor cation channel transducting the external chemical signal elicited by the agonist into membrane depolarization. In addition to this basic knowledgement, the discernment of the specific structural components that drive the binding of each cholinergic ligand will be important for the development of new and better drugs that help to alleviate several neurological disorders.

Acknowledgements

I thank Dr Gustavo Appignanesi for his help with the English language and Marcelo Distéfano for his help with the art work.

References

Abramson, S.N., Pi, Y., Culver, P., Taylor, P., 1989. An analog of lophotoxin reacts covalently with Tyr^{190} in the α-subunit of the nicotinic acetylcholine receptor. J. Biol. Chem. 264, 12666–12672.

Ackermann, E.J., Ang, E.T.-H., Kanter, J.R., Tsigelny, I., Taylor, P., 1998. Identification of pairwise interactions in the α-neurotoxin-nicotinic acetylcholine receptor complex through double mutant cycles. J. Biol. Chem. 273, 10958–10964.

Ackermann, E.J., Taylor, P., 1997. Nonidentity of the α-neurotoxin binding sites on the nicotinic acetylcholine receptor reveales by modification in α-neurotoxin and receptor structures. Biochemistry 36, 12836–12844.

Adams, M.E., Olivera, B.M., 1994. Neurotoxins: overview of an emerging research technology. Trends Neurosci. 17, 151–155.

Addona, G.H., Andrews, S.H., Cafiso, D.S., 1997. Estimating the electrostatic potential at the acetylcholine receptor agonist site using power saturation EPR. Biochim. Biophys. Acta 1329, 74–84.

Aiken, S.P., Sellin, L.C., Schmidt, J.J., Weinstein, S.A., McArdle, J.J., 1992. A novel peptide toxin from *Trimeresurus wagleri* acts pre- and post-synaptically to block transmission at the rat neuromuscular junction. Pharmacol. Toxicol. 70, 459–462.

Akaike, A., Ikeda, S.R., Brookes, N., Pascuzzo, G.J., Rickett, D.L., Alburquerque, E.X., 1984. The nature of interactions of pyridostigmine with the nicotinic acetylcholine receptor–ion channel complex. II. Patch clamp studies. Mol. Pharmacol. 25, 102–112.

Alburquerque, E.X., Deshpande, S.S., Kawabuchi, M., Aracava, Y., Idriss, M., Rickett, D.L., Boyne, A.F., 1985. Multiple actions of anticholinesterase agents on chemosensitive synapes: molecular basis for prophylaxis and treatment of organophosphate poisoning. Fund. Appl. Toxicol. 5, S182–S203.

Alburquerque, E.X., Alkondon, M., Pereira, E.F.R., Castro, N.G., Schrattenholz, A., Barbosa, C.T.F., et al., 1997. Properties of neuronal nicotinic acetylcholine receptors: Pharmacological characterization and modulation of synaptic function. J. Pharmcol. Exp. Ther. 280, 1117–1136.

Alkondon, M., Alburquerque, E.X., 1991. Initial characterization of the nicotinic acetylcholine receptors in rat hippocampal neurons. J. Rec. Res. 11, 1001–1022.

Amin, J., Dickerson, I.M., Weiss, D.S., 1994. The agonist binding site of the gamma-aminobutyric acid-type-a channel is not formed by the extracellular cysteine loop. Mol. Pharmacol. 45, 317–323.

Anand, R., Conroy, W.G., Schoepfer, R., Whiting, P., Lindstrom, J., 1991. Neuronal nicotinic acetylcholine receptors expressed in *Xenopus* oocytes have a pentameric quaternary structure. J. Biol. Chem. 266, 11192–11198.

Arias, H.R., 1996. Luminal and non-luminal non-competitive inhibitor binding sites on the nicotinic acetylcholine receptor (Review). Mol. Membr. Biol. 13, 1–17.

Arias, H.R., 1997. Topology of ligand binding sites on the nicotinic acetylcholine receptor. Brain Res. Rev. 25, 133–191.

Arias, H.R., 1998a. Binding sites for exogenous and endogenous non-competitive inhibitors of the nicotinic acetylcholine receptor. Biochim. Biophys. Acta 1376, 173–220.

Arias, H.R., 1998b. Noncompetitive inhibition of nicotinic acetylcholine receptors by endogenous molecules. J. Neurosci. Res. 52, 369–379.

Arias, H.R., 1999. Role of local anesthetics on both cholinergic and serotonergic ionotropic receptors. Neurosci. Biobehav. Rev. in press, 1–27.

Arias, H.R., 1999. Neurosci. Biobehav. Rev. 23, 817–843.

Arias, H.R., Valenzuela, C.F., Johnson, D.A., 1993. Transverse localization of the quinacrine binding site on the *Torpedo* acetylcholine receptor. J. Biol. Chem. 268, 6348–6355.

Ashcom, J.D., Stiles, B.G., 1997. Characterization of α-conotoxin interactions with the nicotinic acetylcholine receptor and monoclonal antibodies. Biochem. J. 328, 245–250.

Asher, O., Jensen, B.S., Lupu-Meiri, M., Oron, Y., Fuchs, S., 1998. The mongoose acetylcholine receptor α-subunit: analysis of glycosylation and α-bungarotoxin binding. FEBS Lett. 426, 212–216.

Aylwin, M.L., White, M.M., 1994a. Ligand-receptor interactions in the nicotinic acetylcholine receptor probed using multiple substitutions at conserved tyrosines on the α subunit. FEBS Lett. 349, 99–103.

Aylwin, M.L., White, M.M., 1994b. Gating properties of mutant acetylcholine receptor. Mol. Pharmacol. 46, 1149–1155.

Balass, M., Katchalski-Katzir, E., Fuchs, S., 1997. The α-bungarotoxin bidning site on the nicotinic acetylcholine receptor: Analysis using phage-epitope library. Proc. Natl. Acad. Sci. USA 94, 6054–6058.

Barchan, D., Kachalsky, S., Neumann, D., Vogel, Z., Ovadia, M., Kochva, E., Fuchs, S., 1992. How the mongoose can fight the snake: The binding site of the mongoose acetylcholine receptor. Proc. Natl. Acad. Sci. USA 89, 7717–7721.

Barchan, D., Ovadia, M., Kochva, E., Fuchs, S., 1995. The binding site of the nicotinic acetylcholine receptor in animal species resistant to α-bungarotoxin. Biochemistry 34, 9172–9176.

Barnard, E.A., 1996. The transmitter-gated channels: a range of receptor types and structures. Trends Pharmacol. Sci. 17, 305–309.

Basus, V.J., Song, G., Hawrot, E., 1993. NMR solution structure of an α-bungarotoxin/nicotinic receptor peptide complex. Biochemistry 32, 12290–12298.

Bennett, J.A., Dingledine, R., 1995. Topology profile for a glutamate receptor: three transmembrane domains and a channel-lining reentrant membrane loop. Neuron 14, 373–384.

Betzel, C., Lange, G., Pal, G.P., Wilson, K.S., Maelicke, A., Saenger, W., 1991. The refined crystal structure of α-cobratoxin from *Naja naja siamensis* at 2.4 Å resolution. J. Biol. Chem. 266, 21530–21536.

Blount, K., Johnson, A., Prior, C., Marshall, I.G., 1992. α-Conotoxin GI produces tetanic fade at the rat neuromuscular junction. Toxicon 30, 835–842.

Blount, P., Merlie, J.P., 1988. Native folding of an acetylcholine receptor α subunit expressed in the absence of other receptor subunits. J. Biol. Chem. 263, 1072–1080.

Blount, P., Merlie, J.P., 1989. Molecular basis of the two nonequivalent ligand binding sites of the muscle nicotinic acetylcholine receptor. Neuron 3, 349–357.

Boess, F.G., Beroukhim, R., Martin, I.L., 1995. Ultrastructure of the 5-hydroxytryptamine$_3$ receptor. J. Neurochem. 64, 1401–1405.

Boess, F.G., Martin, I.L., 1994. Molecular biology of 5-HT receptors. Neuropharmacol. 33, 275–317.

Boess, F.G., Steward, L.J., Steele, J.A., Liu, D., Reid, J., Glencorse, T.A., Martin, I.L., 1997. Analysis of the ligand binding site of the 5-HT$_3$ receptor using site directed mutagenesis: importance of glutamate 106. Neuropharmacol. 36, 637–647.

Bolger, M.B., Dionne, V., Chrivia, J., Johnson, D.A., Taylor, P., 1984. Interaction of a fluorescent acyldicholine with the nicotinic acetylcholine receptor and acetylcholinesterase. Mol. Pharmacol. 26, 57–69.

Bon, F., Lebrun, E., Gomel, J., Van Rapenbusch, R., Cartaud, J., Popot, J.-L., Changeux, J.-P., 1984. Image analysis of the heavy form of the acetylcholine receptor from *Torpedo marmorata*. J. Mol. Biol. 176, 205–237.

Brake, A.J., Wagenbach, M.J., Julius, D., 1994. New structural motif for ligand-gated ion channels defined by ionotropic ATP receptor. Nature 371, 519–523.

Bren, N., Sine, S.M., 1997. Identification of residues in the adult nicotinic acetylcholine receptor that confer selectivity for curariform antagonists. J. Biol. Chem. 272, 30793–30798.

Brownlee, D.J.A., Fairweather, Y., 1999. Exploring the neurotransmitter labyrinth in nematodes. Trends Neurosci. 22, 16–24.

Broxton, N.M., Down, J.G., Gehrmann, J., Alewood, P.F., Satchell, D.G., Livett, B.G., 1999. α-Conotoxin ImI inhibits the α-bungarotoxin-resistant nicotinic response in bovine adrenal chromaffin cells. J. Neurochem. 72, 1656–1662.

Bufler, J., Kahlert, S., Tzartos, S., Toyka, K.V., Maelicke, A., Franke, C., 1996. Activation and blockade of mouse muscle nicotinic channels by antibodies directed against the binding site of the acetylcholine receptor. J. Physiol. 492.1, 107–114.

Bufler, J., Pitz, R., Czep, M., Wick, M., Franke, C., 1998. Purified IgG from seropositive and seronegative patients with myasthenia gravis reversibly blocks currents through nicotinic acetylcholine receptor channels. Ann. Neurol. 43, 458–464.

Buhr, A., Baur, R., Sigel, E., 1997. Subtle changes in residue 77 of the γ subunit of α1β2γ2 GABA$_A$ receptors drastically alter the affinity for ligands of the benzodiazepine binding site. J. Biol. Chem. 272, 11799–11804.

Canti, C., Bodas, E., Marsal, J., Solsona, C., 1998. Tacrine and physostigmine block nicotinic receptors in *Xenopus* oocytes injected with *Torpedo* electroplaque membranes. Eur. J. Pharmacol. 363, 197–202.

Cartier, G.E., Yoshikami, D., Gray, W.R., Luo, S., Olivera, B.M., McIntosh, J.M., 1996. A new α-conotoxin wich targets α3β2 nicotinic acetylcholine receptors. J. Biol. Chem. 271, 7522–7528.

Changeux, J.-P., Edelstein, S.J., 1998. Allosteric receptors after 30 years. Neuron 21, 959–980.

Changeux, J.-P., Podleski, T., Wofsy, L., 1967. Affinity labeling of the acetylcholine-receptor. Proc. Natl. Acad. Sci. USA 58, 2063–2070.

Chatrenet, B., Trémeau, O., Bontems, F., Goeldner, M.P., Hirth, C.G., Ménez, A., 1990. Topographical studies of toxin–antibody and toxin–acetylcholine receptor complexes using photoactivatable toxin derivatives. Proc. Natl. Acad. Sci. USA 87, 3378–3382.

Chaturvedi, V., Donnelly-Roberts, D.L., Lentz, T.L., 1992. Substitution of *Torpedo* acetylcholine receptor α1-subunit residues with snake α1- and rat nerve α3-subunit residues in recombinant fusion protein: Effect on α-bungarotoxin binding. Biochemistry 31, 1370–1375.

Chavez, R.A., Hall, Z.W., 1992. The transmembrane topology of the amino terminus of the alpha subunit of the nicotinic acetylcholine receptor. J. Biol. Chem. 266, 15532–15538.

Chen, J., Zhang, Y., Akk, G., Sine, S., Auerbach, A., 1995. Activation kinetics of recombinant mouse nicotinic acetylcholine receptors: mutations of α subunit tyrosine 190 affect both binding and gating. Biophys. J. 69, 849–859.

Chiappinelli, V.A., Weaver, W.R., McLane, K.E., Conti-Fine, B.M., Fiordalisi, J.J., Grant, G.A., 1996. Binding of native κ-neurotoxins and site-directed mutants to nicotinic acetylcholine receptors. Toxicon 34, 1243–1256.

Chiara, D.C., Cohen, J.B., 1997. Identification of amino acids contributing to high and low affinity *d*-tubocurarine sites in the *Torpedo* nicotinic acetylcholine receptor. J. Biol. Chem. 272, 32940–32950.

Chiara, D.C., Middleton, R.E., Cohen, J.B., 1998. Identification of tryptophan 55 as the primary site of [^{3}H]nicotine photoincorporation in the γ-subunit of the *Torpedo* nicotinic acetylcholine receptor. FEBS Lett. 423, 223–226.

Chiara, D.C., Xie, Y., Cohen, J.B., 1999. Structure of the agonist-binding sites of the *Torpedo* nicotinic acetylcholine receptor: Affinity-labeling and mutational anlayses identify γTyr-111/δArg-113 as antagonist affinity determinants. Biochemistry 38, 6689–6698.

Clark, J.H., Martínez-Carrión, M., 1986. Labeling of functionally

sensitive sulfhydryl-containing domains of the actylcholine receptor from *Torpedo californica* membranes. J. Biol. Chem. 261, 10063–10072.

Clarke, P.B.S., Reuben, M., El-Bizri, H., 1994. Blockade of nicotinic responses by physostigmine, tacrine and other cholinesterase inhibitors in rat stratium. Br. J. Pharmacol. 111, 695–702.

Codignola, A., McIntosh, J.M., Cattaneo, M.G., Vicentini, L.M., Clementi, F., Sher, E., 1996. α-Conotoxin Imperialis I inhibits nicotine-evoked hormone release and cell proliferation in human neuroendocrine carcinoma cells. Neurosci. Lett. 206, 53–56.

Cohen, B.N., Figl, A., Quick, M.W., Labarca, C., Davidson, N., Lester, H.A., 1995. Regions of β2 and β4 responsible for differences between the steady state dose-response relationship of the α3β2 and α3β4 neuronal nicotinic receptors. J. Gen. Physiol. 105, 745–764.

Cohen, J.B., Sharp, S.D., Liu, W.S., 1991. Structure of the agonist-binding site of the nicotinic acetylcholine receptor. [^{3}H]Acetylcholine mustard identifies residues in the cation-binding subsite. J. Biol. Chem. 266, 23354–23364.

Conti-Fine, B.M., Lei, S., McLane, K.E., 1996. Antibodies as tools to study the structure of membrane proteins: The case of the nicotinic acetylcholine receptor. Annu. Rev. Biophys. Biomol. Struct. 25, 197–229.

Conti-Fine, B.M., Maelicke, A., Reinhardt-Maelicke, S., Chiappinelli, V., McLane, K.E., 1995. Binding sites for neurotoxins and cholinergic ligands in peripheral and neuronal nicotinic receptors. Studies with synthetic receptor sequences. Ann. N.Y. Acad. Sci. 757, 133–152.

Conti-Tronconi, B.M., Diethelm, B.M., Wu, X., Tang, F., Bertazzon, T., Schröder, B., Reinhardt-Maelicke, S., Maelicke, A., 1991. α-Bungarotoxin and the competing antibody WF6 interact with different amino acids within the same cholinergic subsite. Biochemistry 30, 2575–2584.

Conti-Tronconi, B.M., McLane, K.E., Raftery, M.A., Grando, S.A., Protti, M.P., 1994. The nicotinic acetylcholine receptor: Structure and autoimmune pathology. Crit. Rev. Mol. Biol. 29, 69–123.

Conti-Tronconi, B.M., Tang, F., Diethelm, B.M., Spencer, S.R., Reinhardt-Maelicke, S., Maelicke, A., 1990. Mapping of a cholinergic binding site by means of synthetic peptides, monoclonal antibodies, and α-bungarotoxin. Biochemistry 29, 6221–6230.

Corringer, P.-J., Bertrand, S., Bohler, S., Edelstein, S.J., Changeux, J.-P., Bertrand, D., 1998. Critical elements determining diversity in agonist binding and desensitization of neuronal nicotinic acetylcholine receptors. J. Neurosci. 18, 648–657.

Corringer, P.-J., Galzi, J.-L., Eiselé, J.-L., Bertrand, S., Changeux, J.-P., Bertrand, D., 1995. Identification of a new component of the agonist binding site of the nicotinic α7 homooligomeric receptor. J. Biol. Chem. 270, 11749–11752.

Criado, M., Sarin, V., Fox, J.L., Lindstrom, J., 1986. Evidence that the acetylcholine binding site is not formed by the sequence α127–143 of the acetylcholine receptor. Biochemistry 25, 2839–2846.

Cross, K.M.L., Formena, R.C., Chad, J.E., 1995. Enhancement by 5-hydroxytryptamine and analogues of desensitization of neuronal and muscle nicotinic receptors expressed in *Xenopus* oocytes. Br. J. Pharmacol. 114, 1636–1640.

Croxen, R., Newland, C., Beeson, D., Oosterhuis, H., Chauplannaz, G., Vincent, A., Newsom-Davis, J., 1997. Mutations in different functional domains of the human muscle acetylcholine receptor α subunit in patients with the slow-channel congenital myasthenic syndrome. Hum. Mol. Gen. 6, 767–774.

Czajkowski, C., Kaufmann, C., Karlin, A., 1993. Negatively charged amino acid residues in the nicotinic receptor delta subunit that contribute to the binding of acetylcholine. Proc. Natl. Acad. Sci. USA 90, 6285–6289.

Czajkowski, C., Karlin, A., 1991. Agonist binding site of *Torpedo* electric tissue nicotinic acetylcholine receptor. A negatively charged region of the δ subunit within 0.9 nm of the α subunit binding site disulfide. J. Biol. Chem. 266, 22603–22612.

Czajkowski, C., Karlin, A., 1995. Structure of the nicotinic receptor acetylcholine-binding site. J. Biol. Chem. 270, 3160–3164.

Damle, V.N., Karlin, A., 1978. Affinity labeling of one of two α-neurotoxin binding sites in acetylcholine receptor from *Torpedo californica*. Biochemistry 17, 2039–2045.

Damle, V.N., Karlin, A., 1980. Effects of agonists and antagonists on the reactivity of the binding site disulfide in acetylcholine receptor from *Torpedo californica*. Biochemistry 19, 3924–3932.

Damle, V.N., McLaughlin, M., Karlin, A., 1978. Bromoacetylcholine as an affinity label of the acetylcholine receptor from *Torpedo californica*. Biochem. Biophys. Res. Commun. 84, 845–851.

Darlison, M.G., Albrecht, B.E., 1995. $GABA_A$ receptor subtypes: which, where and why? Semin. Neurosci. 7, 115–126.

Dewan, J., Grant, G.A., Sacchettini, J.C., 1994. Crystal structure of κ-bungarotoxin at 2.3-Å resolution. Biochemistry 33, 13147–13154.

diPaola, M., Czajkowski, C., Karlin, A., 1989. The sidedness of the COOH terminus of the acetylcholine receptor δ-subunit. J. Biol. Chem. 264, 1–7.

Dougherty, D.A., 1996. Cation-π interactions in chemistry and biology: a new view of benzene, Phe, Tyr, and Trp. Science 271, 163–167.

Dougherty, D.A., Stauffer, D.A., 1990. Acetylcholine binding by a synthetic receptor: implications for biological recognition. Science 250, 1558–1560.

Dunn, S.M., Conti-Tronconi, B.M., Raftery, M.A., 1993. A high-affinity for acetylcholine ocurrs close to the α–γ subunit interface of *Torpedo* nicotinic acetylcholine receptor. Biochemistry 32, 8616–8621.

Dunn, S.M., Raftery, M.A., 1993. Cholinergic binding sites on the pentameric acetylcholine receptor of *Torpedo californica*. Biochemistry 32, 8608–8615.

Eiselé, J.-L., Bertrand, S., Galzi, J.-L., Devillers-Thiéry, A., Changeux, J.-P., Bertrand, D., 1993. Chimeric nicotinic-serotonergic receptor combines distinct ligand binding and channel especificities. Nature 366, 479–483.

Elgoyhen, A.B., Johnson, D.S., Boulter, J., Vetter, D.E., Heinemann, S., 1994. α9: an acetylcholine receptor with novel pharmacological properties expressed in rat cochlear hair cells. Cell 79, 705–715.

Endo, T., Tamiya, N. 1991. Structure-function relationships of postsynaptic neurotoxins from snake venoms. In: Harvey, A.L. (Ed.), Snake Toxins. Pergamon Press, New York, pp. 165–222.

Fainzilber, M., Hasson, A., Oren, R., Burlingame, A.L., Gordon, D., Spira, M.E., Zlotkin, E., 1994. New mollusc-specific α-conotoxins block *Aplysia* neuronal acetylcholine receptors. Biochemistry 33, 9523–9529.

Fairclough, R.H., Finer-Moore, J., Love, R.A., Kristofferson, D., Desmeules, P.J., Stroud, R.M., 1983. Subunit organization and structures of an acetylcholine receptor. Cold Spring Harbor Symp. Quant. Biol. 48, 9–20.

Fairclough, R.H., Josephs, R., Richman, D.P., 1993. Imaging ligand binding sites on the *Torpedo* acetylcholine receptor. Ann. N.Y. Acad. Sci. 681, 113–125.

Favreau, P., Krimm, Y., Le Gall, F., Bobenrieth, M.-J., Lamthanh, H., Bouet, F., et al., 1999. Biochemical characterization and nuclear magnetic resonance structure of novel αconotoxins isolated from the venom of *Conus consors*. Biochemistry 38, 6317–6326.

Fels, G., Plümer-Wilk, R., Schreiber, M., Maelicke, A., 1986. A monoclonal antibody interfereing with binding and response of the acetylcholine receptor. J. Biol. Chem. 261, 15746–15754.

Fernández, J.M., Granja, R., Izaguirre, V., González-García, C., Ceña, V., 1995. ω-Conotoxin GVIA blocks nicotine-induced catecholamine secretion by blocking the nicotinic receptor-actived

inward currents in bovine chromaffin cells. Neurosci. Lett. 191, 59–62.

Figl, A., Cohen, N.B., Quick, M.W., Davidson, N., Lester, H., 1992. Regions of β4.β2 subunit chimeras that contribute to the agonist selectivity of neuronal nicotinic receptors. FEBS Lett. 3, 243–248.

Fiordalisi, J.J., Al-Rabiee, R., Chiappinelli, V.A., Grant, G., 1994. Site-directed mutagenesis of κ-bungarotoxin: implications for neuronal receptor specificity. Biochemistry 33, 3872–3877.

Fu, D.-X., Sine, S.M., 1994. Competitive antagonists bridge the α–γ subunit interface of the acetylcholine receptor through quaternary ammonium–aromatic interactions. J. Biol. Chem. 269, 26152–26157.

Fulpius, B.W., Miskin, R., Reich, E., 1980. Antibodies from myasthenic patients that compete with cholinergic agents for binding to nicotinic receptors. Proc. Natl. Acad. Sci. USA 77, 4326–4330.

Galzi, J.-L., Bertrand, S., Corringer, P.J., Changeux, J.-P., Bertrand, D., 1996. Identification of calcium binding site that regulate potentiation of a neuronal nicotinic acetylcholine receptor. EMBO J. 15, 5824–5832.

Galzi, J.-L., Revah, F., Bouet, F., Ménez, A., Goeldner, M., Hirth, C., Changeux, J.-P., 1991a. Allosteric transitions of the acetylcholine receptor probed at the amino acid level with a photolabile cholinergic ligand. Proc. Natl. Acad. Sci. USA 88, 5051–5055.

Galzi, J.-L., Bertrand, D., Devillers-Thiéry, A., Revah, F., Bertrand, S., Changeux, J.-P., 1991b. Functional significance of aromatic amino acids from three peptide loops of the α7 neuronal nicotinic receptor site investigated by site-directed mutagenesis. FEBS Lett. 294, 198–202.

Galzi, J.-L., Revah, F., Black, D., Goeldner, M., Hirth, C., Changeux, J.-P., 1990. Identification of a novel amino acid α-Tyr 93 within the cholinergic ligand-binding sites of the acetylcholine receptor by photoaffinity labeling: additional evidence for a three-loop model of the cholinergic ligand-binding sites. J. Biol. Chem. 265, 10430–10437.

Gehle, V.M., Walcott, E.C., Nishizaki, T., Sumikawa, K., 1997. *N*-Glycosylation at the conserved sites ensures the expression of properly folded functional ACh receptors. Mol. Brain Res. 45, 219–229.

Gehrmann, J., Alewood, P.F., Craik, D.J., 1998. Structure determination of the three disulfide bond isomers of α-conotoxin GI: a model for the role of disulfide bonds in structural stability. J. Mol. Biol. 278, 401–415.

Gershoni, J.M., 1987. Expression of the α-bungarotoxin binding site of the nicotinic acetylcholine receptor by *Escherichia coli* transformants. Proc. Natl. Acad. Sci. USA 84, 4318–4321.

Gershoni, J.M., Hawrot, E., Lentz, T.L., 1983. Binding of α-bungarotoxin to isolated α subunit of the acetylcholine receptor of *Torpedo californica*: quantitative analysis with protein blots. Proc. Natl. Acad. Sci. USA 80, 4973–4977.

Goldberg, G., Mochly-Rosen, D., Fuchs, S., Lass, Y., 1983. Monoclonal antibodies modify acetylcholine induced ion channel properties in cultured chick myoballs. J. Membr. Biol. 76, 123–128.

Gouda, H., Yamazaki, K., Hasegawa, J., Kobayashi, Y., Nishiuchi, Y., Sakakibara, S., Hirono, S., 1997. Solution structure of α-conotoxin MI determined by H-1-NMR spectroscopy and molecular dynamics simulation with the explicit solvent water. Biochim. Biophys. Acta 1243, 327–334.

Grant, G.A., Al-Rabiee, R., Xu, X.L., Zhang, Y., 1997. Critical interactions at the dimer interface of κ-bungarotoxin, a neuronal nicotinic acetylcholine receptor antagonist. Biochemistry 36, 3353–3358.

Grant, G.A., Luetje, C.W., Summers, R., Xu, X.L., 1998. Differential roles for disulfide bonds in the structural integrity and biological activity of κ-bungarotoxin, a neuronal nicotinic receptor antagonist. Biochemistry 37, 12166–12171.

Green, W.N., Wanamaker, C.P., 1998. Formation of the nicotinic acetylcholine receptor binding sites. J. Neurosci. 18, 5555–5564.

Greismann, G.E., McCormick, D.J., De Aizpurua, H.J., Lennon, V.A., 1990. α-Bungarotoxin binds to human acetylcholine receptor α-subunit peptide 185–199 in solution and solid phase but not to peptides 125–147 and 389–409. J. Neurochem. 54, 1541–1547.

Groebe, D.R., Dumm, J.M., Abramson, S.N., 1994. Irreversible inhibition of nicotinic acetylcholine receptors by the bipinnatins: Toxin activation and kinetics of receptor inhibition. J. Biol. Chem. 269, 8885–8891.

Groebe, D.R., Dumm, J.M., Levitan, E.S., Abramson, S.N., 1995. α-Conotoxins selectively inhibit one of the two acetylcholine binding sites of nicotinic receptors. Mol. Pharmacol. 48, 105–111.

Groebe, D.R., Gray, W.R., Abramson, S.N., 1997. Determinants involved in the affinity of α-conotoxins GI and SI for the muscle subtype of the nicotinic acetylcholine receptors. Biochemistry 36, 6469–6474.

Gu, Y., Forsayeth, J.R., Verrall, S., Yu, X.M., Hall, Z.W., 1991. Assembly of the mammalian muscle acetylcholine receptor in transfected COS cells. J. Cell Biol. 114, 799–807.

Guddat, L.W., Martin, J.A., Shan, L., Edmundson, A.B., Gray, W.R., 1996. Three-dimensional structure of the α-conotoxin GI at 1.2 Å resolution. Biochemistry 35, 11329–11335.

Gurley, D.A., Lanthorn, T.H., 1998. Nicotinic agonists competitively antagonize serotonin at mouse 5-HT_3 receptor expressed in *Xenopus* oocytes. Neurosci. Lett. 247, 107–110.

Hamilton, S.L., Pratt, D.R., Eaton, D.C., 1985. Arrangement of the subunits of the nicotinic acetylcholine receptor from *Torpedo californica* as determined by α-neurotoxin cross-linking. Biochemistry 24, 2210–2219.

Han, K.-H., Hwang, K.J., Kim, S.M., Gray, W.R., Olivera, B.M., Rivier, J., Shon, K.J., 1997. NMR structure determination of a novel conotoxin, [Pro7, 13] α_A-conotoxin PIVA. Biochemistry 34, 1669–1677.

Hann, R.M., Pagán, O.R., Eterovic, V.A., 1994. The α-conotoxins GI and MI distinguish between the nicotinic acetylcholine receptor agonist sites while SI does not. Biochemistry 33, 14058–14063.

Hann, R.M., Pagán, O.R., Gregory, L.M., Jácome, T., Eterovic, V.A., 1997. The 9-arginine residue of α-conotoxin GI is responsible for its selective high affinity for the αγ agonist site on the electric organ acetylcholine receptor. Biochemistry 36, 9051–9056.

Harvey, S.C., McIntosh, J.M., Cartier, G.E., Maddox, F.N., Luetje, C.W., 1997. Determinants of specificity for α-conotoxin MII on α3β2 neuronal nicotinic receptors. Mol. Pharmacol. 51, 336–342.

Harvey, S.C., Luetje, C.W., 1996. Determinants of competitive antagonist sensitivity on neuronal nicotinic receptor β subunits. J. Neurosci. 16, 3798–3806.

Heidmann, T., Changeux, J.-P., 1979. Fast kinetic studies on the interaction of a fluorescent agonist with the membrane-bound acetylcholine receptor from *Torpedo marmorata*. Eur. J. Biochem. 94, 255–279.

Hervé, M., Pillet, L., Humbert, P., Trémeau, O., Ducanel, F., Hirth, C., Ménez, A., 1992. Role and environment of conserved Lys27 of snake curaremimetic toxins as probed by chemical modifications, site-directed mutagenesis and photolabelling experiments. Eur. J. Biochem. 208, 125–131.

Herz, J.M., Johnson, D.A., Taylor, P., 1989. Distance between the agonist and the noncompetitive inhibitor sites on the nicotinic acetylcholine receptor. J. Biol. Chem. 264, 12439–12448.

Holtzman, E., Wise, D., Wall, J., Karlin, A., 1982. Electron microscopy of complexes of isolated acetylcholine receptor, biotynil-toxin, and avidin. Proc. Natl. Acad. Sci. USA 79, 310–314.

Hopkins, C., Grilley, M., Miller, C., Shon, K.-J., Cruz, L.J., Gray, W.R., et al., 1995. A new family of *Conus* peptides targeted to the nicotinic acetylcholine receptor. J. Biol. Chem. 270, 22361–22367.

Horne, W.A., Hawrot, E., Tsien, R.W., 1991. ω-Conotoxin GVIA

receptors of discopyge electric organ. Characterization of ω-conotoxin binding to the nicotinic acetylcholine receptor. J. Biol. Chem. 266, 13719–13725.

Hu, S.-H., Gehrmann, J., Guddat, L.W., Alewood, P.F., Craik, D.J., Martin, J.L., 1996. The 1.1 Å crystal structure of the neuronal acetylcholine receptor antagonist, α-conotoxin PnIA from *Conus pennaceus*. Structure 4, 417–423.

Hucho, F., Tsetlin, V.I., Machold, J., 1996. The emerging three-dimensional structure of a receptor. The nicotinic acetylcholine receptor. Eur. J. Biochem. 239, 539–557.

Huganir, R.L., Greengard, P., 1990. Regulation of neurotransmitter receptor desensitization by protein phosphorylation. Neuron 5, 555–567.

Hussy, N., Ballivet, M., Bertrand, D., 1994. Agonist and antagonist effects of nicotine on chick neuronal nicotinic receptors are defined by α-subunits and β-subunits. J. Neurophysiol. 72, 1317–1326.

Ikari, H., Spangler, E.L., Greig, N.H., Pei, X.-F., Brossi, A., Speer, D., et al., 1995. Maze learning in aged rats is enhanced by phenserine, a novel anticholinesterase. NeuroReport 6, 481–484.

Jacobsen, R., Yoshikami, D., Ellison, M., Martínez, J., Gray, W.R., Cartier, G.E., et al., 1997. Differential targeting of nicotinic acetylcholine receptors by novel αA-conotoxins. J. Biol. Chem. 272, 22531–22537.

Jackson, M.B., 1989. Perfection of a synaptic receptor: the kinetics and energetics of the acetylcholine receptor. Proc. Natl. Acad. Sci. USA 86, 2199–2203.

Johnson, D.A., Cushman, P., Malekzadeh, R., 1990. Orientation of α-toxin on the surface of the nicotinic acetylcholine receptor: a fluorescent spectroscopic study. J. Biol. Chem. 265, 7360–7368.

Johnson, D.A., Nuss, J.M., 1994. The histrionicotoxin-sensitive ethidium binding site is located outside of the transmembrane domain of the nicotinic acetylcholine receptor: a fluorescence study. Biochemistry 33, 9070–9077.

Johnson, D.A., Voet, J.G., Taylor, P., 1984. Fluorescence energy transfer between cobra α-toxin molecules bound to the acetylcholine receptor. J. Biol. Chem. 259, 5717–5725.

Johnson, D.S., Martínez, J., Elgoyhen, A.B., Heinemann, S.F., McIntosh, J.M., 1995. α-Conotoxin ImI exhibits subtype-specific nicotinic acetylcholine receptor blockade: preferential inhibition of homomeric α7 and α9 receptors. Mol. Pharmacol. 48, 194–199.

Jones, M.V., Westbrook, G.L., 1996. The impact of receptor desensitization on fast synaptic transmission. Trends Neurosci. 19, 96–101.

Kachalsky, S.G., Aladjem, M., Barchan, D., Fuchs, S., 1993. The ligand binding domain of the nicotinic acetylcholine receptor. Immunological analysis. FEBS Lett. 318, 264–268.

Kachalsky, S.G., Jensen, B.S., Barchan, D., Fuchs, S., 1995. Two subsites in the binding domain of the acetylcholine receptor: An aromatic subsite and a proline subsite. Proc. Natl. Acad. Sci. USA 92, 10801–10805.

Kaiser, S.A., Soliakov, L., Harvey, S.C., Luetje, C.W., Wonnacott, S., 1998. Differential inhibition by α-conotoxin MII of the nicotinic stimulation of [^{3}H]-dopamine release from rat striatal synaptosomes and slices. J. Neurochem. 70, 1069–1076.

Kang, S., Maelicke, A., 1980. Fluorescein isothiocyanate-labeled alpha-cobratoxin: biochemical characterization and interaction with acetylcholine receptor from *Electrophorus electricus*. J. Biol. Chem. 256, 7326–7332.

Kao, P.N., Karlin, A., 1986. Acetylcholine receptor binding site contains a disulfide cross-link between adjacent half-cystinyl residues. J. Biol. Chem. 261, 8085–8088.

Karlin, A., Akabas, M.H., 1995. Toward a structural basis for the function of nicotinic acetylcholine receptors and their cousins. Neuron 15, 1231–1244.

Kasheverov, Y., Zhmak, M., Chivilyov, E., Saezbrionez, P., Utkin, Y., Hucho, F., Tsetlin, V., 1999. Benzophenone-type photoactivatable derivatives of α-neurotoxins and α-conotoxins in studies on *Torpedo* nicotinic acetylcholine receptor. J. Rec. Signal Transd. Res. 19, 559–571.

Kehoe, J.-S., McIntosh, J.M., 1998. Two distinct nicotinic receptors, one pharmacologically similar to the vertebrate α7-containing receptor, mediate Cl currents in *Aplysia* neurons. J. Neurosci. 18, 8198–8213.

Keller, S.H., Kreienkamp, H.-J., Kawanishi, C., Taylor, P., 1995. Molecular determinants conferring α-toxin resistence in recombinant dNA-derived acetylcholine receptors. J. Biol. Chem. 270, 4165–4171.

Keyser, K.T., Britto, L.R.G., Schoepfer, R., Whitting, P., Cooper, J., Conroy, W., et al., 1993. Three subtypes of α-bungarotoxin-sensitive nicotinic acetylcholine receptors are expressed in chick retina. J. Neurosci. 13, 442–454.

Khakh, B.S., Bao, X.R., Labarca, C., Lester, H.A., 1999. Neuronal P2X transmitter-gated cation channels change their ion selectivity in seconds. Nature Neurosci. 2, 322–330.

Kistler, J., Stroud, R.M., Klymkowsky, M.W., Lalancette, R.A., Fairclough, R.H., 1982. Structure and function of an acetylcholine receptor. Biophys. J. 37, 371–383.

Kreienkamp, H.-J., Maeda, R.K., Sine, S.M., Taylor, P., 1995. Intersubunit contacts governing assembly of the mammalian nicotinic acetylcholine receptor. Neuron 14, 635–644.

Kreienkamp, H.-J., Sine, S.M., Maeda, R.K., Taylor, P., 1994. Glycosylation sites selectively interfere with α-toxin binding to the nicotinic acetylcholine receptor. J. Biol. Chem. 269, 8108–8114.

Kreienkamp, H.-J., Utkin, Y.N., Weise, C., Machold, J., Tsetlin, V.I., Hucho, F., 1992. Investigation of ligand-binding sites of the acetylcholine receptor using photoactivatable derivatives of neurotoxin II from *Naja naja oxiana*. Biochemistry 31, 8239–8244.

Kriegler, S., Sudweeks, S., Yakel, J.L., 1999. The nicotinic α4 receptor subunit contributes to the lining of the ion channel pore when expressed with the 5-HT_3 receptor subunit. J. Biol. Chem. 274, 3934–3936.

Kuhlmann, J., Okonjo, K.O., Maelicke, A., 1991. Desensitization is a property of the cholinergic binding region of the nicotinic acetylcholine receptor, not of the receptor-integral ion channel. FEBS Lett. 279, 216–218.

Kulak, J.M., Nguyen, T.A., Olivera, B.M., McIntosh, J.M., 1997. α-Conotoxin MII blocks nicotine-stimulated release in rat striatal synaptosomes. J. Neurosci. 17, 5263–5270.

Kuner, T., Wollmuth, L.P., Karlin, A., Seeburg, P.H., Sakmann, B., 1996. Structure of the NMDA receptor channel M2 segment inferred from the accessibility of substituted cysteines. Neuron 17, 343–352.

Langosch, D., Becker, C.-M., Betz, H., 1990. The inhibitory glycine receptor: a ligand-gated chloride channel of the central nervous system. Eur. J. Biochem. 194, 1–8.

Laube, B., Kuhse, J., Betz, H., 1998. Evidence for a tetrameric structure of recombinant NMDA receptors. J. Neurosci. 18, 2954–2961.

Lee, Y.-H., Li, L., Lasalde, J., Rojas, L., McNamee, M.G., Ortiz-Miranda, S.I., Pappone, P., 1994. Mutations in the M4 domain of *Torpedo californica* acetylcholine receptor dramatically alter ion channel function. Biophys. J. 66, 646–653.

Le Novère, N., Changeux, J.-P., 1995. Molecular evolution of the nicotinic acetylcholine receptor: An example of multigene family in excitable cells. J. Mol. Evol. 40, 155–172.

Le Novère, N., Corringer, P.-J., Changeux, J.-P., 1999. Improved secondary structure predictions from a nicotinic receptor subunit: Incorporation of solvent accessibility and experimental data into a two-dimensional representation. Biophys. J. 76, 2329–2345.

Lentz, T.L., 1995. Differential binding of nicotine and α-bungarotoxin to residues 173–204 of the nicotinic acetylcholine receptor α1-subunit. Biochemistry 34, 1316–1322.

Lentz, T.L., Chaturvedi, V., Conti-Fine, B.M., 1998. Amino acids within residues 181–200 of the nicotinic acetylcholine receptor α1 subunit involved in nicotine binding. Biochem. Pharmacol. 55, 341–347.

Lester, R.A.J., McIntosh, J.M., Quick, M.W., 1998. Relationship between nicotinic acetylcholine receptor subunit mRNA levels and channel function in central neurons. Soc. Neurosci. Abstr. 24, 1342.

Levitan, I.B., 1994. Modulation of ion channels by protein phosphorylation and dephosphorylation. Annu. Rev. Physiol. 56, 193–212.

Li, L., Schuchard, M., Palma, A., Pradier, L., McNamee, M.G., 1990. Functional role of the cysteine 451 thiol group in the M4 helix of the γ subunit of *Torpedo californica* acetylcholine receptor. Biochemistry 29, 5428–5436.

Li, L., Lee, Y.-H., Pappone, P., Palma, A., McNamee, M.G., 1992. Site-specific mutations of nicotinic acetylcholine receptor at the lipid–protein interface dramatically alter ion channel gating. Biophys. J. 62, 61–63.

Lindstrom, J., 1986. Probing nicotinic acetylcholine receptors with monoclonal antibodies. Trends Neurosci. 9, 401–407.

Lo, D.C., Pinkham, J.L., Stevens, C.F., 1991. Role of a key cysteine residue in the gating of the acetylcholine receptor. Neuron 6, 31–40.

Lopez, M.G., Montiel, C., Herrero, C.J., Garcia-Palomero, E., Mayorgas, Y., Hernandez-Guijo, J.M., et al., 1998. Unmasking the functions of the chromaffin cell alpha7 nicotinic receptor by using short pulses of acetylcholine and selective blockers. Proc. Natl. Acad. Sci. USA 95, 14184–14189.

Loughnan, M., Bond, T., Atkins, A., Cuevas, J., Adams, D.J., Broxton, N.M., et al., 1998. α-Conotoxin EpI, a novel sulfated peptide from *Conus episcopatus* that selectively targets neuronal nicotinic acetylcholine receptors. J. Biol. Chem. 273, 15667–15674.

Luetje, C.W., Piattoni, M., Patrick, J., 1993. Mapping of ligand binding sites of neuronal nicotinic acetylcholine receptors using chimeric α subunits. Mol. Pharmacol. 44, 657–666.

Lukas, R.J., Morimoto, H., Hanley, M.R., Bennett, E., 1981. Radiolabeled α-bungarotoxin derivatives: kinetic interaction with nicotinic acetylcholine receptors. Biochemistry 20, 7373–7378.

Luo, S., Kulak, J.M., Cartier, G.E., Jacobsen, R.B., Yoshikami, D., Olivera, B.M., McIntosh, J.M., 1998. α-Conotoxin AuIB selectively blocks α3β4 nicotinic acetylcholine receptors and nicotine-evoked norepinephrine release. J. Neurosci. 18, 8571–8579.

Machold, J., Utkin, Y., Kirsch, D., Kaufmann, R., Tsetlin, V., Hucho, F., 1995a. Photolabeling reveals the proximity of the α-neurotoxin binding site to the M2 helix of the ion channel in the nicotinic acetylcholine receptor. Proc. Natl. Acad. Sci. USA 92, 7282–7286.

Machold, J., Weise, C., Utkin, Y.N., Franke, P., Tsetlin, V.I., Hucho, F., 1995b. A new class of photoactivatable and cleavable derivatives of neurotoxin II from *Naja naja oxiana*. Synthesis, characterisation, and application for affinity labelling of the nicotinic acetylcholine receptor from *Torpedo californica*. Eur. J. Biochem. 228, 947–954.

Machold, J., Weise, C., Utkin, Y.N., Franke, P., Tsetlin, V.I., Hucho, F., 1995c. The handedness of the subunit arrangement of the nicotinic acetylcholine receptor from *Torpedo californica*. Eur. J. Biochem. 234, 427–430.

Maelicke, A., Alburquerque, E.X., 1996. New approach to drug therapy in Alzheimer's dementia. Drug Disc Today 1, 53–59.

Maelicke, A., Coban, T., Storch, A., Schrattenholz, A., Pereira, E.F.R., Alburquerque, E.X., 1997. Allosteric modulation of *Torpedo nicotinic* acetylcholine receptor ion channel activity by noncompetitive agonists. J. Rec. Signal Transd. Res. 17, 11–28.

Maelicke, A., Schrattenholz, A., Schröder, B., 1995a. Modulatory control by noncompetitive agonists of nicotinic cholinergic neurotransmission in the central nervous system. Semin. Neurosci. 7, 103–114.

Maelicke, A., Schrattenholz, A., Storch, A., Schröder, B., Gutbrod, O., Methfessel, C., et al., 1995b. Noncompetitive agonism at nicotinic acetylcholine receptor. Functional signficance for CNS signal transduction. J. Rec. Sign. Transd. Res. 15, 333–353.

Martin, M., Czajkowski, C., Karlin, A., 1996. The contributions of aspartyl residues in the acetylcholine receptor γ and δ subunits to the binding of agonists and competitive antagonists. J. Biol. Chem. 271, 13497–13503.

Martin, M., Karlin, A., 1997. Functional effects on the acetylcholine receptor of multiple mutations of γAsp174 and δAsp180. Biochemistry 36, 10742–10750.

Martínez, J.S., Olivera, B., Gray, W.R., Craig, A.G., Groebe, D.R., Abramson, S.N., McIntosh, J.M., 1995. α-Conotoxin EI, a new nicotinic acetylcholine receptor antagonist with novel selectivity. Biochemistry 34, 14519–14526.

Maslennikov, I.V., Sobol, A.G., Gladky, K.V., Lugovskoy, A.A., Ostrovsky, A.G., Tsetlin, V.I., et al., 1998. Two distinct structures of α-conotoxin GI in aqueous solution. Eur. J. Biochem. 254, 238–247.

Maslennikov, I.V., Shenkarev, Z.O., Zhmak, M.N., Ivanov, V.T., Methfessel, C., Tsetlin, V.I., Arseniev, A.S., 1999. NMR spatial structure of α-conotoxin ImI reveals a common scaffold in snail and snake toxins recognizing neuronal nicotinic acetylcholine receptors. FEBS Lett. 444, 275–280.

Matsubayashi, H., Alkondon, M., Pereira, E.F.R., Swanson, K.L., Alburquerque, E.X., 1998. Strychnine. A potent competitive antagonist of α-bungarotoxin-sensitive nicotinic acetylcholine receptors in rat hippocampal neurons. J. Pharm. Exp. Ther. 284, 904–913.

McArdle, J.J., Lentz, T.L., Witzemann, V., Schwarz, H., Weinstein, S.A., Schmidt, J.J., 1999. Waglerin-1 selectively blocks the ϵ-form of the muscle nicotinic acetylcholine receptor. J. Pharm. Exp. Ther. 289, 543–550.

McBain, C.J., Mayer, M.L., 1994. *N*-methyl-D-aspartic acid receptor structure and function. Physiol. Rev. 74, 723–760.

McDonald, R.L., Twyman, R.E., 1992. Kinetic properties and regulation of $GABA_A$ receptor channels. Ion Chann. 3, 315–343.

McGehee, D.S., Role, L.W., 1995. Physiological diversity of nicotinic acetylcholine receptors expressed by vertebrate neurons. Annu. Rev. Physiol. 57, 521–546.

McIntosh, J.M., Yoshikami, D., Mahe, E., Nielsen, D.B., Rivier, J.E., Gray, W.R., Olivera, B.M., 1994. A nicotinic acetylcholine receptor ligand of unique specificity, α-conotoxin ImI. J. Biol. Chem. 269, 16733–16739.

McLane, K.E., Tang, F., Conti-Tronconi, B.M., 1990. Localization of sequence segments forming a kappa-bungarotoxin-binding site on the α3 neuronal nicotinic receptor. J. Biol. Chem. 265, 1537–1544.

McLane, K.E., Wu, X., Conti-Tronconi, B.M., 1994. An α-bungarotoxin-binding sequence on the *Torpedo* nicotinic acetylcholine receptor α-subunit: Conservative amino acids substitutions reveal side-chain specific interactions. Biochemistry 33, 2576–2585.

McLaughlin, J.T., Hawrot, E., Yellen, G., 1995. Covalent modification of engineered cysteines in the nicotinic acetylcholine receptor agonist-binding domain inhibits receptor activation. Biochem. J. 310, 765–769.

Middleton, R.E., Cohen, J.B., 1991. Mapping the acetylcholine binding site of the nicotinic acetylcholine receptor: [^{3}H]nicotine as an agonist photoaffinity label. Biochemistry 30, 6987–6997.

Mishina, M., Tobimatsu, T., Imoto, K., Tanaka, K., Fujita, Y., Fukuda, K., et al., 1985. Location of functional regions of acetylcholine receptor α-subunit by site-directed mutagenesis. Nature 313, 364–369.

Mochly-Rosen, D., Fuchs, S., 1981. Monoclonal anti-acetylcholine-

receptor antibodies directed against the cholinergic binding site. Biochemistry 20, 5920–5924.

Moore, H.P., Raftery, M.A., 1979. Studies of reversible and irreversible interactions of an alkylating agonist with *Torpedo californica* acetylcholine receptor in membrane-bound and purified states. Biochemistry 18, 1907–1911.

Mulle, C., Léna, C., Changeux, J.-P., 1992. Potentiation of nicotinic receptor response by external calcium in rat central neurons. Neuron 8, 937–945.

Myers, R.A., Cruz, L.J., Rivier, J.E., Olivera, B.M., 1993. Conus peptides as chemical probes for receptors and ion channels. Chem. Rev. 93, 1923–1936.

Myers, R.A., Zafaralla, G.C., Gray, W.R., Abbott, J., Cruz, L.J., Olivera, B.M., 1991. α-Conotoxin, small peptide probes of nicotinic acetylcholine receptor. Biochemistry 30, 9370–9377.

Nakazawa, K., Ohno, Y., 1999. Block by 5-hydroxytryptamine and apomorphine of recombinant human neuronal nicotinic receptors. Eur. J. Pharmacol. 374, 293–299.

Nathanson, N.M., Hall, Z.W., 1980. In situ labeling of *Torpedo* and rat muscle acetylcholine receptor by a photoaffinity derivative of α-bungarotoxin. J. Biol. Chem. 255, 1698–1703.

Nayeem, N., Green, T.P., Martin, I.L., Barnard, E.A., 1994. Quaternary structure of the native $GABA_A$ receptor determined by electron microscopic image analysis. J. Neurochem. 62, 815–818.

Neumann, D., Barchan, D., Fridkin, M., Fuchs, S., 1986. Analysis of ligand binding to the synthetic dodecapeptide 185–196 of the acetylcholine receptor α subunit. Proc. Natl. Acad. Sci. USA 83, 9250–9253.

Newbolt, A., Stoop, R., Virginio, C., Suprenant, A., North, R.A., Buell, G., Rassendren, F., 1998. Membrane topology of an ATP-gated ion channel (P2X receptor). J. Biol. Chem. 273, 15177–15782.

Nicke, A., Baumert, H.G., Rettinger, J., Eichele, A., Lambrecht, G., Mutschler, E., Schmalzing, G., 1998. P2X1 and P2X2 receptors form stable trimers: a novel structural motif of ligand-gated channels. EMBO J. 17, 3016–3028.

Nowak, M.W., Kearney, P.C., Sampson, J.R., Saks, M.E., Labarca, C.G., Silverman, S.K., et al., 1995. Nicotinic receptor binding site probed with unnatural amino acid incorporation in intact cells. Science 268, 439–442.

Ohana, B., Gershoni, J.M., 1990. Comparison of the toxin binding sites of the nicotinic acetylcholine receptor from *Drosophila* to human. Biochemistry 29, 6409–6415.

Ohno, K., Wang, H.-L., Milone, M., Bren, N., Brengman, J.M., Nakano, S., et al., 1996. Congenital myasthenic syndrome caused by decreased agonist binding affinity due to a mutation in the acetylcholine receptor ϵ subunit. Neuron 17, 157–170.

Okonjo, K.O., Kuhlmann, J., Maelicke, A., 1991. A second pathway for the activation of the *Torpedo* actylcholine receptor. Eur. J. Biochem. 200, 671–677.

O'Leary, M.E., Filatov, G.N., White, M.M., 1994. Characterization of *d*-tubocurarine binding site of *Torpedo* acetylcholine receptor. Am. J. Physiol. 266, C648–C653.

O'Leary, M.E., White, M.M., 1992. Mutational analysis of ligand-induced activation of the *Torpedo* acetylcholine receptor. J. Biol. Chem. 267, 8360–8365.

Olivera, B.M., Rivier, J., Clark, C., Corpuz, G.P., Mena, E., Ramilo, C.A., Cruz, L.J., 1990. Diversity of *Conus* neuropeptides. Science 249, 257–263.

Ortells, M.O., Lunt, G.G., 1995. Evolutionary history of the ligand-gated ion-channel superfamily of receptors. Trends Neurosci. 18, 121–127.

Osaka, H., Malany, S., Kanter, J.R., Sine, M.S., Taylor, P., 1999. Subunit interface selectivity of the α-neurotoxins for the nicotinic acetylcholine receptor. J. Biol. Chem. 274, 9581–9586.

Osaka, H., Sugiyama, N., Taylor, P., 1998. Distinctions in agonist and antagonist specificity conferred by anionic residues of the nicotinic acetylcholine receptor. J. Biol. Chem. 273, 12758–12765.

Oswald, R.E., Changeux, J.-P., 1982. Crosslinking of alpha-bungarotoxin to the acetylcholine receptor from *Torpedo marmorata* by ultraviolet light irradiation. FEBS Lett. 139, 225–229.

Paas, Y., 1998. The macro- and microarchitectures of the ligand-binding domain of glutamate receptors. Trends Neurosci. 21, 117–125.

Paas, Y., Eisenstein, M., Medevielle, F., Teichberg, V.I., Devillers-Thiéry, A., 1996. Identification of the amino acid subsets accounting for the ligand binding specificity of a glutamate receptor. Neuron 17, 979–990.

Palma, E., Bertrand, S., Binzoni, T., Bertrand, D., 1996a. Neuronal nicotinic α7 receptor expressed in *Xenopus* oocytes present five putative binding sites for methyllycaconitine. J. Physiol. 491.1, 151–161.

Palma, A., Maggi, L., Eusebi, F., Miledi, R., 1997. Neuronal nicotinic threonine-for-leucine 247 α7 mutant receptors show different gating kinetics when activated by acetylcholine or by the noncompetitive agonist 5-hydroxytryptamine. Proc. Natl. Acad. Sci. USA 94, 9915–9919.

Palma, A., Mileo, A.M., Eusebi, F., Miledi, R., 1996b. Threonine-for-leucine mutation within domain M2 of the neuronal α7 nicotinic receptor converts 5-hydroxytryptamine from antagonist to agonist. Proc. Natl. Acad. Sci. USA 93, 11231–11235.

Papke, R.L., Duvoisin, R.M., Heinemann, S.F., 1993. The amino terminal half of the nicotinic β-subunit extracellular domain regulates the kinetic of inhibition by neuronal bungarotoxin. Proc. R. Soc. London Biol. 252, 141–148.

Pascual, J.M., Karlin, A., 1998. State-dependent accessibility and electrostatic potential in the channel of the acetylcholine receptor. Inferences from rates of reaction of thiosulfonates with substituted cysteines in the M2 segment of the α subunit. J. Gen. Physiol. 111, 717–739.

Pascuzzo, G.J., Akaide, A., Maleque, M.A., Shaw, K.-P., Aronstam, R.S., Rickett, D.L., Alburquerque, E.X., 1984. The nature of the interaction of pyridostigmine with the nicotinic acetylcholine receptor-ion channel complex in rat myotubes. Mol. Pharmacol. 25, 92–101.

Pearce, S.F., Hawrot, E., 1990. Intrinsic fluorescence of binding-site fragments of the nicotinic acetylcholine receptor: perturbations produced upon binding α-bungarotoxin. Biochemistry 29, 10649–10659.

Pedersen, S.E., 1995. Site-selective photoaffinity-labeling of the *Torpedo californica* nicotinic acetylcholine receptor by azide derivatives of ethidium bromide. Mol. Pharmacol. 47, 1–9.

Pedersen, S.E., Cohen, J.B., 1990. *d*-Tubocurarine binding sites are located at α–γ and α–δ subunit interfaces of the nicotinic acetylcholine receptor. Proc. Natl. Acad. Sci. USA 87, 2785–2789.

Pedersen, S.E., Papineni, R.V.L., 1995. Interaction of *d*-tubocurarine anlogs with the *Torpedo nicotinic* acetylcholine receptor. Methylation and stereoisomerization affect site-selective competitive binding and binding to the noncompetitive site. J. Biol. Chem. 270, 31141–31150.

Pedersen, S.E., Sharp, S.D., Liu, W.-S., Cohen, J.B., 1992. Structure of the non-competitive antagonist-binding site of the *Torpedo nicotinic* acetylcholine receptor. [^{3}H]Meproadifen mustard reacts selectively with α-subunit Glu-262. J. Biol. Chem. 267, 10489–10499.

Pereira, E.F., Alkondon, M., McIntosh, J.M., Alburquerque, E.X., 1996. α-Conotoxin ImI: a competitive antagonist at α-bungarotoxin-sensitive neuronal nicotinic receptors in hippocampal neurons. J. Pharmacol. Exp. Ther. 278, 1472–1483.

Pereira, E.F.R., Alkondon, M., Reinhardt, S., Maelicke, A., Peng, X., Lindstrom, J., et al., 1994. Physostigmine and galanthamine: Probes for a novel binding site on the α4β2 subtype of neuronal

nicotinic acetylcholine receptors stably expressed in fibroblast cells. J. Pharmacol. Exp. Ther. 270, 768–778.

Pereira, E.F.R., Alkondon, M., Tano, T., Castro, N.G., Fróes-Ferrão, M.M., Rozental, R., et al., 1993. A novel agonist binding site on nicotinic acetylcholine receptors. J. Rec. Res. 13, 413–436.

Phillips, W.D., Maimone, M.M., Merlie, J.P., 1991. Mutagenesis of the 43-kDa postsynaptic protein defines domains involved in plasma membrne targeting and AChR clustering. J. Cell. Biol. 115, 1713–1723.

Picciotto, M.R., Zoli, M., Léna, C., Bessis, A., Lallemand, Y., LeNovére, N., et al., 1995. Abnormal avoidance learning in mice lacking functional high-affinity nicotine receptor in the brain. Nature 374, 65–67.

Picciotto, M.R., Zoli, M., Zachariou, V., Changeux, J.-P., 1997. Contribution of nicotine acetylcholine receptors containing the β2-subunit to the behavioural effects of nicotine. Biochem. Soc. Trans. 25, 824–829.

Pillet, L., Trémeau, O., Ducancel, F., Drevet, P., Zinn-Justin, S., Pinkasfeld, S., et al., 1993. Genetic engineering of snake toxins. Role of invariant residues in the structural and functinal properties of a curaremimetic toxin, as probed by site-directed mutagenesis. J. Biol. Chem. 268, 909–916.

Pradier, L., Yee, A., McNamee, M.G., 1989. Use of chemical modifications and site-directed mutagenesis to probe the functional role of thiol groups on the γ subunit of *Torpedo californica* acetylcholine receptor. Biochemistry 28, 6562–6571.

Preston-Hurlburt, P., Wilson, P.T., Dowding, A.J., Hawrot, E., 1990. Monoclonal antibodies directed against a synthetic peptide corresponding to the α-bungarotoxin binding region of the acetylcholine receptor. Biochim. Biophys. Acta 1033, 324–328.

Prince, R.J., Sine, S.M., 1996. Molecular dissection of subunit interfaces in the acetylcholine receptor. Identification of residues that determine agonist selectivity. J. Biol. Chem. 271, 25770–25777.

Prince, R.J., Sine, S.M., 1998a. Epibatidine binds with unique site and state selectivity to muscle nicotinic acetylcholine receptors. J. Biol. Chem. 273, 7843–7849.

Prince, R.J., Sine, S.M. 1998b. The ligand binding domains of nicotinic acetylcholine receptor. In: Barrantes, F.J. (Ed.), The Nicotinic Acetylcholine Receptor: Current Views and Future Trends. Landes Bioscience, Austin, TX, pp. 31–59.

Quiram, P.A., Sine, S.M., 1998a. Identification of residues in the neuronal α7 acetylcholine receptor that confer selectivity for conotoxin ImI. J. Biol. Chem. 273, 11001–11006.

Quiram, P.A., Sine, S.M., 1998b. Structural elements in α-conotoxin ImI essential for binding to neuronal α7 receptors. J. Biol. Chem. 273, 11007–11011.

Rajendra, S., Lynch, J.W., Pierce, K.D., French, C.R., Barry, P.H., Schofield, P.R., 1995a. Mutation of an arginine residue in the human glycine receptor transforms β-alanine and taurine from agonists into competitive antagonists. Neuron 14, 169–175.

Rajendra, S., Vandenberg, R.J., Pierce, K.D., Cunninham, A.M., French, P.W., Barry, P.H., Schofield, P.R., 1995b. The unique extracellular disulfide loop of the glycine receptor is a principal ligand binding element. EMBO J. 14, 2987–2998.

Ramilo, C.A., Zafaralla, G., Nadasdi, L., Hammerland, L.G., Yoshikami, D., Gray, W.R., et al., 1992. Novel α- and ω-conotoxins from *Conus striatus* venom. Biochemistry 31, 9919–9926.

Role, L.W., 1992. Diversity in primary structure and function of neuronal nicotinic acetylcholine receptor channels. Curr. Opin. Neurobiol. 2, 254–262.

Rossant, C.J., Lindstrom, J., Loring, R.H., 1994. Effects of redox agents and arsenical compounds on [^{3}H]cytisine binding to immunoisolated nicotinic acetylcholine receptors from chick brain containing α4β2 subunits. J. Neurochem. 62, 1368–1374.

Rothlin, C.V., Katz, E., Verbitsky, M., Elgoyhen, A.B., 1999. The α9 nicotinic acetylcholine receptor shares pharmacological properties with type A γ-aminobutyric acid, glycine, and type 3 serotonin receptors. Mol. Pharmacol. 55, 248–254.

Rousselet, A., Faure, G., Boulain, J.-C., Ménez, A., 1984. The interaction of neurotoxin derivatives with either acetylcholine receptor or as monoclonal antibody. An electron-spin-resonance study. Eur. J. Biochem. 140, 31–37.

Ruan, K.-H., Stiles, B., Atassi, M.Z., 1991. The short-neurotoxin-binding regions on the α-chain of human and *Torpedo californica* acetylcholine receptors. Biochem. J. 274, 849–854.

Rübsamen, H., Eldefrawi, A.T., Eldefrawi, M.E., Hess, G., 1978. Characterization of the calcium-binding sites of the purified acetylcholine receptor and identification of the calcium binding site subunit. Biochemistry 17, 3818–3825.

Scherf, T., Balass, M., Fuchs, S., Katchalski-Katzir, E., Anglister, J., 1997. Three-dimensional solution structure of the complex of α-bungarotoxin with a library-derived peptide. Proc. Natl. Acad. Sci. USA 94, 6059–6064.

Schrattenholz, A., Coban, T., Schröder, B., Okonjo, K.O., Kuhlmann, J., Pereira, E.F., et al., 1993a. Biochemical characterization of a novel channel-activating site on nicotinic acetylcholine receptors. J. Rec. Res. 13, 393–412.

Schrattenholz, A., Godovac-Zimmerman, J., Schäfer, H.-J., Alburquerque, E.X., Maelicke, A., 1993b. Photoaffinity labeling of *Torpedo* acetylcholine receptor by physostigmine. Eur. J. Biochem. 216, 671–677.

Schrattenholz, A., Pereira, E.F.R., Roth, U., Weber, K.-H., Alburquerque, E.X., Maelicke, A., 1996. Agonist responses of neuronal nicotinic acetylcholine receptors are potentiated by a novel class of allosterically acting ligands. Mol. Pharmacol. 49, 1–6.

Schröder, B., Reinhardt-Maelicke, S., Schrattenholz, A., McLane, K.E., Kretschmer, A., Conti-Tronconi, B.M., Maelicke, A., 1994. Monoclonal antibodies FK1 and WF6 define two neighboring ligand binding sites on *Torpedo* actylcholine receptor α-polypeptide. J. Biol. Chem. 269, 10407–10416.

Schulte, M., Bloom, K.E., White, M.M., 1995. Evidence for the involvement of tryptophan in the binding of curare to 5-HT$_3$ receptors. Society Neurosci. Abstr. 21, 30.6.

Seifert, S.A., Eldefrawi, M.E., 1974. Affinity of myasthenia drugs to acetylcholinesterase and acetylcholine receptor. Biochem. Med. 18, 258–265.

Sellin, L.C., Mattila, K., Annila, A., Schmidt, J.J., McArdle, J.J., Hyvönen, M., et al., 1996. Conformational analysis of a toxic peptide from *Trimeresurus wagleri* which blocks the nicotinic acetylcholine receptor. Biophys. J. 70, 3–13.

Servent, D., Ménez, A., Kessler, P., 1995. Site-directed disulfide reduction using an affinity reagent: application on the nicotinic acetylcholine receptor. FEBS Lett. 360, 261–265.

Servent, D., Mourier, G., Antil, S., Ménez, A., 1998. Curaremimetic toxins discriminate between nicotinic acetylcholine receptor subtypes. Toxicol. Lett. 103, 199–203.

Sgard, F., Fraser, S.P., Katkowska, M.J., Djamgoz, M.B.A., Dunbar, S.J., Windass, J.D., 1998. Cloning and functional characterisation of two novel nicotinic acetylcholine receptor α subunits from the insect pest *Myzus persicae*. J. Neurochem. 71, 903–912.

Shaw, K.-P., Aracava, Y., Akaike, A., Daly, J.W., Rickett, D.L., Alburquerque, E.X., 1985. The reversible cholinesterase inhibitor physostigmine has channel-blocking and agonist effects on the acetylcholine receptor-ion channel complex. Mol. Pharmacol. 28, 527–538.

Shon, K.-J., Koerber, S.C., Rivier, J.E., Olivera, B.M., McIntoch, J.M., 1997. Three-dimensional solution structure of α-conotoxin MII, and $\alpha_3\beta_2$ neuronal nicotinic acetylcholine receptor-targeted ligand. Biochemistry 36, 15693–15700.

Sieghart, W., 1995. Structure and pharmacology of γ-aminobutyric acid$_A$ receptor subtypes. Pharmacol. Rev. 47, 181–234.

Sigel, E., Baur, R., Kellenberger, S., Malherbe, P., 1992. Point mutations affecting antagonist affinity and agonist dependent gating of $GABA_A$ receptor channels. EMBO J. 11, 2017–2023.

Sine, S.M., 1993. Molecular dissection of subunit interfaces in the acetylcholine receptor: Identification of residues that determine curare selectivity. Proc. Natl. Acad. Sci. USA 90, 9436–9440.

Sine, S.M., 1997. Identification of equivalent residues in the γ, δ, and ϵ subunit of the nicotinic acetylcholine receptor that contribute to α-bugarotoxin binding. J. Biol. Chem. 272, 23521–23527.

Sine, S.M., Bren, N., Quiram, P.A., 1998. Molecular dissection of subunit interfaces in the nicotinic acetylcholine receptor. J. Physiol. 92, 101–105.

Sine, S.M., Claudio, T., 1991. γ- and δ-subunits regulate the affinity and the cooperativity of ligand binding to the acetylcholine receptor. J. Biol. Chem. 266, 19369–19377.

Sine, S.M., Claudio, T., Sigworth, F.J., 1990. Activation of *Torpedo* acetylcholine receptors expressed in mouse fibroblasts. Single channel current kinetics reveal distinct agonist binding affinities. J. Gen. Physiol. 96, 395–437.

Sine, S.M., Kreienkamp, H.-J., Bren, N., Maeda, R., Taylor, P., 1995b. Molecular dissection of subunit interfaces in the acetylcholine receptor: identification of determinants of α-conotoxin M1 selectivity. Neuron 15, 205–211.

Sine, S.M., Ohno, K., Bouzat, C., Auerbach, A., Milone, M., Pruitt, J.N., Engel, A.G., 1995a. Mutation of the actylcholine receptor α subunit causes a slow-channel myasthenic syndrome by enhancing agonist binding affinity. Neuron 15, 229–239.

Sine, S.M., Quiram, P., Papanikolaou, F., Kreienkamp, H.-J., Taylor, P., 1994. Conserved tyrosines in the α subunit of the nicotinic acetylcholine receptor stabilize quaternary ammonium groups of agonists and curariform antagonists. J. Biol. Chem. 269, 8808–8816.

Sobel, A., Heidmann, T., Cartaud, J., Changeux, J.-P., 1980. Reconstitution of a functional acetylcholine receptor. Polypeptide chains, ultrastructure and binding sites for acetylcholine and local anesthetics. Eur. J. Biochem. 110, 13–33.

Spivak, C.E., 1995. Correlations among Hill parameters reflect models of activating ligand-gated ion channels. Trends Pharmacol. Sci. 16, 39–42.

Spura, A., Russin, T.S., Freedman, N.D., Grant, M., McLaughlin, J.T., Hawrot, E., 1999. Probing the agonist domain of the nicotinic acetylcholine receptor by cysteine scanning mutagenesis reveals residues in proximity to the α-bungarotoxin binding site. Biochemistry 38, 4912–4921.

Stauffer, D.A., Karlin, A., 1994. Electrostatic potential of the acetylcholine binding sites in the nicotinic receptor probed by reactions of binding-site cysteines with charged methanethiosulfonates. Biochemistry 33, 6840–6849.

Starter, M., 1991. Taking stock of cognition enhancers. Trends Pharmacol. Sci. 12, 456–461.

Storch, A., Schrattenholz, A., Cooper, J.C., Ghani, E.M.A., Gutbrod, O., Weber, K.-H., et al., 1995. Physostigmine, galanthamine and codeine act as 'noncompetitive nicotinic receptor agonists' on clonal rat pheochromocytoma cells. Eur. J. Pharmacol. 290, 207–219.

Stroud, R.M., McCarthy, M.P., Shuster, M., 1990. Nicotinic acetylcholine receptor superfamily of ligand-gated ion channels. Biochemistry 29, 11009–11023.

Sugiyama, N., Boyd, A.E., Taylor, P., 1996. Anionic residue in the α-subunit of the nicotinic acetylcholine receptor contributing to subunit assembly and ligand binding. J. Biol. Chem. 271, 26575–26581.

Sugiyama, N., Marchot, P., Kawanishi, C., Osaka, H., Molles, B., Sine, S.M., Taylor, P., 1998. Residues at the subunit interfaces of the nicotinic acetylcholine receptor that contribute to α-conotoxin M1 binding. Mol. Pharmacol. 53, 787–794.

Sung, J.J., Kim, S.J., Lee, H.B., Chung, J.M., Choi, Y.M., Cha, C.I., et al., 1998. Anticholinesterase induces nicotinic receptor modulation. Musc. Nerv. 21, 1135–1144.

Sussman, J.L., Harel, M., Frolow, F., Oefner, C., Goldman, A., Toker, L., Silman, I., 1991. Atomic structure of acetylcholinesterase from *Torpedo californica*. Science 253, 872–879.

Svensson, A.-L., Nordberg, A., 1996. Tacrine interacts with an allosteric site on α4β2 nAChRs in M10 cells. NeuroReport 7, 2201–2205.

Swope, S.L., Moss, S.J., Blackstone, C.D., Huganir, R.L., 1992. Phosphorylation of ligand-gated ion channels: a possible mode of synaptic plasticity. FASEB J. 6, 2514–2523.

Tamamizu, S., Butler, D.H., Lasalde, J.A., McNamee, M.G., 1996. Effects of antibody binding on structural transitions of the nicotinic acetylcholine receptor. Biochemistry 35, 11773–11781.

Tavazoie, S.F., Tavazoie, M.F., McIntosh, J.M., Olivera, B.M., Yoshikami, D., 1996. Differential block of nicotinic synapses on B versus C neurons in sympathetic ganglia of frog by α-conotoxins MII and ImI. Br. J. Pharmacol. 120, 995–1000.

Taylor, P., Osaka, H., Molles, B.E., Sugiyama, N., Marchot, P., Ackermann, E.J., et al., 1998. Toxins selective for subunit interafces as probes of nicotinic acetylcholine receptor structure. J. Physiol. 92, 79–83.

Thal, L.J., Fuld, P.A., Masur, D.M., Sharpless, N.S., 1983. Oral physostigmine and lecithin improve memory in Alzheimer's disease. Ann. Neurol. 13, 491–496.

Tine, S.-J., Raftery, M.A., 1993. Photoaffinity labeling of *Torpedo* acetylcholine receptor at multiple sites. Proc. Natl. Acad. Sci. USA 90, 7308–7311.

Tomaselli, G.F., McLaughlin, J.T., Jurman, M.E., Hawrot, E., Yellen, G., 1991. Mutations affecting agonist sensitivity of the nicotinic acetylcholine receptor. Biophys. J. 60, 721–727.

Tomizawa, M., Casida, J.E., 1997. (I^{125}) Azidonicotinoid ptotoaffinity labeling of insecticide-binding subunit of *Drosophila* nicotinic acetylcholine receptor. Neurosci. Lett. 237, 61–64.

Toyoshima, C., Unwin, P.N.T., 1990. Three-dimensional structure of the acetylcholine receptor by cryoelectron microscopy and helical image reconstruction. J. Cell. Biol. 111, 2623–2635.

Trémeau, O., Lemaire, C., Drevet, P., Pinkasfeld, S., Ducancel, F., Boulain, J.-C., Ménez, A., 1995. Genetic engineering of snake toxins. The functional site of erabutoxin a, as delineated by site-directed mutagenesis, includes variant residues. J. Biol. Chem. 270, 9362–9369.

Tsigelny, I., Sugiyama, N., Sine, S.M., Taylor, P., 1997. A model of the nicotinic receptor extracellular domain based on sequence identity and residue location. Biophys. J. 73, 52–66.

Tzartos, S.J., Remoundos, M.S., 1990. Fine localization of the major α-bungarotoxin binding site to residues α189–195 of the *Torpedo* acetylcholine receptor: residues 189, 190, and 195 are indispensable for binding. J. Biol. Chem. 265, 21462–21467.

Ullian, E.M., McIntosh, J.M., Sargent, P.B., 1997. Rapid synaptic transmission in the avian ciliary ganglion is mediated by two distinct classes of nicotinic receptors. J. Neurosci. 17, 7210–7219.

Unwin, N., 1993. Nicotinic acetycholine receptor at 9 Å resolution. J. Mol. Biol. 229, 1101–1124.

Unwin, N., 1995. Acetylcholine receptor channel imaged in the open state. Nature 373, 37–43.

Unwin, N., 1996. Projection structure of the nicotinic acetylcholine receptor. Distinct conformations of the α-subunit. J. Mol. Biol. 257, 586–596.

Utkin, Y.N., Kobayashi, Y., Hucho, F., Tsetlin, V.I., 1994a. Relationship between the binding sites for α-conotoxin and snake venom neurotoxins in the nicotinic acetylcholine receptor from *Torpedo californica*. Toxicon 32, 1153–1157.

Utkin, Y.N., Krivoshein, A.V., Davydov, V.L., Kasheverov, I.E., Franke, P., Maslennikov, I.V., et al., 1998. Labeling of *Torpedo californica* nicotinic acetylcholine receptor subunits by cobratoxin

derivatives with photoactivatable groups of different chemical nature at Lys23. Eur. J. Biochem. 253, 229–235.

Utkin, Y.N., Weise, C., Tritscher, E., Machold, J., Franke, P., Tsetlin, V.I., Hucho, F., 1994b. Structure determination of peptide fragments from the cross-linked complex of Lys26-*p*-azidobenzoyl neurotoxin II from *Naja naja oxiana* with the nicotinic acetylcholine receptor from *Torpedo californica*. Bioorganicheskaya Khimiya 20, 1047–1059.

Valenzuela, C.F., Dowding, A.J., Arias, H.R., Johnson, D.A., 1994b. Antibody-induced conformational changes in the *Torpedo* nicotinic acetylcholine receptor: A fluorescence study. Biochemistry 33, 6586–6594.

Valenzuela, C.F., Weign, P., Yguerabide, J., Johnson, D.A., 1994a. Transverse distance between the membrane and the agonist binding sites on the *Torpedo* acetylcholine receptor: a fluorescence study. Biophys. J. 66, 674–682.

Van den Beukel, Y., Van Kleef, R.G.D.M., Zwart, R., Oortgiesen, M., 1998. Physostigmine and acetylcholine differentially activate nicotinic receptor subpopulations in *Locusta migratoria* neurons. Brain Res. 789, 263–273.

van Hooft, J.A., Spier, A.D., Yakel, J.L., Lummis, S.C.R., Vijverberg, H.P.M., 1997. Promiscuous coassambly of serotonin 5-HT_3 and nicotinic α4 receptor subunits into Ca^{2+} pemeable ion channels. Proc. Natl. Acad. Sci. USA 95, 11456–11461.

Vazquez, R.W., Oswald, R.E., 1999. Identification of a new amino acid residue capable of modulating agonist efficacy at the homomeric nicotinic acetylcholine receptor, α7. Mol. Pharmacol. 55, 1–7.

Venera, G.D., Testai, F.D., Pena, C., Lacorazza, H.D., Bonino, M.J.B.D., 1997. Involvement of Histidine-134 in the binding of α-bungarotoxin to the nicotinic acetylcholine receptor. Neurochem. Int. 31, 151–157.

Verrall, S., Hall, Z.W., 1992. The *N*-terminal domain of acetylcholine receptor subunits contain recognition signals for the initial steps of receptor assembly. Cell 68, 23–31.

Villarroya, M., Delafuente, M.T., Lopez, M.G., Gandia, L., García, A.G., 1997. Distinct effects of ω-toxins and various groups of Ca^{2+} entry inhibitors on nicotinic acetylcholine receptor and Ca^{2+} channels of chromaffin cells. Eur. J. Pharmacol. 320, 249–257.

Vincent, A., Newland, C., Croxen, R., Beeson, D., 1997. Genes at the junction — candidates for congenital myasthenic syndromes. Trends Neurosci. 20, 15–22.

Virginio, C., MacKenzie, A., Rassendren, F.A., North, R.A., Surprenant, A., 1999. Pore dilation of neuronal P2X receptor channels. Nature Neurosci. 2, 315–321.

Wahlsten, J.L., Lindstrom, J.M., Conti-Tronconi, B.M., 1993. Amino acid residues within the sequence region α55–74 of *Torpedo* nicotinic acetylcholine receptor interacting with antibodies to the main immunogenic region and with snake α-neurotoxins. J. Rec. Res. 13, 989–1008.

Walker, J.W., Richardson, C.A., McNamee, M.G., 1984. Effects of thiol group modifications of *Torpedo californica* acetylcholine receptor ion flux activation and inactivation kinetics. Biochemistry 23, 2329–2338.

Walkinshaw, M.D., Saenger, W., Maelicke, A., 1980. Three-dimensional structure of the 'long' neurotoxin from cobra venom. Proc. Natl. Acad. Sci. USA 77, 2400–2404.

Wang, D., Xie, Y., Cohen, J.B., 1996. Probing the structure of the nicotinic acetylcholine receptor (nAChR) with 4-benzoylbenzoylcholine (Bz2-choline), a novel photoaffinity competitive antagonist. Biophys. J. 70, A76 Abst.

Watters, D., Maelicke, A., 1983. Organization of ligand binding sites at the acetylcholine receptor: A study with monoclonal antibodies. Biochemistry 22, 1811–1819.

Wheeler, S.V., Chad, J.E., Foreman, R., 1993. Residues 1 to 80 of the N-terminal domain of the β subunit confer neuronal bungarotoxin sensitivity and agonist selectivity on neuronal nicotinic receptors. FEBS Lett. 332, 139–142.

Williamson, P.T.F., Gröbner, G., Spooner, P.J.R., Miller, K.W., Watts, A., 1998. Probing the agonist binding pocket in the nicotinic acetylcholine receptor: A high-resolution solid-state NMR approach. Biochemistry 37, 10854–10859.

Wilson, G.G., Karlin, A., 1998. The location of the gate in the acetylcholine receptor channel. Neuron 20, 1269–1281.

Witzemann, V., Raftery, M.A., 1977. Selective photoaffinity labeling of acetylcholine receptor using a cholinergic analogue. Biochemistry 16, 5862–5868.

Wu, T.I., Liu, C.I., Chang, Y.C., 1996. A study of the oligomeric state of the alpha-amino-3-hydroxy-5-methyl-4-isoxazolepropionic acid-preferring glutamate receptors in the synaptic junction of porcine brain. Biochem. J. 319, 731–739.

Yan, D., Pedersen, S.E., White, M.M., 1998. Interaction of *d*-tubocurarine analogs with the 5HT_3 receptor. Neuropharmacol. 37, 251–257.

Yan, D., Shulte, M.K., Bloom, K.E., White, M.M., 1999. Structural features of the ligand-binding domain of the Serotonin 5HT_3 receptor. J. Biol. Chem. 274, 5537–5541.

Yguerabide, J., 1994. Theory for establishing proximity relations in biological membranes by excitation energy transfer measurements. Biophys. J. 66, 683–693.

Zafaralla, G.C., Ramilo, C., Gray, W.R., Karlstrom, R., Olivera, B.M., Cruz, L.J., 1988. Phylogenetic specificity of cholinergic ligands: α-conotoxin SI. Biochemistry 27, 7102–7105.

Zhang, Y., Chen, J., Auerbach, A., 1995. Activation of recombinant mouse acetylcholine receptors by acetylcholine, carbamylcholine and tetramethylammonium. J. Physiol. 486, 189–206.